

AD-A008 716

HIGH ACCURACY AIRCRAFT TO SATELLITE  
TRACKING USING AN EXTENDED KALMAN  
FILTER

Robert A. K. Mitchell

Air Force Institute of Technology  
Wright-Patterson Air Force Base, Ohio

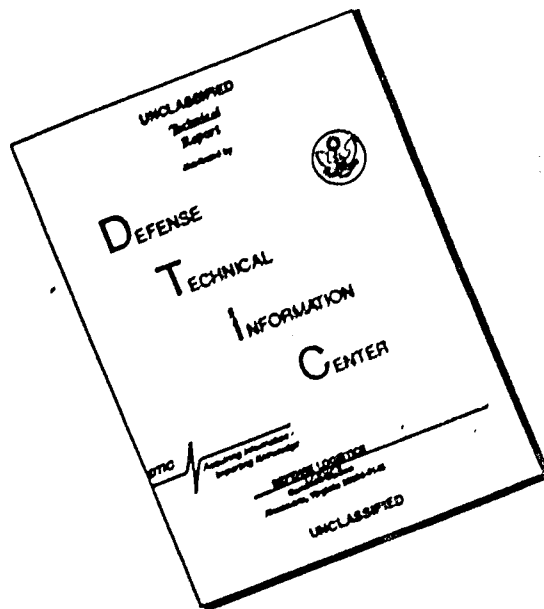
December 1974

DISTRIBUTED BY:

**NTIS**

National Technical Information Service  
U. S. DEPARTMENT OF COMMERCE

# DISCLAIMER NOTICE



THIS DOCUMENT IS BEST QUALITY AVAILABLE. THE COPY FURNISHED TO DTIC CONTAINED A SIGNIFICANT NUMBER OF PAGES WHICH DO NOT REPRODUCE LEGIBLY.

REPORT DOCUMENTATION PAGE		REPORT NUMBER
1. REPORT NUMBER GA/15/74-3	2. GOVT ACCESSION NO.	3. RECIPIENT CATALOG NUMBER AD-ACC8 416
4. TITLE (and Subtitle) HIGH ACCURACY AIRCRAFT TO SATELLITE TRACKING USING <del>AN</del> EXTENDED KALMAN FILTER <b>AN</b>	5. TYPE OF REPORT & PERIOD COVERED MS Thesis	
	6. PERFORMING ORG. REPORT NUMBER	
7. AUTHOR(s) Robert A.E. Mitchell Squadron Leader, RAF	8. CONTRACT OR GRANT NUMBER(s)	
9. PERFORMING ORGANIZATION NAME AND ADDRESS Air Force Institute of Technology (AFIT-DN) Wright-Patterson AFB, Ohio 45433	10. PROGRAM ELEMENT, PROJECT, TASK AREA & WORK UNIT NUMBERS	
11. CONTROLLING OFFICE NAME AND ADDRESS Air Force Avionics Laboratory (AFAL) Wright-Patterson AFB, Ohio 45433	12. REPORT DATE December 1974	
	13. NUMBER OF PAGES 166	
14. MONITORING AGENCY NAME & ADDRESS (if different from Controlling Office)	15. SECURITY CLASS. (of this report) Unclassified	
	15a. DECLASSIFICATION DOWNGRADING SCHEDULE	
16. DISTRIBUTION STATEMENT (of this Report)  Approved for public release; distribution unlimited		
17. DISTRIBUTION STATEMENT (of the abstract entered in Block 20, if different from Report)  Approved for public release; LIT REF 190-17 Jerry C. Hill, Captain, USAF Director of Information		
18. SUPPLEMENTARY NOTES		
19. KEY WORDS (Continue on reverse side if necessary and identify by block number) Kalman Filter Tracking Satellite Covariance Analysis  Reproduced by NATIONAL TECHNICAL INFORMATION SERVICE US Department of Commerce Springfield, VA 22151  <b>PRICES SUBJECT TO CHANGE</b>		
20. ABSTRACT (Continue on reverse side if necessary and identify by block number)  A 61-state truth model is developed for the aircraft to satellite tracking problem. The equations for the Extended Kalman Filter are described and the truth model is examined and simplified to give a 12-state reduced order filter model of the system. Using the method of Covariance Analysis which is described, the performance of the 12-state filter model against the 61-state truth model is evaluated with the dynamics profile of a high altitude aircraft tracking a near earth satellite in a circular polar orbit.		

Unclassified

SECURITY CLASSIFICATION OF THIS PAGE (When Data Entered)

The measurement equations for the truth model are adjusted over a range of measuring instrument precision and the filter model re-evaluated. The resultant tracking accuracies are discussed.

1a  
SECURITY CLASSIFICATION OF THIS PAGE (When Data Entered)

HIGH ACCURACY AIRCRAFT TO SATELLITE TRACKING USING  
AN EXTENDED KALMAN FILTER

THESIS

Presented to the Faculty of the School of Engineering  
of the Air Force Institute of Technology

Air University

in Partial Fulfillment of the  
Requirements for the Degree of  
Master of Science

by

Robert A. K. Mitchell, BSc  
Squadron Leader, Royal Air Force

Graduate Astronautics

December 1974

Approved for public release; distribution unlimited.

Preface

This work is a continuation of research carried out by my sponsor Captain Robert B. Asher into the air to air tracking problem, while at the Air Force Avionics Laboratory, Wright-Patterson Air Force Base. The study utilizes essentially the same techniques used for air to air tracking but introduces an accurate model of the satellite orbit.

I would like to thank Captain J. Gary Reid and Major Parker D. Sproul for their advice and assistance in the preparation of this thesis. I especially appreciate the enthusiastic and professional advice and help I have received from my advisor Lieutenant Peter S. Maybeck throughout all phases of the project.

Finally, I thank my wife Chris, for her understanding and patience during the year in which this thesis was prepared.

Contents

	Page
Preface . . . . .	ii
List of Figures . . . . .	v
List of Symbols . . . . .	vii
Abstract . . . . .	xii
I. Introduction . . . . .	1
Statement of the Problem . . . . .	1
Objectives of the Study . . . . .	1
Assumptions and Limitations . . . . .	2
II. System Modeling . . . . .	5
Physical Description of the System . . . . .	5
Target State Equations . . . . .	5
Tracker State Equations . . . . .	11
Measurement Equations . . . . .	24
Summary of System Truth Model State and Measurement Equations . . . . .	34
III. Extended Kalman Filter . . . . .	41
Basic Kalman Filter . . . . .	41
Extended Kalman Filter Formulation . . . . .	44
Summary of Propagation and Update Equations . . . . .	48
Comparison with Basic Kalman Filter . . . . .	49
Application to Tracking Problem . . . . .	50
IV. Covariance Analysis of Suboptimal Filter Design . . . . .	52
Objective . . . . .	52
The Equations for Sensitivity Analysis. . . . .	52
Summary of Propagation and Update Equations for Covariance Analysis . . . . .	61
Application of Covariance Analysis to Extended Kalman Filter . . . . .	62
V. Initial Choice of Filter Model . . . . .	64
Objective . . . . .	64
Filter Model State Equations . . . . .	64
Filter Model Measurement Equations . . . . .	68
Summary of State and Measurement Equations . . . . .	70

	Page
VI. Results . . . . .	73
Test Simulation Data . . . . .	73
Test Objective . . . . .	73
Tuning the Filter Model . . . . .	73
Transient Behaviour of the Filter . . . . .	77
Determination of Vehicle Orbit . . . . .	82
Tracking Accuracy . . . . .	92
Modifications to Truth Model . . . . .	96
Summary of Effects of Truth Model Modifications . . . . .	104
VII. Recommendations and Conclusions . . . . .	106
Addition of Further Measurements . . . . .	106
Alternate Methods of Modeling . . . . .	107
Method of Analysis . . . . .	108
Summary of Recommendations . . . . .	109
Conclusions . . . . .	109
Bibliography . . . . .	111
Appendix A: Derivation of Gravitational Forces Due to Earth . .	113
Appendix B: Linearization of Truth Model State and Measurement Equations . . . . .	119
Appendix C: Linearization of Filter Model State and Measurement Equations . . . . .	143
Appendix D: Initial Truth Model Simulation Data . . . . .	148
Vita . . . . .	151

List of Figures

Figure		Page
1.	Geocentric Equatorial Non-rotating Coordinate System . . . . .	6
2.	Tracking Antenna Configuration . . . . .	12
3.	Inertial and Tracker Coordinate Frames . . . . .	12
4.	Target and Line of Sight Coordinate Frames . . . . .	15
5.	Linear System Representation for $C_{gx}$ . . . . .	27
6.	Filter Range Rate Error Standard Deviation . . . . .	75
7.	System Range Rate Error Standard Deviation . . . . .	76
8.	Filter $X_1$ Position Error Standard Deviation with Initial Condition of 100 km . . . . .	78
9.	System $X_1$ Position Error Standard Deviation with Initial Condition of 0 km . . . . .	79
10.	Filter $X_1$ Position Error Standard Deviation with Initial Condition of 63 km . . . . .	80
11.	System $X_1$ Position Error Standard Deviation with Initial Condition of 63 km . . . . .	81
12.	Filter $\omega_{LSY}$ Error Standard Deviation-Incorrect Tuning . . . . .	83
13.	System $\omega_{LSY}$ Error Standard Deviation-Incorrect Tuning . . . . .	84
14.	Filter $\omega_{LSY}$ Error Standard Deviation-Tuned . . . . .	85
15.	System $\omega_{LSY}$ Error Standard Deviation-Tuned . . . . .	86
16.	Filter $X_2$ Position Error Standard Deviation . . . . .	88
17.	System $X_2$ Position Error Standard Deviation . . . . .	89
18.	Filter $X_4$ Velocity Error Standard Deviation . . . . .	90
19.	System $X_4$ Velocity Error Standard Deviation . . . . .	91
20.	Filter $\delta n$ Error Standard Deviation-Initial Measurements . . . . .	93
21.	System $\delta n$ Error Standard Deviation-Initial Measurements . . . . .	94
22.	Filter $\delta \epsilon$ Error Standard Deviation-Improved Gyro Drift . . . . .	98
23.	System $\delta \epsilon$ Error Standard Deviation-Improved Gyro Drift . . . . .	99

Figure		Page
24.	Filter $\delta\epsilon$ Error Standard Deviation-Final Measurements	100
25.	System $\delta\epsilon$ Error Standard Deviation-Final Measurements	101
26.	Filter $X_1$ Position Error Standard Deviation-Final Measurements . . . . .	102
27.	System $X_1$ Position Error Standard Deviation-Final Measurements . . . . .	103
28.	Summary of Effects of Measurement Improvements . . . . .	105
29.	Inertial and Rotating Coordinate Frames . . . . .	113
30.	Gravity Harmonics . . . . .	117

List of Symbols

Symbol	Description
X, Y, Z	Geocentric nonrotating coordinate frame axes (I-frame)
$x_T, y_T, z_T$	Tracker coordinate frame axes (T-frame)
$x_{LS}, y_{LS}, z_{LS}$	Line of sight coordinate frame axes (LS-frame)
$\theta, \phi$	Euler rotation angles from I-frame to T-frame
$\delta\epsilon, \delta\eta$	Euler rotation angles from T-frame to LS-frame
$X_1, X_2, X_3$	Satellite position vector coordinates in I-frame
$X_4, X_5, X_6$	Satellite velocity vector coordinates in I-frame
$\underline{A_g}$	Earth gravity vector
$\underline{A_d}$	Atmospheric drag perturbation vector
$\underline{A_s}$	Solar perturbation vector
$\underline{A_m}$	Lunar perturbation vector
$\underline{A_p}$	Solar pressure perturbation vector
$\underline{\omega}_T$	Tracker angular velocity vector
$\underline{\omega}_{LS}$	Line of sight angular velocity vector
$W_T$	Tracker angular velocity skew symmetric matrix
$W_{LS}$	Line of sight angular velocity skew symmetric matrix

$\underline{R}$	Target to tracker relative position vector
$A_{rel_x}, A_{rel_y},$ $A_{rel_z}$	Components of acceleration of target relative to tracker in LS-frame
$A_{rx}, A_{ry}, A_{rz}$	Components of acceleration of target relative to tracker in T-frame
$R_M$	Measurement of range
$\omega_{MX}$	Measurement of $\omega_{TX}$ -component of $\underline{\omega}_T$ along $x_T$ axis
$A_{TXM}$	Measurement of $A_{TX}$
$\delta\epsilon_M$	Measurement of $\delta\epsilon$
$B_{gsf}$	Gyro scale factor
$B_{gm}$	Gyro g-sensitive mass unbalance coefficient
$B_{gma}$	Gyro misalignment coefficient
$C_g$	Gyro drift
$B_{as}$	Accelerometer scale factor
$B_{ama}$	Accelerometer misalignment coefficient
$B_{non}$	Accelerometer $g^2$ or $g^3$ sensitive nonlinear coefficient
$C_a$	Accelerometer drift
$\delta\epsilon, \delta\eta$	Angle track scintillations

$B_{AT}$	Angle track bias
$C_{SF}$	Angle measurement scale factor
$S_R$	Range scintillation
$B_R$	Range bias
$\beta_i$	Reciprocal of process correlation time $\tau_i$
$\sigma_i$	Process rms value (steady state)
$\underline{x}(t)$	State vector
$\hat{\underline{x}}(t)$	State vector estimate
$\Phi(t_i, t_i - 1)$	State transition matrix
$P(t)$	State covariance matrix
$K(t_i)$	Kalman gain matrix
$F(t)$	System dynamics matrix
$G(t)$	System noise input matrix
$H(t_i)$	Measurement matrix
$\underline{w}(t)$	Zero mean Gaussian white noise vector
$Q(t)$	Positive semi-definite noise covariance matrix
$\underline{v}(t_i)$	Zero mean Gaussian white noise vector sequence.
$R(t_i)$	Positive definite symmetric noise covariance matrix

$\underline{z}(t_i)$	Measurement vector
$f[\underline{x}(t), t]$	Nonlinear vector function of $\underline{x}(t)$ and $t$ describing propagation of $\underline{x}(t)$
$h[\underline{x}(t_i), t_i]$	Nonlinear vector function of $\underline{x}(t_i)$ and $t_i$ describing $\underline{z}(t_i)$
$\underline{x}_n(t)$	Nominal reference trajectory
$F[t; \underline{x}_{no}]$	Linearized system matrix which is a function of time and is evaluated along $\underline{x}_n$ which is a function of $\underline{x}_{no}$
$H[t_i; \underline{x}_n(t_i)]$	Linearized measurement matrix which is a function of the sequence $t_i$ and is evaluated along $\underline{x}_n(t_i)$
$\underline{e}(t)$	Error vector
$P_{ee}(t)$	Covariance matrix describing $\underline{e}(t)$
$\underline{y}(t)$	Augmented state vector
$\omega_E$	Earth rotation rate
$\rho$	Atmospheric density
$\rho_0$	Mean sea level atmospheric density
$\beta$	Altitude atmospheric decay rate
$h$	Satellite altitude
$R_0$	Mean Earth radius
$B$	Satellite ballistic coefficient

S	Satellite solar pressure coefficient
$\mu_{\oplus}$	Earth gravitational constant
$\mu_{\odot}$	Sun gravitational constant
$\mu_{\text{M}}$	Moon gravitational constant

Abstract

A 61-state truth model is developed for the aircraft to satellite tracking problem. The equations for the Extended Kalman Filter are described and the truth model is examined and simplified to give a 12-state reduced order filter model of the system. Using the method of Covariance Analysis which is described, the performance of the 12-state filter model against the 61-state truth model is evaluated with the dynamics profile of a high altitude aircraft tracking a near earth satellite in a circular polar orbit. The measurement equations for the truth model are adjusted over a range of measuring instrument precision and the filter model reevaluated. The resultant tracking accuracies are discussed.

HIGH ACCURACY AIRCRAFT TO SATELLITE  
TRACKING USING EXTENDED KALMAN  
FILTER

I. INTRODUCTION

Statement of the Problem

Given two accelerating vehicles, there are many situations in which it is necessary to track one vehicle from the other with a high degree of accuracy. In general, such a system cannot be modeled deterministically and stochastic estimation techniques must be employed.

This thesis addresses the problem of tracking a satellite from an aircraft. Again, this problem is varied and might include tracking of navigation satellites from long range transport aircraft or tracking of low orbit satellites from high altitude aircraft using laser devices. The latter will be investigated in particular. Ideally, the satellite would transmit a beacon signal to facilitate tracking but in practice this cannot be guaranteed. For the purposes of this report, the satellite is assumed to be completely passive.

Various methods are available for formulating and solving the tracking problem. One such method which uses an Extended Kalman Filter to provide the system state estimate is investigated in detail.

Objectives of the Study

The primary objective of the study will be to determine the feasibility of using a reduced order (simplified) system model to propagate the system state. Propagation will be carried out using the Extended Kalman Filter. To investigate feasibility, the following breakdown of

the problem will be followed:

1. Develop the full truth model representing true system performance.
2. Generate a tracking profile representing a typical tracking 'pass'.
3. Using the truth model from 1. and the tracking profile from 2. carry out a covariance analysis with a reduced order system model.
4. Adjust the reduced order model until satisfactory performance is obtained.

Thus, given a system truth model, a reduced order system model will be found and tested using the covariance analysis. A secondary objective will be to modify the system truth model and correspondingly modify the reduced order system model and repeat the tests of the reduced order model. The modifications will involve changes to the measuring devices to represent increased or degraded quality. This will be done to determine the quality of measuring instrument required in practice to achieve some specified level of tracking performance.

#### Assumptions and Limitations

The system investigated here is in fact non-linear so that the basic Kalman Filter cannot be used to propagate state estimate and associated covariance. Various methods are available for handling non-linear problems among which is the Extended Kalman Filter. This formulation, in common with most methods for handling non-linear problems, assumes that the non-linear system can adequately be represented by a linear system about some trajectory. That is, deviations from this trajectory can be handled using linear methods. The assumptions inherent in the lineari-

zation process will be described in detail under section III which describes the Extended Kalman Filter.

This study attempts to find a simplified reduced order system model which will adequately describe the true system performance. For a true linear system, the covariance analysis is complete in that it accurately describes the filter performance. However, in applying linear techniques to non-linear systems, it is sometimes possible to obtain apparently good performance when in reality the performance is bad. This possibility is usually overcome by carrying out a 'Monte-Carlo' system analysis in addition to the covariance analysis. This would be desirable for the problem but will not be done in this study.

Only one aircraft/satellite dynamics profile is investigated in this study. The profile chosen uses a low orbit satellite in a polar orbit tracked by an aircraft flying east/west. This was chosen to represent as near as possible one of the worst case situations in which the satellite passes almost directly overhead. Clearly, confidence in the models would improve if several representative profiles are tested. Also, the tracking state equations are modeled in the line of sight coordinate system. The equations could have been modeled entirely in inertial coordinates or aircraft coordinates possibly with different results.

It is assumed that the tracking antenna is controlled by some closed loop control system. The dynamics of such a system have not been incorporated into the models. In fact, the system assumes that deviations from nominal can instantaneously be corrected at regular intervals.

Finally, it will be assumed that the coordinate transformation matrix from the tracking coordinate frame to the inertial non-rotating earth centered coordinate frame is known. This assumption implies that the

tracker orientation relative to the inertial coordinate frame is known. For the purposes of this study, it will be further assumed that the tracker elevation axis always lies in the inertial X-Y plane (See Fig. 1 Section II). Thus an inertial reference must be available on board the aircraft. The problem could be considered by introducing a body (aircraft) coordinate system and assuming that the tracker orientation relative to the body is known. It would then be necessary to assume also that the body orientation relative to the inertial coordinate system is known. The simplest assumption which implies no loss of generality is the first. That is, the tracker-orientation relative to the inertial coordinate frame is known.

## II. SYSTEM MODELING

Physical Description of the System

Physically, the system consists of a satellite and an aircraft equipped with some type of satellite tracking device, typically a high resolution radar or laser. The tracking device is equipped with three rate gyros which measure the tracker inertial angular velocity in three components. Three accelerometers measure the three components of specific force of the tracker origin. Some control system is available to correct the estimated tracker angular deviations. These estimates will be found using the Extended Kalman Filter and the control system will have the capability of instantaneous corrections. The tracking device is able to measure the satellite range, range rate and small angular deviations of the tracker from the true line of sight. The measurements are all assumed to be imperfect. The nature of the corrupting noises will be discussed later.

The tracker depends for its operation on the availability of a reference coordinate system. This could be the aircraft to body system assuming the orientation is known or the inertial earth centered coordinate system. For this problem, it is assumed that the tracker base always lies in a plane parallel to the inertial X-Y plane (see Fig. 1, next page). In practice this would be accomplished with a closed loop control system using some inertial reference sensing device. Note that the possibility that the tracker base is translating or accelerating is not excluded.

Target State Equations

The target state equations are expressed in the geocentric - equatorial non-rotating coordinate system illustrated in Fig. 1. The state

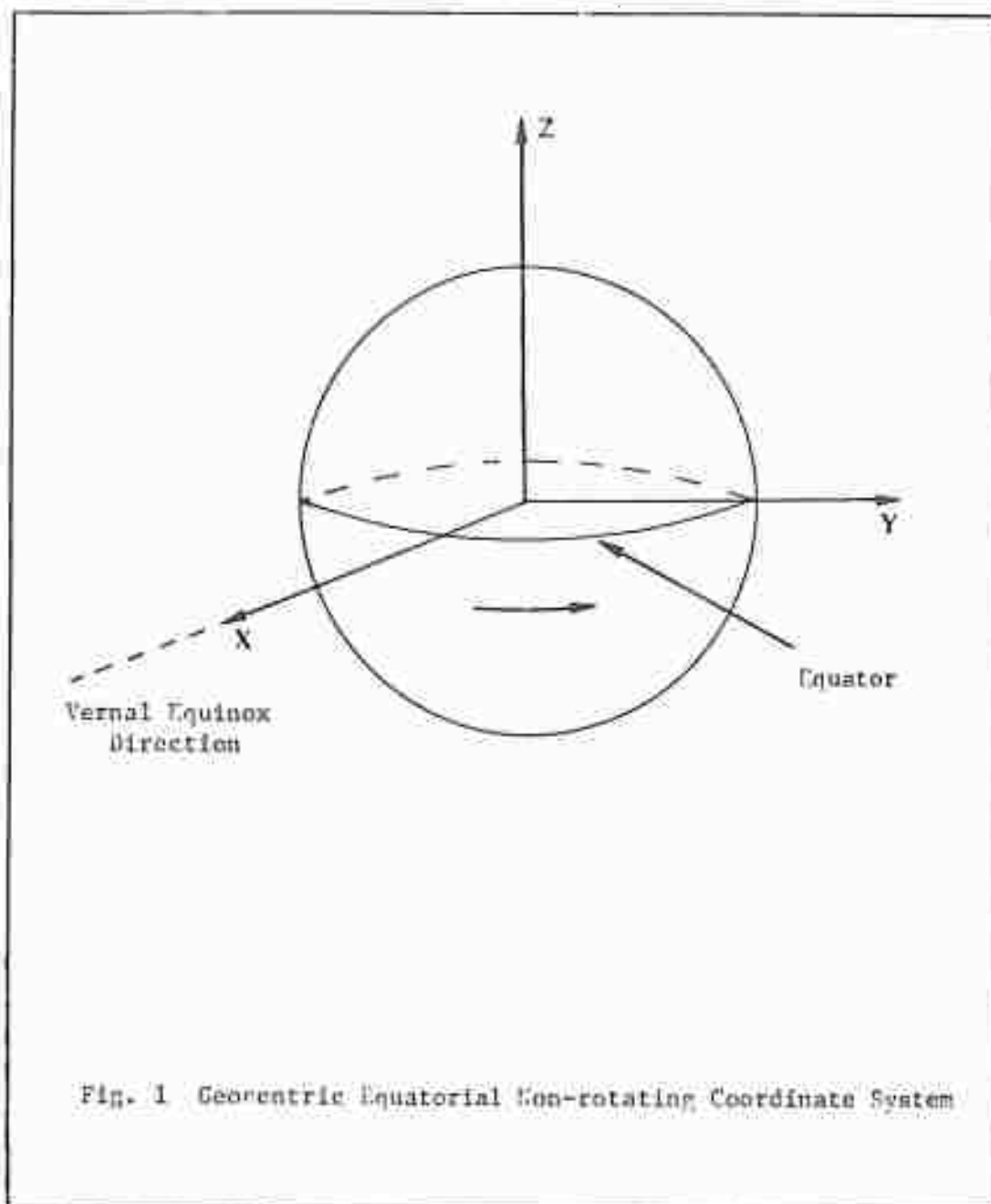


Fig. 1 Geocentric Equatorial Non-rotating Coordinate System

equations are:

$$\begin{aligned}
 \dot{X}_1 &= X_4 \\
 \dot{X}_2 &= X_5 \\
 \dot{X}_3 &= X_6 \\
 \dot{X}_4 &= Ag_1 + Ad_1 + As_1 + Am_1 + Ap_1 + W_1 \\
 \dot{X}_5 &= Ag_2 + Ad_2 + As_2 + Am_2 + Ap_2 + W_2 \\
 \dot{X}_6 &= Ag_3 + Ad_3 + As_3 + Am_3 + Ap_3 + W_3
 \end{aligned} \tag{2-1}$$

$X_1, X_2, X_3$  - represent the target inertial position from earth center.

$X_4, X_5, X_6$  - represent the target inertial velocity

$Ag_1, Ag_2, Ag_3$  - are the gravitational forces along the  $X_1, X_2, X_3$  directions

$Ad_1, Ad_2, Ad_3$  - are the forces due to aerodynamic drag.

$As_1, As_2, As_3$  - are the solar perturbations (gravitational).

$Am_1, Am_2, Am_3$  - are the lunar perturbations (gravitational).

$Ap_1, Ap_2, Ap_3$  - are the perturbations due to solar pressure.

$W_1, W_2, W_2$  - are zero mean independent Gaussian white noises added to model unknown perturbations and to account for approximations in the above terms.

Appendix A indicates the method of obtaining the earth's gravitational attracting forces  $Ag_1, Ag_2, Ag_3$  and the method of finding the second partials of the gravity gradient for the earth. These will be required during the state equation linearization process.

#### Force Due to Drag

The drag perturbational accelerations are modeled as follows:

Ad is the drag vector in inertial non-rotating coordinates

r is the inertial position vector from earth center to target

$$\begin{bmatrix} X_1 \\ X_2 \\ X_3 \end{bmatrix}$$

$\dot{\underline{r}}$  is the inertial velocity vector of the target  $\begin{bmatrix} X_4 \\ X_5 \\ X_6 \end{bmatrix}$

$$\text{Then } \underline{Ad} = -\frac{1}{2} \rho B V_a \dot{\underline{r}}_a \quad (2-2)$$

where:

$\rho$  = atmospheric density modeled as:  $\rho = \rho_0 e^{-\beta h}$

$\rho_0$  = mean sea level atmospheric density

$\beta$  = altitude atmospheric density decay rate

$h = (X_1^2 + X_2^2 + X_3^2)^{1/2} - R_0$

$R_0$  = mean earth radius

$V_a$  = magnitude of the vehicle velocity relative to the rotating atmosphere.  $V_a = \left| \dot{\underline{r}}_a \right|$

WE = earth rotation rate, and by the law of Coriolis:

$$\dot{\underline{r}}_a = \begin{bmatrix} X_4 + WE X_2 \\ X_5 - WE X_1 \\ X_6 \end{bmatrix} = \underline{Va} \quad (2-3)$$

$B$  = vehicle ballistic coefficient

In general, the ballistic properties of the vehicle will be unknown. However, the ballistic coefficient  $B$  will not change with time and can therefore be modeled stochastically as a random bias. Such a model implies 100% correlation with time.  $B$  is therefore represented by the system state  $X_7$  with the state equation

$$\dot{X}_7 = 0 \quad (2-4)$$

Thus appropriate choice of an initial condition for  $X_7$  can be made to adequately model a range of vehicle types.

Sun and Moon Gravitational Perturbations

The sun and moon perturbing acceleration vectors are defined respectively as:

$$\underline{A_s} = \begin{bmatrix} A_{s1} \\ A_{s2} \\ A_{s3} \end{bmatrix}, \quad \underline{A_m} = \begin{bmatrix} A_{m1} \\ A_{m2} \\ A_{m3} \end{bmatrix}$$

For the purposes of this report, the sun and moon are considered stationary in space relative to the vehicle and earth. This assumption is valid since the time for a particular pass for a low orbit satellite will be of the order of minutes only.

If the sun and moon have position vectors relative to the non-rotating inertial coordinate system of:

$$\begin{bmatrix} X_s \\ Y_s \\ Z_s \end{bmatrix} \quad \text{and} \quad \begin{bmatrix} X_m \\ Y_m \\ Z_m \end{bmatrix} \quad \text{respectively}$$

then the perturbational acceleration vectors  $\underline{A_s}$  and  $\underline{A_m}$  will be given by:

$$\underline{A_s} = \mu_{\odot} \begin{bmatrix} \frac{X_s - X_1}{r_{vs}^3} - \frac{X_s}{rs^3} \\ \frac{Y_s - X_2}{r_{vs}^3} - \frac{Y_s}{rs^3} \\ \frac{Z_s - X_3}{r_{vs}^3} - \frac{Z_s}{rs^3} \end{bmatrix}$$

and

$$\frac{A_m}{\mu_D} = \begin{bmatrix} \frac{(X_m - X_1)}{r_{vm}^3} - \frac{X_m}{r_m^3} \\ \frac{(Y_m - X_2)}{r_{vm}^3} - \frac{Y_m}{r_m^3} \\ \frac{(Z_m - X_3)}{r_{vm}^3} - \frac{Z_m}{r_m^3} \end{bmatrix} \quad (2-6)$$

where

$$X_{vm} = X_m - X_1$$

$$Y_{vm} = Y_m - X_2$$

$$Z_{vm} = Z_m - X_3$$

$$X_{vs} = X_s - X_1$$

$$Y_{vs} = Y_s - X_2$$

$$Z_{vs} = Z_s - X_3$$

$$r_{vs} = \sqrt{X_{vs}^2 + Y_{vs}^2 + Z_{vs}^2}$$

$$r_{vm} = \sqrt{X_{vm}^2 + Y_{vm}^2 + Z_{vm}^2}$$

$$r_m = \sqrt{X_m^2 + Y_m^2 + Z_m^2}$$

$$r_s = \sqrt{X_s^2 + Y_s^2 + Z_s^2}$$

Solar Pressure The force acting due to solar pressure is modeled in a simple way using the relationship:

$$\begin{aligned} \Delta p_1 &= -K S \frac{\dot{X}_{vs}}{r_{vs}} \\ \Delta p_2 &= -K S \frac{\dot{Y}_{vs}}{r_{vs}} \\ \Delta p_3 &= -K S \frac{\dot{Z}_{vs}}{r_{vs}} \end{aligned} \quad (2-7)$$

K is a proportionality constant of  $4.5 \times 10^{-7}$  m/sec (Ref. 1) and S is the solar pressure coefficient. This latter coefficient depends directly on the vehicle surface area presented towards the sun and inversely on the mass of the vehicle. Again, no information is available about the vehicle and S is again modeled as a random bias  $X_8$ . The state equation for  $X_8$  is therefore:

$$\dot{X}_8 = 0 \quad (2-8)$$

and appropriate choice of the initial condition for X will adequately model the range of vehicles of primary interest.

#### Tracker State Equations

Fig. 2 illustrates the geometry of the typical tracker. The table is aligned with a reference plane which in this case will be the inertial plane. The tracker is thus restricted to rotate about the azimuth vertical axis and the elevation axis. The vertical axis of rotation will always stay aligned with the inertial vertical axis while the elevation axis will be restricted to lie in the inertial horizontal plane only. Note that the tracker is configured such that the tracker  $x_T$  axis points along the antenna center line, while the tracker  $y_T$  axis points out through the tracker elevation axis and therefore always lies in the plane of the table as shown. The tracker  $z_T$  axis forms the third vector in an orthogonal system.

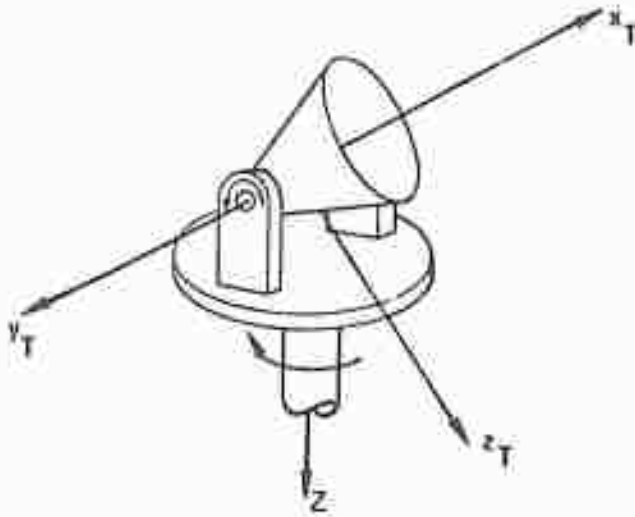


Fig. 2 Tracking Antenna Configuration

Fig. 3 shows the relation between the inertial  $X, Y, Z$  frame, which is an earth centered non-rotating frame, and the tracker  $x_T, y_T, z_T$  frame.

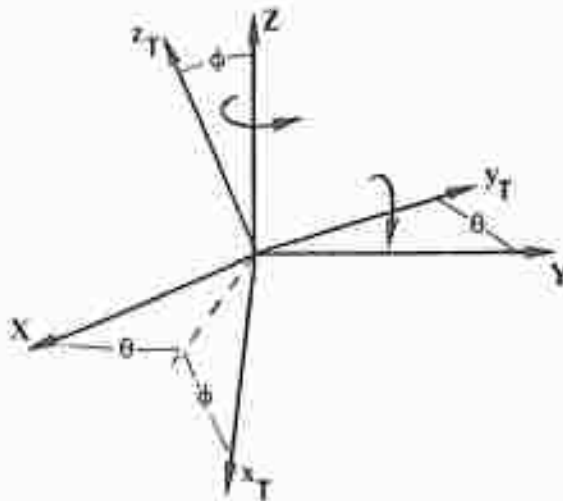


Fig. 3 Inertial and Tracker Coordinate Frames

From the above figure it can be seen that the tracker frame orientation is obtained via two Euler angle rotations  $\theta$  and  $\phi$  in the azimuth and elevation directions respectively from the inertial frame. Denoting

the inertial frame as the I-frame and the tracking frame as the T-frame we define the coordinate transformation matrix  $C_I^T$  as the transformation matrix from I-coordinates into T-coordinates, then:

$$\begin{aligned}
 C_I^T &= \begin{bmatrix} \cos \phi & 0 & -\sin \phi \\ 0 & 1 & 0 \\ \sin \phi & 0 & \cos \phi \end{bmatrix} \begin{bmatrix} \cos \theta & \sin \theta & 0 \\ -\sin \theta & \cos \theta & 0 \\ 0 & 0 & 1 \end{bmatrix} \\
 &= \begin{bmatrix} \cos \theta \cos \phi & \sin \theta \cos \phi & -\sin \phi \\ -\sin \theta & \cos \theta & 0 \\ \cos \theta \sin \phi & \sin \theta \sin \phi & \cos \phi \end{bmatrix} \quad (2-9)
 \end{aligned}$$

Now, the Euler rotation angles  $\theta$  and  $\phi$  can be determined by considering the geometry of the tracking problem. Let the relative position vector of the target from the aircraft be expressed in inertial X, Y, Z coordinates as  $\underline{R}^I$ :

Defining  $\underline{R}^I$  as the relative position vector expressed in inertial I-coordinates and  $\underline{R}^T$  as the relative position vector expressed in tracker T-coordinates then:

$$\underline{R}^I = \begin{bmatrix} R_X \\ R_Y \\ R_Z \end{bmatrix}, \quad \text{and} \quad \underline{R}^T = C_I^T \underline{R}^I \quad (2-10)$$

$$\underline{R}^T = \begin{bmatrix} R_X \cos \theta \cos \phi + R_Y \sin \theta \cos \phi - R_Z \sin \phi \\ -R_X \sin \theta + R_Y \cos \theta \\ R_X \cos \theta \sin \phi + R_Y \sin \theta \sin \phi + R_Z \cos \phi \end{bmatrix}$$

If we define the range from aircraft to target as the scalar variable  $R$ , then  $R =$  the X-component of the vector  $\underline{R}^T$  and the Y and Z components are both zero for perfect tracking.

Thus

$$R = R_X \cos \theta \cos \phi + R_Y \sin \theta \cos \phi + R_Z \sin \phi$$

And

$$-R_X \sin \theta + R_Y \cos \theta = 0$$

$$\tan \theta = \frac{R_Y}{R_X}$$

is determined as follows:

$$\theta = \arctan (R_Y/R_X) \text{ if } R_X > 0, R_Y \text{ arbitrary} \quad (2-12)$$

$$= \arctan (R_Y/R_X) + \pi \text{ if } R_X < 0, R_Y \text{ arbitrary}$$

Similarly,

$$R_X \cos \theta \sin \phi + R_Y \sin \theta \sin \phi + R_Z \cos \phi = 0$$

$$\frac{R_X}{\tan \theta} + R_Y + \frac{R_Z}{\tan \phi \sin \theta} = 0$$

but

$$\sin \theta = \frac{R_Y}{(R_X^2 + R_Y^2)^{1/2}}$$

So

$$\frac{(R_X^2 + R_Y^2)}{R_Y} + \frac{R_Z \cdot (R_X^2 + R_Y^2)^{1/2}}{R_Y \cdot \tan \phi} = 0$$

$$\tan \phi = \frac{-R_Z}{(R_X^2 + R_Y^2)^{1/2}} \quad (2-13)$$

Thus far, the relationship between the tracker and inertial coordinate frames has been established and it has been shown that the coordinate transformation matrix is dependent entirely on the relative position vector from aircraft to target expressed in inertial coordinates.

In practice, perfect tracking, in which the  $x_T$  vector aligns perfectly with the target line of sight, will not be possible. The tracker frame will in fact be slightly misaligned from the true line of sight coordinate system denoted  $LS$ . This system has the  $x_{LS}$  axis pointing directly towards the target and is related to the target coordinate system as shown by Fig. 4.

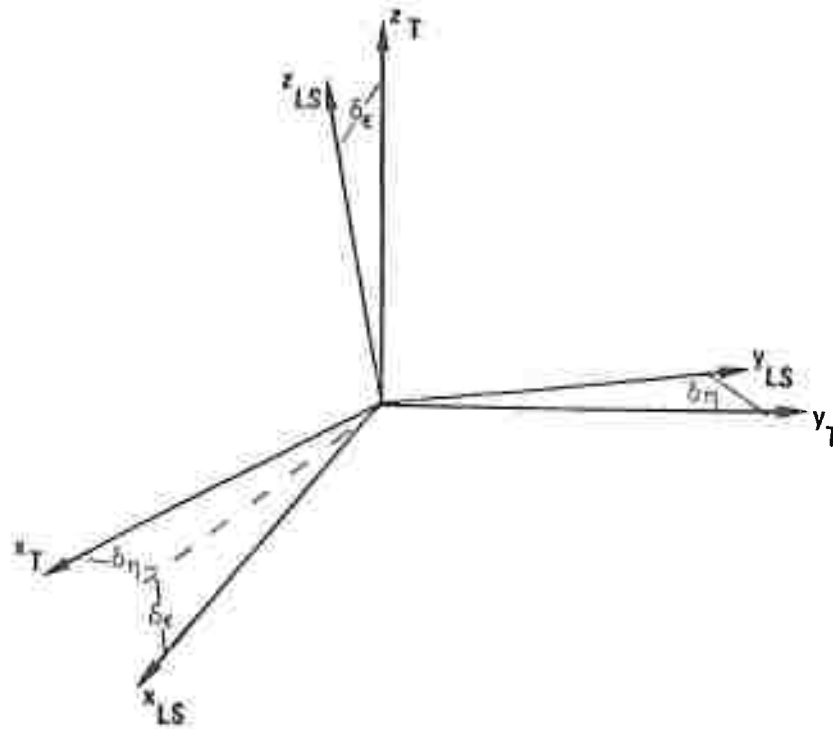


Fig. 4 Target and Line of Sight Coordinate Frames

Once again, the two frames can be coincided through two small Euler rotations  $\delta\epsilon$  and  $\delta\eta$ .  $\delta\eta$  rotates the LS - frame about the tracker  $z_T$  axis and  $\delta\epsilon$  rotates the LS - frame about the line of sight  $y_{LS}$  axis. The coordinate transformation matrix  $C_T^{LS}$  transforms a vector from T - coordinates into LS - coordinates and:

$$C_T^{LS} = \begin{bmatrix} \cos \delta\eta & \cos \delta\epsilon & \sin \delta\eta & \cos \delta\epsilon & -\sin \delta\epsilon \\ -\sin \delta\eta & & \cos \delta\eta & & 0 \\ \cos \delta\eta & \sin \delta\epsilon & \sin \delta\eta & \sin \delta\epsilon & \cos \delta\epsilon \end{bmatrix}$$

For near-perfect tracking in which the angles  $\delta\epsilon$  and  $\delta\eta$  are small, it is possible to make the small angle assumptions:

$$\cos \delta\eta \approx \cos \delta\epsilon \approx 1$$

$$\sin \delta\eta \approx \delta\eta, \sin \delta\epsilon \approx \delta\epsilon$$

$$\delta\epsilon\delta\eta \approx 0$$

then:

$$C_T^{LS} = \begin{bmatrix} 1 & \delta\eta & -\delta\epsilon \\ -\delta\eta & 1 & 0 \\ \delta\epsilon & 0 & 1 \end{bmatrix} \quad (2-14)$$

In practice, the tracking device will be capable of providing measurement information concerning the two small angles  $\delta\epsilon$  and  $\delta\eta$ ; hence it is necessary to establish the state equations expressing the time rate of change of the two angles.

The motion between the T-rotating frame and the LS-rotating frame

is characterized by the following differential equation: (Ref. 7)

$$\dot{C}_{LS}^T = C_{LS}^T W_{LS} - W_T C_{LS}^T \quad (2-15)$$

where  $W_{LS}$  and  $W_T$  are the skew symmetric matrices defined as

$$W_{LS} = \begin{bmatrix} 0 & -\omega_{LSZ} & \omega_{LSY} \\ \omega_{LSZ} & 0 & -\omega_{LSX} \\ -\omega_{LSY} & \omega_{LSX} & 0 \end{bmatrix}, \quad W_T = \begin{bmatrix} 0 & -\omega_{TZ} & \omega_{TY} \\ \omega_{TZ} & 0 & -\omega_{TX} \\ \omega_{TY} & \omega_{TX} & 0 \end{bmatrix}$$

and the elements of these matrices represent the angular velocities about the particular axes subscripted.

Now, the two vectors:

$$\underline{\omega}_{LS}^{LS} = \begin{bmatrix} \omega_{LSX} \\ \omega_{LSY} \\ \omega_{LSZ} \end{bmatrix} \quad \text{and} \quad \underline{\omega}_T^T = \begin{bmatrix} \omega_{TX} \\ \omega_{TY} \\ \omega_{TZ} \end{bmatrix}$$

are inertial angular velocity vectors expressed in line of sight LS - coordinates and tracker T - coordinates respectively.

From (2-15),

$$C_T^{LS} \dot{C}_{LS}^T = W_{LS} - C_T^{LS} W_T C_{LS}^T$$

or

$$(I + A)(-\dot{A}) = W_{LS} - C_T^{LS} W_T C_{LS}^T$$

where:

$$A = \begin{bmatrix} 0 & \delta\eta & -\delta\varepsilon \\ -\delta\eta & 0 & 0 \\ \delta\varepsilon & 0 & 0 \end{bmatrix} \quad (2-17)$$

Neglecting second order quantities gives:

$$-\dot{A} = W_{LS} - C_T^{LS} W_T C_{LS}^T \quad (2-18)$$

The above equation can be written out as:

$$\begin{bmatrix} 0 & -\delta\dot{\eta} & \delta\dot{\varepsilon} \\ \delta\dot{\eta} & 0 & 0 \\ -\delta\dot{\varepsilon} & 0 & 0 \end{bmatrix} = \begin{bmatrix} 0 & -\omega_{LSZ} & \omega_{LSY} \\ \omega_{LSZ} & 0 & -\omega_{LSX} \\ -\omega_{LSY} & \omega_{LSX} & 0 \end{bmatrix} -$$

$$\begin{bmatrix} 1 & \delta\eta & -\delta\varepsilon \\ -\delta\eta & 1 & 0 \\ \delta\varepsilon & 0 & 1 \end{bmatrix} \begin{bmatrix} 0 & -\omega_{TZ} & \omega_{TY} \\ \omega_{TZ} & 0 & -\omega_{TX} \\ -\omega_{TY} & \omega_{TX} & 0 \end{bmatrix} \begin{bmatrix} 1 & -\delta\eta & \delta\varepsilon \\ \delta\eta & 1 & 0 \\ -\delta\varepsilon & 0 & 1 \end{bmatrix}$$

$$= W_{LS} - \begin{bmatrix} 0 & (-\omega_{TZ} - \delta\varepsilon \omega_{TX}) & (\omega_{TY} - \delta\eta \omega_{TX}) \\ (\omega_{TZ} + \delta\varepsilon \omega_{TX}) & 0 & (-\omega_{TX} - \delta\eta \omega_{TY} + \delta\varepsilon \omega_{TZ}) \\ (-\omega_{TY} + \delta\eta \omega_{TX}) & (\omega_{TX} + \delta\eta \omega_{TY} - \delta\varepsilon \omega_{TZ}) & 0 \end{bmatrix}$$

which provides the two required state equations for  $\delta\epsilon$  and  $\delta\eta$  as:

$$\begin{aligned}\dot{\delta\eta} &= \omega_{LSZ} - \omega_{TZ} - \delta\epsilon \omega_{TX} \\ \dot{\delta\epsilon} &= \omega_{LSY} - \omega_{TY} + \delta\eta \omega_{TX}\end{aligned}$$

In order to determine the time evolution of the line of sight angular velocity vector  $\underline{\omega}_{LS}$ , consider the position vector of the target relative to the aircraft which was defined as  $\underline{R}$  (Note that the magnitude of  $\underline{R}$  is the scalar range variable  $R$  also previously defined).

Differentiating  $\underline{R}$  twice with respect to inertial space and applying the theorem of Coriolis each time gives the equation:

$$\begin{aligned}\left. \frac{d^2 \underline{R}}{dt^2} \right|_I &= \left. \frac{d^2 \underline{R}}{dt^2} \right|_{LS} + 2 \underline{\omega}_{LS} \times \left. \frac{d \underline{R}}{dt} \right|_{LS} + \left. \frac{d \underline{\omega}_{LS}}{dt} \right|_{LS} \times \underline{R} \\ &+ \underline{\omega}_{LS} \times (\underline{\omega}_{LS} \times \underline{R})\end{aligned}\quad (2-20)$$

where the vertical line denotes the frame relative to which the derivatives are taken, so that the left hand side of equation (20) i.e.

$\left. \frac{d^2 \underline{R}}{dt^2} \right|_I$  represents the total rate of change of  $\left. \frac{d \underline{R}}{dt} \right|_I$  which is also

the total rate of change of the relative position vector  $\underline{R}$ .

Equation (2-20) is entirely general and not referenced to any particular coordinate system. Choosing the line of sight coordinate

system and expression  $\left. \frac{d^2 \underline{R}}{dt^2} \right|_I$  in the line of sight system as  $\begin{bmatrix} A_{rel_x} \\ A_{rel_y} \\ A_{rel_z} \end{bmatrix}$

then:

$$\begin{aligned}
 \begin{bmatrix} A_{relx} \\ A_{rely} \\ A_{relz} \end{bmatrix} &= \begin{bmatrix} \dot{V}_r \\ 0 \\ 0 \end{bmatrix} + 2 \begin{bmatrix} 0 \\ \dot{R} \omega_{LSz} \\ -\dot{R} \omega_{LSy} \end{bmatrix} + \begin{bmatrix} 0 \\ R \dot{\omega}_{LSz} \\ -R \dot{\omega}_{LSy} \end{bmatrix} \\
 &+ \begin{bmatrix} -R(\omega_{LSy}^2 + \omega_{LSz}^2) \\ R \omega_{LSx} \omega_{LSy} \\ R \omega_{LSx} \omega_{LSz} \end{bmatrix} \tag{2-21}
 \end{aligned}$$

and the above vector state equation yields the following four scalar state equations:

$$\dot{R} = V_r \tag{2-22}$$

$$\dot{V}_r = A_{relx} + R(\omega_{LSy}^2 + \omega_{LSz}^2) \tag{2-23}$$

$$\dot{\omega}_{LSy} = -\frac{1}{R} A_{relz} - \frac{2 V_r}{R} + \omega_{LSx} \omega_{LSz} \tag{2-24}$$

$$\dot{\omega}_{LSz} = \frac{1}{R} A_{rely} - \frac{2 V_r}{R} \omega_{LSz} - \omega_{LSx} \omega_{LSy} \tag{2-25}$$

where:

$R$  = Range

$V_r$  = Range rate

$A_{relx}$  = Acceleration of target relative to tracker measured along the line of sight X - axis

$A_{relY}$  = Relative acceleration measured along line of sight Y - axis

$A_{relZ}$  = Relative acceleration measured along line of sight Z - axis

thus, if  $A_{TARX}^{\Delta}$  = target acceleration along line of sight X - axis

and  $A_{TRX}^{\Delta}$  = tracker acceleration along line of sight X - axis

then:  $A_{relX} = A_{TARX}^{\Delta} - A_{TRX}^{\Delta}$  etc.

Equations (2-22) to (2-25) thus represent the exact relationships for the aircraft/satellite tracking problem. It should be noted that there is no state equation relating the motion of the tracker about the X - axis in the line of sight coordinate system, i.e.  $\omega_{LSX}$ . The reason is simple, for the purposes of tracking, angular velocity about the line of sight has no significance. This does not however preclude the requirement to measure the tracker angular velocity in that direction but since there is no state equation for  $\omega_{LSX}$ , it must be eliminated from equations (2-24) and (2-25).

In practice, angular velocities will be measured in the tracking coordinate frame since there is no physical way in which they could be measured in the line of sight frame. The substitution from equation (2-18) is made, i.e.

$$\omega_{LSX} = \omega_{TX} + \delta\eta \omega_{TY} - \delta\epsilon \omega_{TZ} \quad (2-26)$$

and equations (2-24) and (2-25) now become:

$$\dot{\omega}_{LSY} = -\frac{1}{R} A_{relZ} - \frac{2 V_T}{R} \omega_{LSY} + \omega_{LSZ} (\omega_{TX} + \delta\eta \omega_{TY} - \delta\epsilon \omega_{TZ}) \quad (2-27)$$

$$\dot{\omega}_{LSZ} = \frac{1}{R} A_{relY} - \frac{2 V_T}{R} \omega_{LSZ} - \omega_{LSY} (\omega_{TX} + \delta\eta \omega_{TY} - \delta\epsilon \omega_{TZ}) \quad (2-28)$$

The definitions for  $A_{relX}$ ,  $A_{relY}$ , and  $A_{relZ}$  again are made in the line of sight coordinate system. Acceleration measurements for the tracker are only available in the tracker coordinate system in which the tracker acceleration vector is defined as:

$$\underline{A}_T^T = \begin{bmatrix} A_{TX} \\ A_{TY} \\ A_{TZ} \end{bmatrix}$$

and accelerations of the target (satellite) are only available in the inertial coordinate system as:

$$\underline{A}_S^I = \begin{bmatrix} \dot{X}_4 \\ \dot{X}_5 \\ \dot{X}_6 \end{bmatrix}$$

$\underline{A}_S$  can be transformed from the inertial coordinate frame into the tracker coordinate frame by the transformation

$$\underline{A}_S^T = C_I^T \underline{A}_S^I \quad (2-29)$$

Thus, the vector of relative accelerations in the tracker coordinate frame defined as:

$$\underline{A}_R = \begin{bmatrix} A_{rX} \\ A_{rY} \\ A_{rZ} \end{bmatrix} = \underline{A}_S^T - \underline{A}_T^T \quad (2-30)$$

must be used to obtain the vector  $\underline{A}_{rel}$ , i.e.

$$\underline{A}_{rel} = C_T^{LS} \underline{A}_R \quad (2-31)$$

where

$$C_T^{LS} = \begin{bmatrix} 1 & \delta\eta & -\delta\epsilon \\ -\delta\eta & 1 & 0 \\ \delta\epsilon & 0 & 1 \end{bmatrix}$$

or

$$\begin{bmatrix} A_{relX} \\ A_{relY} \\ A_{relZ} \end{bmatrix} = \begin{bmatrix} 1 & \delta\eta & -\delta\epsilon \\ -\delta\eta & 1 & 0 \\ \delta\epsilon & 0 & 1 \end{bmatrix} \begin{bmatrix} A_{rX} \\ A_{rY} \\ A_{rZ} \end{bmatrix} \quad (2-32)$$

Substitution from equations (2-31) and (2-32) into (2-27) and (2-28) gives the final form of the two line of sight angular velocity equations as:

$$\begin{aligned} \dot{\omega}_{LSY} = & \frac{-2 V_R}{R} \omega_{LSY} - \frac{1}{R} A_{rZ} + \omega_{LSZ} \omega_{TX} \\ & + \left\{ \frac{-\delta\epsilon}{R} A_{rX} + \omega_{LSZ} \left[ \delta\eta \omega_{TY} - \delta\epsilon \omega_{TZ} \right] \right\} \end{aligned} \quad (2-33)$$

$$\begin{aligned} \dot{\omega}_{LSZ} = & \frac{-2 V_R}{R} \omega_{LSZ} + \frac{1}{R} A_{rY} - \omega_{LSY} \omega_{TX} \\ & + \left\{ \frac{-\delta\eta}{R} A_{rX} - \omega_{LSY} \left[ \delta\eta \omega_{TY} - \delta\epsilon \omega_{TZ} \right] \right\} \end{aligned} \quad (2-34)$$

Note that in equations (2-33) and (2-34), the two bracketed terms represent modifications to the state equations for perfect tracking. These modifications account for the small angular deviations  $\delta\epsilon$  and  $\delta\eta$  from the perfect tracking situation.

Finally, equation (2-32) is substituted into equation (2-23) to give:

$$\dot{V}_R = A_{rX} + R(\omega_{LSY}^2 + \omega_{LSZ}^2) + \delta\eta A_{rY} - \delta\epsilon A_{rZ} \quad (2-35)$$

which is the final state equation for  $V_R$ .

#### Measurement Equations (Ref. 2, 3, and 5)

Measurements to the tracking system as already stated will consist of inertial angular velocity of the tracker measured in the tracker coordinate frame by three rate gyros. measurements of tracker inertial acceleration again in the tracker coordinate frame, measurements of range and range rate and measurements of the two small angular deviations  $\delta\epsilon$  and  $\delta\eta$ . None of the measurements are assumed perfect. Now the system propagates the true line of sight angular velocities  $\omega_{LSY}$  and  $\omega_{LSZ}$ , whereas measurements are available only of the tracker angular velocities

$\omega_{TX}$ ,  $\omega_{TY}$ ,  $\omega_{TZ}$ . Measurements of  $\omega_{TX}$  thus constitute true measurements of parameter  $\omega_{TX}$  while measurements of  $\omega_{TY}$  and  $\omega_{TZ}$  are interpreted as pseudo-measurements of  $\omega_{LSY}$  and  $\omega_{LSZ}$  respectively. If the tracking is good, these measurements approach true measurements. Measurements of angular velocities in the line of sight system would be most desirable but in a practical system such measurements would not be available. It should also be noted that the tracker accelerations are not states of the system. Thus measurements of tracker accelerations are measurements of system parameters.

#### Measurement of Tracker Angular Velocities

These are provided by three rate gyros mounted approximately in the tracking coordinate frame. The approximation arises because in practice, the gyros will always be slightly misaligned from the true frame alignment. To simplify the discussion, only the measurement of  $\omega_{TX}$  will be described. Measurements of the other two angular velocity components are modeled identically in form. The measurement of angular velocity in the  $X_T$  direction is thus modeled as:

$$\omega_{TX}' = \omega_{TX} + B_{gsf_X} \omega_{TX} + \sum_{i=1}^3 B_{gm_X i} A_i + C_{g_X} + \left[ \Delta C_{gma} \frac{\omega_T}{X} \right] + V_1 \quad (2-36)$$

The terms in equation (2-36) are as follows:

$\omega_{M_X}$  = measured angular velocity along  $X_T$  - axis (see Fig. 2)

$\omega_{T_X}$  = true angular velocity along  $x_T$  axis

$B_{gsf_X}$  = constant (bias) gyro scale factor

$B_{gm_{X_i}}$  = coefficients (along X, Y, and Z directions of tracker coordinate frame) of the g - sensitive mass unbalance to which the gyro is subject

$A_i$  = Accelerations ( $A_{T_X}$ ,  $A_{T_Y}$ ,  $A_{T_Z}$ ) of the tracker origin

$C_{gX}$  = gyro drift term along the  $X_T$  axis.

$\Delta C_{gma}$  = the error angle transformation resulting from the misalignments of the three gyros

$$\Delta C_{gma} = \Delta \begin{bmatrix} 0 & B_{gma_{12}} & B_{gma_{13}} \\ B_{gma_{21}} & 0 & B_{gma_{23}} \\ B_{gma_{31}} & B_{gma_{32}} & 0 \end{bmatrix}$$

Note that for the purposes of this study, the terms in the above matrix are considered constant and result from the small angle approximation.

$V_1$  is an additive white noise used to compensate for any unmodeled effects such as aniso-elastic drift.

The above terms can be modeled stochastically as follows: The gyro drift term  $C_{gX}$  can be modeled as a first order exponentially time correlated random variable. Drift is not a white random noise process

but does show a degree of correlation in time. Laboratory data indicates that the exponential model adequately describes this correlation. The state equation for  $C_{gX}$  will thus be:

$$\dot{C}_{gX} = -\beta_4 C_{gX} + \sqrt{2\beta_4} \sigma_4 U_4 \quad (2-37)$$

where if  $\tau_4$  represents the system correlation time,

$$\beta_4 \triangleq \frac{1}{\tau_4}$$

$\sigma_4$  is the rms value of the process, and  $U_4$  is a unity variance white driving noise. Fig. 5 below shows the equivalent linear system:

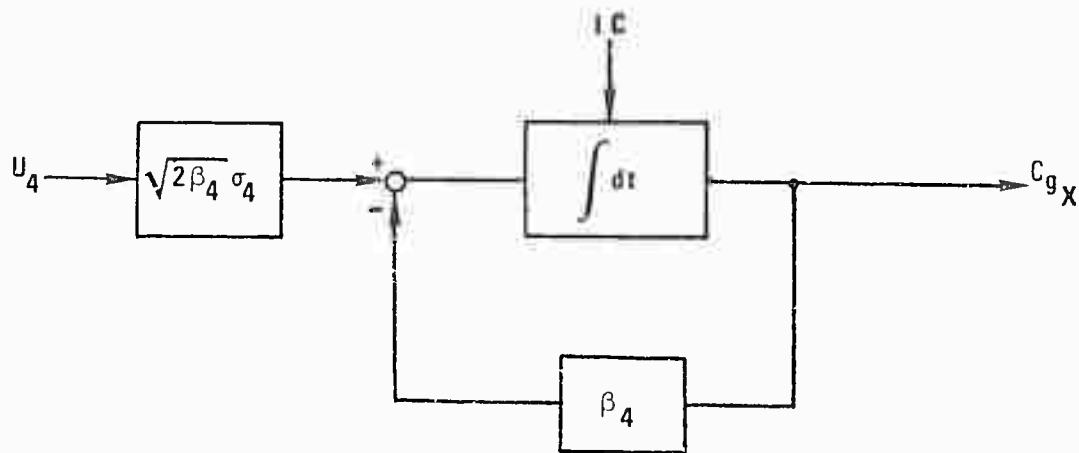


Fig. 5 Linear System Representation for  $C_{gX}$

$U_4$  in Fig. 5 is a white driving noise of variance  $q = 1$ .

The autocorrelation function for  $C_{g_X}$  is given by:

$$E \left\{ C_{g_X}(t) C_{g_X}(t + \tau) \right\} = \sigma_4^2 e^{-\beta_4 |\tau|}$$

Note that by appropriate choice of initial condition for  $C_{g_X}$ , an initial known bias in drift can be accounted for.

The remaining coefficients represent unknowns in the system. One fact is certain however; none of these coefficients will vary with time. For example, the gyro misalignment coefficients have values which describe how the gyros are displaced during assembly from their true orientations. While these displacements may not be known, it is certain that in the time scale of a typical satellite pass, they will not change. The model chosen to represent the coefficients therefore will have the general form:

$$\dot{X} = 0$$

This is a linear equation and the covariance equation which correspondingly describes the way in which the covariance of a coefficient will change in time is given by the general form:

$$\dot{P} = F P + P F^T \quad (\text{where } F^T \text{ denotes the transpose of } F, \text{ and } F \text{ is the system matrix})$$

$$\text{Thus, } \dot{P} = 0,$$

and this implies that the variance of a coefficient likewise will not change with time. Choice of initial conditions on  $X$  and  $P$  completely describe a coefficient. The initial condition on  $X$  represents the mean value of the coefficient and the initial condition on  $P$  represents the

variance of the distribution of  $X$  about its mean. Often, however, the only information available about the coefficient will be the variance, in which case, the most reasonable choice for an initial condition on  $X$  is zero.

#### Measurements of Tracker Accelerations

The tracker accelerations are parameters of the system rather than states. The measurements are modeled as follows. Note that only the measurement equation for the acceleration in the  $X_T$  direction is given. The remaining equations are identical in form.

$$A_{TX_M} = A_{TX} + Bas_X A_{TX} + C_{aX} + Bnon_{X_1} A_{TX}^2 + Bnon_{X_2} A_{TX}^3 + \left[ \frac{\Delta C_{ma}}{A_T} \right]_X + v_4 \quad (2-38)$$

The terms in equation (2-33) are defined as follows:

$A_{TX_M}$  = measured acceleration along  $X_T$  direction in tracker coordinate frame

$A_{TX}$  = true acceleration

$Bas_X$  = accelerometer scale factor

$C_{aX}$  = accelerometer drift and bias

$Bnon_{X_1}$  = accelerometer ( $g^2$ ) non-linear coefficient

$Bnon_{X_2}$  = accelerometer ( $g^3$ ) non-linear coefficient

$$\Delta Cna = \begin{bmatrix} 0 & Bama_{12} & Bama_{13} \\ Bama_{21} & 0 & Bama_{23} \\ Bama_{31} & Bama_{32} & 0 \end{bmatrix} \quad \text{is the error angle}$$

transformation matrix which supplies the accelerometer misalignment coefficients.

Note that the small angle approximation has been made in using this matrix.

$V_4$  = white noise to account for unmodeled effects.

Once again, as in the case of the rate gyros, the coefficients in the measurement equations are modeled as states of the system. The accelerometer drift and bias is modeled as a first order exponentially correlated random variable. This choice of model is justified since the magnitude of the drift will in fact vary with time. The degree of correlation in time is expressed by the constant  $\beta_1$  used in the state equation. Note that equation (2-37) describing the gyro drift shows the form of these equations. In addition, the remaining coefficients are once again modeled as random biases.

#### Measurement of Angular Misalignments $\delta\epsilon$ and $\delta\eta$

The tracking device will be capable of providing measurements in the tracking coordinate frame of the two angular misalignment angles  $\delta\epsilon$  and  $\delta\eta$ . See Fig. 4 for a description of the geometry.  $\delta\eta$  is measured about the  $z_T$  - axis and  $\delta\epsilon$  is measured about the  $y_{LS}$  - axis. In practice, the LS - coordinate frame and the T - coordinate frame will be closely

aligned and  $\delta\epsilon$  will in fact be assumed to be measured about the  $y_T$  - axis.

Now there are clearly many different measuring devices. If a radar scanner were used, the measurement device might be different to that used with a laser tracker. However, a somewhat representative model is chosen which could easily be adjusted to suit the particular device. The measurement model for the two error angles has the following form:

$$\begin{aligned}\delta\epsilon_M &= K_1(\delta\epsilon + S_\epsilon) + C_{SF_\epsilon} \cdot \delta\epsilon + B_{AT_\epsilon} + V_7 \\ \delta\eta_M &= K_2(\delta\eta + S_\eta) + C_{SF_\eta} \cdot \delta\eta + B_{AT_\eta} + V_8\end{aligned}\tag{2-39}$$

where the various coefficient are as follows:

$K_1, K_2$  - deterministic scale factors

$S_\epsilon, S_\eta$  - angle track scintillation noises

$C_{SF_\epsilon}, C_{SF_\eta}$  - scale factor errors

$B_{AT_\epsilon}, B_{AT_\eta}$  - angle track biases

$V_7, V_8$  - white gaussian additive noises to account for unmodeled effects

$K_1$  and  $K_2$  are assumed to be known.  $S_\epsilon$  and  $S_\eta$  are modeled as first order exponentially time correlated random variables. This model is used since the scintillation noise is dependent on various factors such as atmospheric propagation, amplifier characteristics, etc. This type of

factor does not change instantaneously with time but fluctuates. Again the state equation used will have the form:

$$\dot{S}_\epsilon = -\beta_1 S_\epsilon + \sqrt{2\beta_1} \sigma_1 U_1 \quad (2-40)$$

where  $\beta_1 = \frac{1}{\tau_1}$ , and  $\tau_1$  is the correlation time of the process.  $\sigma_1^2$  is the steady state covariance of the noise and  $U_1$  is a white driving noise with unity covariance.

The scale factor errors  $C_{SF_\epsilon}$  and  $C_{SF_\eta}$  are modeled also as first order exponentially correlated random variables with state equations of the form shown in (2-40) above. This is another way of stating that the constants  $K_1$  and  $K_2$  are not really constants but random variables which are exponentially time correlated and have a non-zero mean. Again, the justification for using this model is that the scale factors are really determined within some type of electronic equipment which exhibits time correlated behaviour.

The remaining coefficients  $B_{AT_\epsilon}$  and  $B_{AT_\eta}$  can be adequately modeled as random biases. i.e. The actual values are unknown, the covariance is known and the variable has 100% time correlation.

#### Measurement of Range

The measurement of range is very similar to those of the angular misalignment angles except that the scale factor error is omitted.

The measurement equation is thus:

$$R_M = K_R(R + S_R) + B_R + V_9 \quad (2-41)$$

where:

$R_M$  - measured range

$R$  - true range

$S_R$  - range scintillation noise

$B_R$  - range bias

$V_g$  - white gaussian additive noise to account for unmodeled effects

The actual electronic methods by which range is measured vary from those by which the angular misalignments are measured. In general, the latter depend to some extent on analog equipment (linear amplifiers, etc.) while the range measurement can usually be accomplished digitally with very little analog equipment. The digital equipment can usually be accurately calibrated so that only the scintillation noise and bias need be stochastically estimated. The bias will be small in magnitude compared to the scintillation noise and will result from the equipment. The scintillation noise will however be the additive effect of the digitization of the range and the atmospheric fluctuations. These can be combined and modeled as the familiar first order exponentially time correlated random variable. The bias is considered to be fixed but unknown and can therefore be modeled as a random bias.

#### Measurement of Range Rate

The experiments performed with this model have shown that the measurement of range rate is usually redundant since range measurements made at a high frequency will yield the same information. The possibility

of a range rate measurement is therefore not investigated.

Summary of System Truth Model State and Measurement Equations

The above state and measurement equations for the system truth model are summarized as follows:

State Equations

$$(1) \dot{X}_1 = X_4$$

$$(2) \dot{X}_2 = X_5 \quad \text{Satellite Inertial Position}$$

$$(3) \dot{X}_3 = X_6$$

$$(4) \dot{X}_4 = A_{g1} + A_{d1} + A_{s1} + A_{m1} + A_{p1} + W_1$$

$$(5) \dot{X}_5 = A_{g2} + A_{d2} + A_{s2} + A_{m2} + A_{p2} + W_2 \quad \text{Satellite Inertial Velocity}$$

$$(6) \dot{X}_6 = A_{g3} + A_{d3} + A_{s3} + A_{m3} + A_{p3} + W_3$$

$$(7) \dot{X}_7 = 0 \quad \text{Satellite Ballistic Coefficient}$$

$$(8) \dot{X}_8 = 0 \quad \text{Satellite Solar Pressure Coefficient}$$

$$(9) \dot{\omega}_{LSY} = -\frac{1}{R} A_{rZ} - \frac{2 V_r}{R} \omega_{LSY} + \omega_{LSZ} \omega_{TX}$$

$$+ \left\{ \frac{-\delta\epsilon A_{rX}}{R} + \omega_{LSZ} \left[ \delta\eta \omega_{TY} - \delta\epsilon \omega_{TZ} \right] \right\} \quad \text{Tracker Angular Velocity}$$

$$(10) \quad \dot{\omega}_{LSZ} = \frac{1}{R} A_{rY} - \frac{2 V_r}{R} \omega_{LSZ} - \omega_{LSY} \omega_{rX} \\ + \left\{ \frac{-\delta\eta A_{rX}}{R} - \omega_{LSY} \left[ \delta\eta \omega_{rY} - \delta\epsilon \omega_{rZ} \right] \right\} \quad \text{Tracker Angular Velocity}$$

$$(11) \quad \dot{\delta\eta} = \omega_{LSZ} - \omega_{rZ} - \delta\epsilon \omega_{rX} \\ (12) \quad \dot{\delta\epsilon} = \omega_{LSY} - \omega_{rY} + \delta\eta \omega_{rX} \quad \left. \vphantom{\begin{matrix} (11) \\ (12) \end{matrix}} \right\} \text{Tracker Misalignments}$$

$$(13) \quad \dot{R} = V_r \quad \text{Range}$$

$$(14) \quad \dot{V}_r = A_{rX} + R (\omega_{LSY}^2 + \omega_{LSZ}^2) + \delta\eta A_{rY} - \delta\epsilon A_{rZ} \quad \text{Range Rate}$$

$$(15) \quad \dot{S}_\epsilon = -\beta_1 S_\epsilon + \sqrt{2 \beta_1} \sigma_1 U_1 \\ (16) \quad \dot{S}_\eta = -\beta_2 S_\eta + \sqrt{2 \beta_2} \sigma_2 U_2 \quad \left. \vphantom{\begin{matrix} (15) \\ (16) \end{matrix}} \right\} \text{Angle Track Scintillations}$$

$$(17) \quad \dot{S}_R = -\beta_3 S_R + \sqrt{2 \beta_3} \sigma_3 U_3 \quad \text{Range Scintillation}$$

$$(18) \quad \dot{C}_{GX} = -\beta_4 C_{GX} + \sqrt{2 \beta_4} \sigma_4 U_4 \\ (19) \quad \dot{C}_{GY} = -\beta_5 C_{GY} + \sqrt{2 \beta_5} \sigma_5 U_5 \\ (20) \quad \dot{C}_{GZ} = -\beta_6 C_{GZ} + \sqrt{2 \beta_6} \sigma_6 U_6 \quad \left. \vphantom{\begin{matrix} (18) \\ (19) \\ (20) \end{matrix}} \right\} \text{Gyro Drift}$$

$$(21) \quad \dot{C}_{aX} = -\beta_7 C_{aX} + \sqrt{2 \beta_7} \sigma_7 U_7 \quad \left. \vphantom{\begin{matrix} (21) \\ (22) \\ (23) \end{matrix}} \right\} \text{Accelerometer Drift}$$

$$(22) \quad \dot{C}_{aY} = -\beta_8 C_{aY} + \sqrt{2 \beta_8} \sigma_8 U_8$$

$$(23) \quad \dot{C}_{aZ} = -\beta_9 C_{aZ} + \sqrt{2 \beta_9} \sigma_9 U_9$$

$$(24) \quad \dot{C}_{SF_\epsilon} = -\beta_{10} C_{SF_\epsilon} + \sqrt{2 \beta_{10}} \sigma_{10} U_{10}$$

$$(25) \quad \dot{C}_{SF_\eta} = -\beta_{11} C_{SF_\eta} + \sqrt{2 \beta_{11}} \sigma_{11} U_{11} \quad \left. \vphantom{\begin{matrix} (24) \\ (25) \end{matrix}} \right\} \text{Angle Measurement Scale Factors}$$

$$(26) \quad \dot{B}_{gmX_1} = 0$$

$$(34) \quad \dot{B}_{gmZ_3} = 0$$

Coefficients of Gyro Mass Unbalance  
(nine equations)

$$(35) \quad \dot{B}_{ASX} = 0$$

$$(36) \quad \dot{B}_{ASY} = 0$$

$$(37) \quad \dot{B}_{ASZ} = 0$$

Accelerometer Scale Factors

$$(38) \quad \dot{B}_{gma_{12}} = 0$$

$$(39) \quad \dot{B}_{gma_{13}} = 0$$

$$(40) \quad \dot{B}_{gma_{21}} = 0$$

$$(41) \quad \dot{B}_{gma_{23}} = 0$$

$$(42) \quad \dot{B}_{gma_{31}} = 0$$

$$(43) \quad \dot{B}_{gma_{32}} = 0$$

Gyro Misalignment Coefficients

$$(44) \quad \dot{B}_{ama_{12}} = 0$$

$$(45) \quad \dot{B}_{ama_{13}} = 0$$

$$(46) \quad \dot{B}_{ama_{21}} = 0$$

$$(47) \quad \dot{B}_{ama_{23}} = 0$$

$$(48) \quad \dot{B}_{ama_{31}} = 0$$

$$(49) \quad \dot{B}_{ama_{32}} = 0$$

Accelerometer Misalignment Coefficients

$$\begin{array}{rcl}
 (50) & \dot{B}_{\text{non}X_1} = 0 & \left. \vphantom{\dot{B}_{\text{non}X_1}} \right\} \\
 (51) & \dot{B}_{\text{non}X_2} = 0 & \left. \vphantom{\dot{B}_{\text{non}X_2}} \right\} \\
 (52) & \dot{B}_{\text{non}Y_1} = 0 & \left. \vphantom{\dot{B}_{\text{non}Y_1}} \right\} \\
 (53) & \dot{B}_{\text{non}Y_2} = 0 & \left. \vphantom{\dot{B}_{\text{non}Y_2}} \right\} \\
 (54) & \dot{B}_{\text{non}Z_1} = 0 & \left. \vphantom{\dot{B}_{\text{non}Z_1}} \right\} \\
 (55) & \dot{B}_{\text{non}Z_2} = 0 & \left. \vphantom{\dot{B}_{\text{non}Z_2}} \right\} \\
 (56) & \dot{B}_R = 0 & \text{Range Bias} \\
 (57) & \dot{B}_{\text{AT}_\varepsilon} = 0 & \left. \vphantom{\dot{B}_{\text{AT}_\varepsilon}} \right\} \\
 (58) & \dot{B}_{\text{AT}_\eta} = 0 & \left. \vphantom{\dot{B}_{\text{AT}_\eta}} \right\} \\
 (59) & \dot{B}_{\text{gsf}_X} = 0 & \left. \vphantom{\dot{B}_{\text{gsf}_X}} \right\} \\
 (60) & \dot{B}_{\text{gsf}_Y} = 0 & \left. \vphantom{\dot{B}_{\text{gsf}_Y}} \right\} \\
 (61) & \dot{B}_{\text{gsf}_Z} = 0 & \left. \vphantom{\dot{B}_{\text{gsf}_Z}} \right\} \\
 & & \text{Accelerometer (g}^2 \text{ and g}^3\text{) non-linear} \\
 & & \text{coefficients} \\
 & & \text{Angle Track Bias} \\
 & & \text{Gyro Scale Factors}
 \end{array}$$

The truth model therefore has a total of 61 state equations. Of these, the first 14 represent the true system dynamics while the remaining 47 equations are introduced to model the measurements to the System.

Measurement Equations

$$(1) \quad \omega_{M_X} = \omega_{T_X} + B_{gsf_X} \omega_{T_X} + \sum_{i=1}^3 B_{gm_{X_i}} A_i + C_{g_X}$$

$$+ \left[ \Delta C_{gma} \frac{\omega_T}{\cdot} \right]_X + V_1 \quad \text{measurement of } \omega_{T_X}$$

$$(2) \quad \omega_{M_Y} = \omega_{T_Y} + B_{gsf_Y} \omega_{T_Y} + \sum_{i=1}^3 B_{gm_{Y_i}} A_i + C_{g_Y}$$

$$+ \left[ \Delta C_{gma} \frac{\omega_T}{\cdot} \right]_Y + V_2 \quad \text{measurement of } \omega_{T_Y}$$

$$(3) \quad \omega_{M_Z} = \omega_{T_Z} + B_{gsf_Z} \omega_{T_Z} + \sum_{i=1}^3 B_{gm_{Z_i}} A_i + C_{g_Z}$$

$$+ \left[ \Delta C_{gma} \frac{\omega_T}{\cdot} \right]_Z + V_3 \quad \text{measurement of } \omega_{T_Z}$$

where

$$\Delta C_{gma} \triangleq \begin{bmatrix} 0 & B_{gma_{12}} & B_{gma_{13}} \\ B_{gma_{21}} & 0 & B_{gma_{23}} \\ B_{gma_{31}} & B_{gma_{32}} & 0 \end{bmatrix}$$

and

$$A_1 \triangleq A_{T_X}$$

$$A_2 \triangleq A_{T_Y}$$

$$A_3 \triangleq A_{T_Z}$$

acceleration of tracker origin  
in tracker coordinates

$$(4) \quad A_{T_{XM}} = A_{T_X} + B_{asX} A_{T_X} + C_{aX} + B_{nonX_1} A_{T_X}^2 + B_{nonX_2} A_{T_X}^3$$

$$+ \left[ \Delta C_{ma} \frac{A_T}{\underline{T}} \right]_X + v_4 \quad \text{Measurement of } A_{T_X}$$

$$(5) \quad A_{T_{YM}} = A_{T_Y} + B_{asY} A_{T_Y} + C_{aY} + B_{nonY_1} A_{T_Y}^2 + B_{nonY} A_{T_Y}^3$$

$$+ \left[ \Delta C_{ma} \frac{A_T}{\underline{T}} \right]_Y + v_5 \quad \text{Measurement of } A_{T_Y}$$

$$(6) \quad A_{T_{ZM}} = A_{T_Z} + B_{asZ} A_{T_Z} + C_{aZ} + B_{nonZ_1} A_{T_Z}^2 + B_{nonZ_2} A_{T_Z}^3$$

$$+ \left[ \Delta C_{ma} \frac{A_T}{\underline{T}} \right]_Z + v_6 \quad \text{Measurement of } A_{T_Z}$$

where  $\Delta C_{ma} = \begin{bmatrix} 0 & B_{ama12} & B_{ama13} \\ B_{ama21} & 0 & B_{ama23} \\ B_{ama31} & B_{ama32} & 0 \end{bmatrix}$

$$(7) \quad \delta \epsilon_M = K_1 (\delta \epsilon + S_\epsilon) + C_{SF_\epsilon} \delta \epsilon + B_{AT_\epsilon} + v_7$$

Measurement of  $\delta \epsilon$

$$(8) \quad \delta \eta_M = K_2 (\delta \eta + S_\eta) + C_{SF_\eta} \delta \eta + B_{AT_\eta} + v_8$$

Measurement of  $\delta \eta$

$$(9) \quad R_M = K_R(R + S_R) + B_R + V_g \quad \text{Measurement of } R$$

Appendix D lists a typical data set for use with the above measurement equations.

#### Use of Measurements

The above measurement equations are the total measurements available to the system. However, only equations (2), (3), (7), (8), and (9) correspond to measurements of the states of the system. The remaining equations are measurements of system parameters. Thus the true system measurement vector has only the above 5 elements. There are two ways in which the other measurements can be incorporated into the system. One method would be to consider the true system measurement vector to contain all 9 elements and the other method would be to rewrite the state equations and substitute the measured value of a parameter for the true value. The latter method limits the number of measurement equations to 5 which is desirable. In addition, since the true parameter values will not be known and the best information about these parameters is contained in the measurements, the latter method would be implemented in practice. For this problem therefore, the measured parameter values replace the true values in the state equations and the number of measurement equations will actually be 5.

#### Linearization of State and Measurement Equations

Appendix B shows how the state and measurement equations for the truth model are linearized for application to a covariance analysis of an Extended Kalman Filter.

## III. EXTENDED KALMAN FILTER

Basic Kalman Filter (Ref. 12)

To understand the Extended Kalman Filter formulation used in the study, it is first necessary to examine the equations for the Basic Kalman Filter. For this study, the state equations of motion are continuous in time. Computationally, the equations are discretized but choice of an integration interval short compared to the system time behaviour ensures that the system is effectively continuous. Measurements are incorporated at discrete points in time. Thus the continuous form of the Kalman Filter with discrete measurement updates is appropriate. The following definitions will be required:

$$\underline{x}(t_i) = \text{system state at time } t_i - (\text{n vector})$$

$$\underline{\hat{x}}(t) = \text{filter estimate of the system state at time } t - (\text{n vector})$$

$$\underline{\hat{x}}(t_i^-) = \text{filter estimate of the system state at time } t_i \text{ before a measurement is incorporated} - (\text{n vector})$$

$$\underline{\hat{x}}(t_i^+) = \text{filter estimate of system state at time } t_i \text{ after a measurement is incorporated} - (\text{n vector})$$

$$\Phi(t_i, t_{i-1}) = \text{system state transition matrix from time } t_{i-1} \text{ to time } t_i - (\text{n x n matrix})$$

$$P(t_i) = \text{covariance matrix of the filter state estimate } \underline{\hat{x}}(t_i) - \text{note that the '-' and '+' convention is used here also} - (\text{n x n matrix})$$

$K(t_i)$  = Kalman gain matrix at time  $t_i$  - (n matrix)

$F(t)$  = systems dynamics matrix defined at all  $t$  -  
(n x n matrix)

$G(t)$  = system noise input matrix defined at all time  $t$  -  
(n x s matrix)

$H(t_i)$  = measurement matrix defined only at time  $t_i$  -  
(m x n matrix)

$\underline{w}(t)$  = Gaussian white noise vector with statistics

$$E \{ \underline{w}(t) \} = 0 \quad (\text{s vector})$$

$$E \{ \underline{w}(t) \underline{w}^T(s) \} = Q(t) \delta(t - s)$$

$Q(t)$  = positive semi-definite symmetric noise covariance matrix - (s x s matrix)

$\underline{v}(t_i)$  = Gaussian white noise vector sequence with statistics  
(m - vector)

$$E \{ \underline{v}(t_i) \} = 0$$

$$E \{ \underline{v}(t_i) \underline{v}^T(t_j) \} = \begin{cases} R(t_i) & t_i = t_j \\ 0 & t_i \neq t_j \end{cases}$$

$R(t_i)$  = positive definite symmetric noise covariance matrix -  
(m x m matrix)

$\underline{z}(t_i)$  = measurement vector at time  $t_i$  - (m vector)

#### System Description

The system is described by the following state equation:

$$\dot{\underline{x}}(t) = F(t)\underline{x}(t) + G(t)\underline{w}(t) \quad (3-1)$$

and measurement equation:

$$\underline{z}(t_i) = H(t_i)\underline{x}(t_i) + \underline{v}(t_i) \quad (3-2)$$

### Filter Equations

The filter state estimate  $\hat{\underline{x}}(t)$  is propagated from time  $t_{i-1}^+$  to time  $t_i^-$  by the equation:

$$\hat{\underline{x}}(t_i^-) = \Phi(t_i, t_{i-1}) \hat{\underline{x}}(t_{i-1}^+) \quad (3-3)$$

and the covariance propagation is given by:

$$P(t_i^-) = \Phi(t_i, t_{i-1}) P(t_{i-1}^+) \Phi^T(t_i, t_{i-1}) + \int_{t_{i-1}}^{t_i} \Phi(t_i, \tau) G(\tau) Q(\tau) G^T(\tau) \Phi^T(t_i, \tau) d\tau \quad (3-4)$$

The Kalman gain matrix at time  $t_i$  is given by:

$$K(t_i) = P(t_i^-) H^T(t_i) \left[ H(t_i) P(t_i^-) H^T(t_i) + R(t_i) \right]^{-1} \quad (3-5)$$

and at time  $t_i$ , the state estimate is updated by the equation:

$$\hat{\underline{x}}(t_i^+) = \hat{\underline{x}}(t_i^-) + K(t_i) \left[ \underline{z}(t_i) - H(t_i) \hat{\underline{x}}(t_i^-) \right] \quad (3-6)$$

where  $\underline{z}(t_i)$  is the vector of measured values which  $\underline{z}(t_i)$  assumes at time  $t_i$ . The covariance matrix is updated at time  $t_i$  by the equation:

$$P(t_i^+) = P(t_i^-) - K(t_i) H(t_i) P(t_i^-) \quad (3-7)$$

Equations (3-3) and (3-4) are thus the propagation equations for the state estimate and covariance respectively and equations (3-6) and (3-7) are the update equations for state estimate and covariance respectively. Initial conditions for the propagation are:

$$\begin{aligned}\hat{\underline{x}}(t_0) &= E \left\{ \underline{x}(t_0) \right\} \\ P(t_0) &= E \left\{ \left[ \underline{x}(t_0) - \hat{\underline{x}}(t_0) \right] \left[ \underline{x}(t_0) - \hat{\underline{x}}(t_0) \right]^T \right\} \quad (3-8)\end{aligned}$$

#### Extended Kalman Filter Formulation (Ref. 13)

The Extended Kalman Filter is one method of propagating the 'optimal' estimate of the state of a non linear system. In the above linear formulation, the filter estimate was indeed optimal since the equations of motion and measurement equations were totally linear and the basic Kalman Filter provides the optimal or best possible estimate for a linear system driven by white Gaussian noise. The Extended Kalman Filter uses a first order linearization process and hence, the estimate will only be optimal providing deviations from a nominal trajectory remain arbitrarily small.

Consider the non-linear state and measurement equations:

$$\begin{aligned}\dot{\underline{x}}(t) &= \underline{f} \left[ \underline{x}(t), t \right] + G(t) \underline{w}(t) \\ \underline{z}(t_i) &= \underline{h} \left[ \underline{x}(t_i), t_i \right] + \underline{v}(t_i)\end{aligned} \quad (3-9)$$

where once again,  $\underline{w}(t)$  and  $\underline{v}(t_i)$  are as described for the linear formulation with noise covariance matrices  $Q(t)$  and  $R(t_i)$  respectively, but in this case, the system dynamics is non-linear and expressed by the non linear function  $\underline{f}( , )$  and the measurement is a non linear function of the state  $\underline{x}(t)$  and described by the non linear function  $\underline{h}( , )$ . Note however that the driving noise  $\underline{w}(t)$  is still additive in a linear fashion

respect to the state  $\underline{x}$  and which is evaluated along the nominal reference trajectory, i.e.

$$F \left[ t; \underline{x}_{no} \right] \triangleq \left. \frac{\partial \underline{f} \left[ \underline{x}(t), t \right]}{\partial \underline{x}} \right|_{\underline{x}(t) = \underline{x}_n(t)} \quad (3-15)$$

Equation (3-14) represents the first order approximation to equation (3-13) and propagates from the initial condition  $\underline{\delta x}(t_0)$  which is modeled as a Gaussian random variable with mean  $(\hat{x}_0 - x_{no})$  and covariance  $P_0$ . The notation  $F \left[ t; \underline{x}_{no} \right]$  implies that  $F$  is a function of time and that  $F$  is evaluated along the nominal trajectory, which is a function of  $\underline{x}_{no}$ .

Similarly, the measurement equation can be approximated to first order by the equation

$$\underline{\delta z}(t_i) = H \left[ t_i; \underline{x}_n(t_i) \right] \underline{\delta x}(t_i) + \underline{v}(t_i) \quad (3-16)$$

where:

$$H \left[ t_i; \underline{x}_n(t_i) \right] = \left. \frac{\partial \underline{h} \left[ \underline{x}(t_i), t_i \right]}{\partial \underline{x}} \right|_{\underline{x}(t_i) = \underline{x}_n(t_i)} \quad (3-17)$$

and the notation  $H \left[ t_i, \underline{x}_n(t_i) \right]$  is used to imply that  $H$  is a function of the sequence of times  $t_i$  and is evaluated along the sequence  $\underline{x}_n(t_i)$ .

Equations (3-14) and (3-16) thus represent the linearized variational equations for the system and therefore the theory of linear filtering could be applied. In fact if the variations  $\underline{\delta x}(t)$  and  $\underline{\delta z}(t_i)$  remain sufficiently small, which in turn implies that the true and nominal state trajectories deviate by 'sufficiently' small quantities, then the results of the application of linear filtering theory should be optimal. The word 'sufficient' is of course relative and even small deviations could result in large magnitude errors.

The object of the Extended Kalman Filter is to obtain the state

through the matrix  $G(t)$  and the measurement noise is also additive. The Extended Kalman Filter formulation assumes that the noises are white, Gaussian and additive in the same way as the basic Kalman Filter, although the system dynamics and measurements may be non linear.

Assume some nominal reference trajectory is available, denoted as  $\underline{x}_n(t)$ , which is propagated from the initial condition  $\underline{x}_n(t_0) = \underline{x}_{n0}$  by the equation:

$$\dot{\underline{x}}_n(t) = \underline{f}[\underline{x}_n(t), t] \quad (3-10)$$

and assume also that associated with this nominal reference trajectory is the sequence of nominal measurements:

$$\underline{z}_n(t_i) = \underline{h}[\underline{x}_n(t_i), t_i] \quad (3-11)$$

and consider the perturbation of the state from the assumed nominal reference trajectory such that:

$$\underline{\delta x}(t) \triangleq \underline{x}(t) - \underline{x}_n(t) \quad (3-12)$$

The error is a stochastic process which satisfies the stochastic differential equation:

$$\dot{\underline{\delta x}}(t) = \underline{f}[\underline{x}(t), t] - \underline{f}[\underline{x}_n(t), t] + G(t) \underline{w}(t) \quad (3-13)$$

The first order approximation to this equation usually referred to as the variational equation is:

$$\dot{\underline{\delta x}}(t) = F[t; \underline{x}_{n0}] \underline{\delta x}(t) + G(t) \underline{w}(t) \quad (3-14)$$

where  $F[t; \underline{x}_{n0}]$  is the matrix of partial derivatives of  $\underline{f}(\cdot, \cdot)$  with

estimate  $\hat{\underline{x}}(t_i^+)$  and then relinearize about this estimate. Thus as soon as a new state estimate is made, a better reference trajectory is incorporated into the system. In this manner, the assumption that the deviations from the reference are small remains valid providing the time between estimates is kept small. Now, if the system is relinearized after  $\hat{\underline{x}}(t_i^+)$  is obtained, then the error state  $\underline{\delta\hat{x}}(t_i^+)$  will be zero. Recalling equation (3-3), rewritten here in terms of the error state:

$$\underline{\delta\hat{x}}(t_{i+1}^-) = \phi(t_{i+1}, t_i; \hat{\underline{x}}(t_i^+)) \underline{\delta\hat{x}}(t_i^+) \quad (3-18)$$

where the notation is meant to convey that  $\phi$  is a function of  $\hat{\underline{x}}(t_i^+)$  in addition to  $t_{i+1}$  and  $t_i$ . It is apparent that if  $\underline{\delta\hat{x}}(t_i^+)$  is zero, then  $\underline{\delta\hat{x}}(t_{i+1}^-)$  will also be zero since equation (3-18) is linear. In fact, using the notation  $\underline{\delta\hat{x}}(t/t_i)$  to indicate that the estimate of  $\underline{\delta\hat{x}}$  at time  $t \geq t_i$  is based only on measurements through time  $t_i$ , then  $\underline{\delta\hat{x}}(t/t_i)$  will remain zero throughout the interval  $[t_i, t_{i+1}]$ .

Now, considering the measurement update for the linearized system at the next measurement sample time.

$$\begin{aligned} \underline{\delta\hat{x}}(t_{i+1}^+) &= \underline{\delta\hat{x}}(t_{i+1}^-) + K(t_{i+1}) \underline{\delta z}(t_{i+1}) - H(t_{i+1}) \underline{\delta\hat{x}}(t_{i+1}^-) \\ &= K(t_{i+1}) \underline{\delta z}(t_{i+1}) \\ &= K(t_{i+1}) \underline{z}(t_{i+1}) - \underline{h} \hat{\underline{x}}(t_{i+1}/t_i), t_{i+1} \quad (3-19) \end{aligned}$$

where  $K(t_{i+1})$  is computed using matrices evaluated along the most recent nominal trajectory  $\hat{\underline{x}}(t/t_i)$ . So far, the state deviation has been estimated between measurement instants as zero and at the measurement update point as given by equation (3-19). The full state estimate

$\hat{\underline{x}}(t/t_i)$  between measurement instants  $t_i$  and  $t_i + 1$  must therefore be given by the solution to the equation:

$$\dot{\hat{\underline{x}}}(t/t_i) = \underline{f} \left[ \hat{\underline{x}}(t/t_i), t \right] \quad (3-20)$$

Since the deviation is zero throughout this interval. At the measurement update time  $t_i + 1$ , the state is given by:

$$\begin{aligned} \hat{\underline{x}}(t_i + 1^+) &= \hat{\underline{x}}(t_i + 1/t_i) + \delta \hat{\underline{x}}(t_i + 1^+) \\ &= \hat{\underline{x}}(t_i + 1/t_i) + K(t_i + 1) \left[ \underline{z}(t_i + 1) \right. \\ &\quad \left. - \underline{h} \left[ \hat{\underline{x}}(t_i + 1/t_i), t_i + 1 \right] \right] \end{aligned} \quad (3-21)$$

which is the state estimate update equation for the Extended Kalman Filter.

#### Summary of Propagation and Update Equations

The equations for the Extended Kalman Filter are summarized as follows:

Propagation: The state estimate and covariance are propagated as:

$$\hat{\underline{x}}(t_i + 1^-) = \hat{\underline{x}}(t_i^+) + \int_{t_i}^{t_i + 1} \underline{f} \left[ \hat{\underline{x}}(t/t_i), t \right] dt$$

or equivalently by integrating:  $\dot{\hat{\underline{x}}}(t/t_i) = \underline{f} \left[ \hat{\underline{x}}(t/t_i), t \right]$  from  $t_i$  to  $t_i + 1$  using the initial condition;  $\hat{\underline{x}}(t_i/t_i) = \hat{\underline{x}}(t_i^+)$

$$\begin{aligned} P(t_i + 1^-) &= \phi(t_i + 1, t_i; \hat{\underline{x}}(t_i^+)) P(t_i^+) \phi^T(t_i + 1, t_i; \hat{\underline{x}}(t_i^+)) \\ &+ \int_{t_i}^{t_i + 1} \phi(t_i + 1, \tau; \hat{\underline{x}}(t_i^+)) G(\tau) Q(\tau) G^T(\tau) \phi^T(t_i + 1, \tau; \hat{\underline{x}}(t_i^+)) d\tau \end{aligned}$$

which is equivalent to integrating

$$\begin{aligned} \dot{P}(t/t_i) &= F \left[ t; \hat{x}(t_i^+) \right] P(t/t_i) + P(t/t_i) F^T \left[ t; \hat{x}(t_i^+) \right] \\ &\quad + G(t) Q(t) G^T(t) \end{aligned}$$

from time  $t_i$  to  $t_i + 1$  using the initial condition:

$$P(t_i/t_i) = P(t_i^+)$$

#### Measurement Update

The state estimate and covariance are updated as follows. Define:

$$\begin{aligned} K(t_i; \hat{x}(t_i - 1^+)) &= \\ P(t_i^-) H^T(t_i; \hat{x}(t_i - 1^+)) &\left[ H(t_i; \hat{x}(t_i - 1^+)) P(t_i^-) H^T(t_i; \hat{x}(t_i - 1^+)) \right. \\ &\quad \left. + R(t_i) \right]^{-1} \end{aligned}$$

$$\hat{x}(t_i^+) = \hat{x}(t_i^-) + K(t_i; \hat{x}(t_i - 1^+)) \left[ z(t_i) - h(\hat{x}(t_i^-), t_i) \right]$$

$$P(t_i^+) = P(t_i^-) - K(t_i; \hat{x}(t_i - 1^+)) H(t_i; \hat{x}(t_i - 1^+)) P(t_i^-)$$

#### Comparison with Basic Kalman Filter

The above equations are essentially similar to equations (3-3), (3-4), and (3-6), (3-7) for the basic Kalman Filter. However, the gain matrix  $K$  for the basic Kalman Filter can be precomputed since it does not depend on the current filter estimate at any time. This is not the case for the Extended Kalman Filter in which the matrices  $F$ ,  $H$  (and  $G$ ) are functions of the current filter estimate and consequently

K is a function of that estimate also. Similarly, the transition matrix varies as a function of  $\hat{\underline{x}}$  and thus P is a function of the estimate  $\hat{\underline{x}}$  during propagation. This therefore is one major difference between the basic and Extended Kalman Filter formulations. The equations for the propagation and update of the covariance matrix P are coupled to the state estimate  $\hat{\underline{x}}$ .

#### Application to Tracking Problem

The purpose of this study is to examine the performance of a reduced order filter model of the system. This involves carrying out a covariance analysis which will be described in the next section. The covariance as a function of time will describe the filter and truth model performance and there will not be any requirement to propagate the actual filter estimate  $\hat{\underline{x}}$ . However, the matrices F and H which result from linearization of a non linear functions  $f(, )$  and  $h(, )$  respectively must be linearized about some non-linear reference trajectory. For this reason, the non-linear state equations of motion are in fact propagated. Thus, the true filter would use the matrix  $F [t; \hat{\underline{x}}(t_i - 1^+)]$  to propagate from  $t_i - 1$  to  $t_i$  where  $\hat{\underline{x}}(t_i - 1^+)$  is the initial condition for the trajectory segment, up to measurement time  $t_i$ , along which F is evaluated. Similarly, the matrix  $H [t_i; \hat{\underline{x}}(t_i - 1^+)]$  would be used for the true filter to update the P matrix at time  $t_i$ . For this analysis however, the matrices  $F [t; \underline{x}_n(t_i - 1)]$  and  $H [t_i; \underline{x}_n(t_i)]$  are used. The reason for this is that  $\hat{\underline{x}}(t)$  is not available in the covariance analysis, and to obtain  $\hat{\underline{x}}(t)$  with one run would not suffice. In fact, Monte Carlo techniques would be required to find the RMS performance of the filter if  $\hat{\underline{x}}(t)$  were used. In this case, the benefit of doing the covariance analysis would be lost.

Thus, evaluation of matrices F and H using  $\underline{x}_n(t)$  rather than  $\hat{\underline{x}}(t)$  is one fundamental limitation to the covariance analysis but necessarily this limitation must be accepted and it should be recalled that the covariance analysis is the first step towards a full Monte Carlo analysis.

## IV. COVARIANCE ANALYSIS OF SUBOPTIMAL FILTER DESIGN

Objective

Section II developed the true system state and measurement models for the aircraft to satellite tracker. In fact, to use the expression 'truth model' to describe these equations is incorrect. There is no way of predicting exactly what the precise true system performance will be. However, the equations were developed taking into account all reasonable system disturbances and thus represent the best approximation to the 'truth model'. The resulting model has 61 states and would therefore be impractical to implement on board an aircraft where computational speed and storage capabilities will be limited. A search will thus be conducted to find a reduced order model which will adequately model the true system. This will involve making simplifying assumptions and will result in a sub-optimal design. The Extended Kalman Filter design will be based on this sub-optimal model and its performance will in turn be sub-optimal. Under these circumstances, a study must be undertaken to evaluate the suboptimal filter estimation error performance and the sensitivity of these errors to incorrect or incomplete dynamic or statistical modeling. This study is commonly referred to as a sensitivity analysis.

The Equations for Sensitivity Analysis (Ref. 2 and 14)

The following will develop the equations for the sensitivity analysis of the sub-optimal filter design. In practice, the filter estimates resulting from using the Extended Kalman Filter with a reduced order system model would be used to provide some closed loop control to the system. However, in order to simplify the development, the effect of such control inputs will be ignored. Reference 2 shows how the equations

are extended to include control inputs.

Truth Model The truth model equations representing the most detailed model of the real world were developed in section II and are written below using slightly different notation:

$$\dot{\underline{x}}_S(t) = F_S(t) \underline{x}_S(t) + G_S(t) \underline{w}_S(t) \quad (4-1)$$

where

$\underline{x}_S$  is an  $n_1$  - vector denoting the true state

$F_S$  is an  $n_1 \times n_1$  system matrix

$G_S$  is an  $n_1 \times m_1$  gain matrix

$\underline{w}_S$  is an  $m_1$  vector of white Gaussian noise inputs with zero mean and variance  $E \left\{ \underline{w}_S(t) \underline{w}_S^T(\tau) \right\} = Q_S(t) \delta(t - \tau)$

Note that equation (4-1) is in fact linear whereas the truth model equations are not. Equation (4-1) could be considered to represent the error state system model described by equation (3-14) section III. Since this is a linear equation, the Kalman Filter theory can be applied providing that perturbations from an assumed trajectory are small so that linear effects dominate.

Similarly, the sensitivity analysis to be described here assumes linear equations and could therefore be applied to the linearized error state equations developed in section III within the region of small perturbations.

A set of discrete measurements are available at times  $t_i$  and can be

described by the equation:

$$\underline{z}_S(t_i) = H_S(t_i) \underline{x}_S(t_i) + \underline{v}_S(t_i) \quad (4-2)$$

which is analogous to equation (3-16) section III, and

$\underline{z}_S$  is an  $r$  - vector of measurements

$H_S$  is an  $r \times n$  measurement matrix

$\underline{v}_S$  is an  $r$  - vector of Gaussian white noise inputs with zero mean and variance  $E \left\{ \underline{v}_S(t_i) \underline{v}_S^T(t_j) \right\} = R_S(t_i) \delta_{i,j}$

#### Filter Model

The filter model is defined to be the reduced order model to which the Extended Kalman Filter will be applied. Again, this is assumed to be linear and thus the resultant sensitivity equations will be valid only in a region of small perturbations about the nominal trajectory.

$$\dot{\underline{x}}_F(t) = F_F(t) \underline{x}_F(t) + G_F(t) \underline{w}_F(t) \quad (4-3)$$

where:

$\underline{x}_F$  is an  $n_2$  - vector denoting the filter state ( $n_2 < n_1$ )

$F_F$  is an  $n_2 \times n_2$  system matrix

$G_F$  is an  $n_2 \times m_2$  gain matrix

$\underline{w}_F$  is an  $m_2$  vector of white Gaussian noise inputs with zero mean and covariance:  $E \left\{ \underline{w}_F(t) \underline{w}_F^T(\tau) \right\} = Q_F(t) \delta(t - \tau)$

The filter measurement equation is:

$$\underline{z}_F(t_i) = H_F(t_i) \underline{x}_F(t_i) + \underline{v}_F(t_i) \quad (4-4)$$

where

$\underline{z}_F$  is an  $r$  - vector of measurements

$H_F$  is an  $r \times n_2$  measurement matrix

$\underline{v}_F$  is an  $r$  - vector of white Gaussian noise inputs with zero mean and covariance  $E \left\{ \underline{v}_F(t_i) \underline{v}_F^T(t_j) \right\} = R_F(t_i) \delta_{i,j}$

Applying the basic Kalman filter equations to the above filter model, the filter estimate between measurements is given by:

$$\dot{\hat{\underline{x}}}_F(t) = F_F(t) \hat{\underline{x}}_F(t) \quad (4-5)$$

with associated covariance matrix satisfying the equation:

$$\dot{P}_F(t) = F_F(t) P_F(t) + P_F(t) F_F^T(t) + G_F(t) Q_F(t) G_F^T(t) \quad (4-6)$$

Defining  $t_i^-$  and  $t_i^+$  as before and after a measurement incorporation at time  $t_i$ , then at a measurement update,  $\hat{\underline{x}}_F(t)$  and  $P_F(t)$  are given by:

$$K_F(t_i) = P_F(t_i^-) H_F^T(t_i) \left[ H_F(t_i) P_F(t_i^-) H_F^T(t_i) + R_F(t_i) \right]^{-1}$$

$$\hat{\underline{x}}_F(t_i^+) = \hat{\underline{x}}_F(t_i^-) + K_F(t_i) \left[ \underline{z}_S(t_i) - H_F(t_i) \hat{\underline{x}}_F(t_i^-) \right] \quad (4-7)$$

$$P_F(t_i^+) = P_F(t_i^-) - K_F(t_i) H_F(t_i) P_F(t_i^-) \quad (4-8)$$

where :

$\hat{\underline{x}}_F(t)$  denotes the filter estimate of  $\underline{x}_F$

$P_F(t)$  denotes the covariance matrix associated with  $\hat{\underline{x}}_F(t)$

Note in equation (4-7) the use of the vector of measured values  $\underline{z}_S(t_1)$ , since the actual measurements will in fact be taken from the true system. Now, if the state vectors  $\underline{x}_F$  and  $\underline{x}_S$  are arranged such that:

$$\underline{x}_F = T^T \underline{x}_S \quad \text{and} \quad T \triangleq \begin{bmatrix} I (n_2 \times n_2) \\ 0 ((n_1 - n_2) \times n_2) \end{bmatrix} \quad (4-9)$$

then an error vector  $\underline{e}(t)$  can be defined such that:

$$\underline{e}(t) = \underline{x}_S(t) - T \hat{\underline{x}}_F(t) \quad (4-10)$$

Note that there is a loss of generality in this assumption, the filter model states would not in general be selected truth model states. Rather, the filter states would be linear combinations of the truth model states. However, in practice it is usual that the filter model is in fact the truth model with selected states removed. If this is not the case, then the T matrix could be defined differently without changing the final results.

The objective of the sensitivity analysis is to examine the propagation of the error vector  $\underline{e}(t)$  with time and the propagation of the covariance matrix of  $\underline{e}(t)$  defined as:

$$P_{ee}(t) = E \left\{ \underline{e}(t) \underline{e}^T(t) \right\}$$

Now,  $\underline{e}(t)$  is a vector expressing the error committed by using the particular filter model and  $P_{ee}(t)$  expresses the covariance of that error. The Kalman Filter covariance  $P_F$  is also a measure of the error in the estimate  $\hat{\underline{x}}_F$  but may not necessarily reflect true performance of

the filter. The sensitivity analysis therefore is a method of comparing the filter estimate  $\hat{\underline{x}}_F(t)$  with the true system state  $\underline{x}_S(t)$ , by propagating  $\underline{e}(t)$  and  $P_{ee}(t)$ , and thereby determining the true error obtained by using a particular filter formulation. The evaluation of  $P_{ee}$  and  $P_F$  is commonly referred to as a Covariance Analysis while the examination of  $\underline{e}(t)$  over an ensemble of runs is usually called a Monte Carlo analysis. In order to study the behaviour of  $\underline{e}(t)$ ,  $P_{ee}(t)$ , and  $P_F(t)$ , the augmented state vector  $\underline{y}(t)$  is formed such that:

$$\underline{y}(t) = \begin{bmatrix} \underline{e}(t) \\ \hat{\underline{x}}_F(t) \end{bmatrix} \quad (4-11)$$

where  $\underline{y}(t)$  is an  $n_1 + n_2$  dimensional vector.

The differential equation for this augmented state vector is therefore:

$$\dot{\underline{y}}(t) = \begin{bmatrix} \dot{\underline{e}}(t) \\ \dot{\hat{\underline{x}}}_F(t) \end{bmatrix} = \begin{bmatrix} F_S \underline{x}_S + G_S \underline{w}_S - T F_F \hat{\underline{x}}_F \\ F_F \hat{\underline{x}}_F \end{bmatrix} \quad (4-12)$$

where the time subscripts on the right side are dropped for clarity

Rewriting equation (4-12) gives:

$$\begin{aligned} \dot{\underline{y}}(t) &= \begin{bmatrix} F_S \underline{x}_S + G_S \underline{w}_S - T F_F \hat{\underline{x}}_F + F_S T \hat{\underline{x}}_F - F_S T \hat{\underline{x}}_F \\ F_F \hat{\underline{x}}_F \end{bmatrix} \\ &= \begin{bmatrix} F_S (\underline{x}_S - T \hat{\underline{x}}_F) + (F_S T - T F_F) \hat{\underline{x}}_F + G_S \underline{w}_S \\ F_F \hat{\underline{x}}_F \end{bmatrix} \end{aligned} \quad (4-13)$$

$$= \begin{bmatrix} F_S \underline{e} + (F_S T - T F_F) \hat{\underline{x}}_F + G_S \underline{w}_S \\ F_F \hat{\underline{x}}_F \end{bmatrix}$$

which can now be written in matrix form as:

$$\dot{\underline{y}}(t) = \begin{bmatrix} F_S & (F_S T - T F_F) \\ 0 & F_F \end{bmatrix} \underline{y}(t) + \begin{bmatrix} G_S \\ 0 \end{bmatrix} \underline{w}_S \quad (4-14)$$

or

$$\dot{\underline{y}}(t) = F \underline{y} + G \underline{w}$$

with F and G defined as in equation (4-14)

Between measurements, the covariance of  $\underline{y}(t)$  propagates according to the differential equation:

$$\dot{P} = F P + P F^T + G Q G^T$$

where  $Q = Q_S$  and F and G are defined above.

and

$$P(t) = \begin{bmatrix} P_{ee}(t) & P_{12}(t) \\ P_{21}(t) & P_{22}(t) \end{bmatrix}$$

and  $P_{22}(t)$  is equivalent to the matrix  $P_F(t)$  from the Kalman Filter equations (4-6) and (4-8).

At a measurement update,  $\hat{\underline{x}}_F$  will change according to equation (4-7), while  $\underline{x}_S$  will not change since control inputs are not considered.

i.e.:

$$\underline{x}_S^+ = \underline{x}_S^- \quad (4-15)$$

$$\hat{\underline{x}}_F^+ = \hat{\underline{x}}_F^- + K_F (\underline{z}_S - H_F \hat{\underline{x}}_F^-) \quad (4-16)$$

where the - and + signify before and after incorporation of a measurement respectively.

$$\rightarrow \hat{\underline{x}}_F^+ = \hat{\underline{x}}_F^- + K_F (H_S \underline{x}_S^- - H_F \hat{\underline{x}}_F^- + \underline{v}_S) \quad (4-17)$$

and since:

$$\begin{aligned} \underline{e}^+ &= \underline{x}_S^+ - T \hat{\underline{x}}_F^+ \\ &= \underline{x}_S^- - T \left[ \hat{\underline{x}}_F^- + K_F (H_S \underline{x}_S^- - H_F \hat{\underline{x}}_F^- + \underline{v}_S) \right] \\ &= \underline{x}_S^- - T \hat{\underline{x}}_F^- - T K_F H_S \underline{x}_S^- + T K_F H_F \hat{\underline{x}}_F^- - T K_F \underline{v}_S \\ &= (\underline{x}_S^- - T \hat{\underline{x}}_F^-) - T K_F H_S (\underline{x}_S^- - T \hat{\underline{x}}_F^-) \\ &\quad + T K_F (H_F - H_S T) \hat{\underline{x}}_F^- - T K_F \underline{v}_S \\ &= (I - T K_F H_S) \underline{e}^- + T K_F (H_F - H_S T) \hat{\underline{x}}_F^- - T K_F \underline{v}_S \end{aligned}$$

and from (4-17),

$$\begin{aligned} \hat{\underline{x}}_F^+ &= \hat{\underline{x}}_F^- + K_F H_S \underline{x}_S^- - K_F H_F \hat{\underline{x}}_F^- + K_F \underline{v}_S \\ \rightarrow \hat{\underline{x}}_F^+ &= \hat{\underline{x}}_F^- + K_F H_S \underline{x}_S^- - K_F H_S T \hat{\underline{x}}_F^- + K_F H_S T \hat{\underline{x}}_F^- \\ &\quad - K_F H_F \hat{\underline{x}}_F^- + K_F \underline{v}_S \\ &= K_F H_S (\underline{x}_S^- - T \hat{\underline{x}}_F^-) + (I + K_F H_S T - K_F H_F) \hat{\underline{x}}_F^- + K_F \underline{v}_S \end{aligned}$$

$$= K_F H_S \underline{e}^- + (I + K_F H_S T - K_F H_F) \hat{\underline{x}}_F^- + K_F \underline{v}_S$$

and thus the augmented state vector after incorporation of a measurement is given by:

$$\underline{y}^+ = \begin{bmatrix} \underline{e}^+ \\ \hat{\underline{x}}_F^+ \end{bmatrix} = \begin{bmatrix} I - T K_F H_S & T K_F (H_F - H_S T) \\ K_F H_S & I + K_F H_S T - K_F H_F \end{bmatrix} \begin{bmatrix} \underline{e}^- \\ \hat{\underline{x}}_F^- \end{bmatrix} + \begin{bmatrix} -T K_F \\ K_F \end{bmatrix} \underline{v}_S \quad (4-18)$$

or

$$\underline{y}^+ = A \underline{y}^- + B \underline{v}_S$$

where matrices A and B are as defined in equation (4-18).

The covariance matrix P(t) is updated by a measurement as follows:

$$\begin{aligned} P^+ &= E \left\{ \underline{y}^+ \underline{y}^{+T} \right\} = E \left\{ (A \underline{y}^- + B \underline{v}_S) (A \underline{y}^- + B \underline{v}_S)^T \right\} \\ + \quad P^+ &= E \left\{ (A \underline{y}^- + B \underline{v}_S) (\underline{y}^{-T} A^T + \underline{v}_S^T B^T) \right\} \\ &= E \left\{ A \underline{y}^- \underline{y}^{-T} A^T \right\} + E \left\{ B \underline{v}_S \underline{v}_S^T B^T \right\} \\ &\quad + E \left\{ A \underline{y}^- \underline{v}_S^T B^T \right\} + E \left\{ B \underline{v}_S \underline{y}^{-T} A^T \right\} \end{aligned}$$

$$\begin{aligned}
&= A E \left\{ \underline{y}^- \underline{y}^{-T} \right\} A^T + B E \left\{ \underline{v}_S \underline{y}^{-T} \right\} A^T + A E \left\{ \underline{y}^- \underline{v}_S^T \right\} B^T \\
&\quad + B E \left\{ \underline{v}_S \underline{v}_S^T \right\} B^T \quad (4-19)
\end{aligned}$$

Now, the noise vector is uncorrelated by hypothesis with the state  $\underline{x}_S$  and the state  $\underline{x}_F$  and therefore the transformation of  $\underline{x}_F$ ,  $T \underline{x}_F$ . Similarly, the estimate  $\underline{x}_F$  and  $\underline{v}_S$  are uncorrelated which implies that  $\underline{v}_S$  and  $\underline{y}$  are uncorrelated. Thus the second the third terms in equation (4-19) above are zero leaving:

$$P^+ = A P^- A^T + B R_S B^T \quad (4-20)$$

#### Summary of Propagation and Update Equations for Covariance Analysis

The equations for propagating and updating the covariance matrix  $P$  are summarized as follows:

Propagation:

$$\dot{P}(t) = F(t) P(t) + P(t) F^T(t) + G(t) Q_S(t) G^T(t)$$

where

$$P(t) \triangleq E \left\{ \underline{y}(t) \underline{y}^T(t) \right\}$$

$$\underline{y}(t) \triangleq \begin{bmatrix} \underline{e}^T(t) & \hat{\underline{x}}_F^T(t) \end{bmatrix}^T$$

$$\underline{e}(t) \triangleq (\underline{x}_S(t) - T \hat{\underline{x}}_F(t))$$

$$T \triangleq \begin{bmatrix} I & 0 \end{bmatrix}^T$$

$$F \triangleq \begin{bmatrix} F_S(t) & (F_S(t) T - T F_F(t)) \\ 0 & F_F(t) \end{bmatrix}$$

$$G(t) \stackrel{\Delta}{=} \begin{bmatrix} G_S(t) \\ 0 \end{bmatrix}$$

Update:

$$P^+(t) = A(t) P^-(t) A^T(t) + B(t) R_S(t) B^T(t)$$

where:

$$A(t) \stackrel{\Delta}{=} \begin{bmatrix} I - T K_F(t) H_S(t) & T K_F(t) (H_F(t) - H_S(t) T) \\ K_F(t) H_S(t) & I + K_F(t) H_S(t) T - K_F(t) H_F(t) \end{bmatrix}$$

$$B(t) \stackrel{\Delta}{=} \begin{bmatrix} -T K_F(t) \\ K_F(t) \end{bmatrix}$$

#### Application of Covariance Analysis to Extended Kalman Filter

The problem under study is non-linear and in section III it was shown that the equations could be linearized about some reference trajectory. Application of linear filtering theory to the linearized equations resulted in the Extended Kalman Filter. The above equations for propagation and update for the matrix  $P(t)$  are linear however and it is necessary to examine the method of implementation of these equations to a non-linear problem. The state equations for both truth and filter models must be linearized about the reference trajectory. The resulting linearized equations will be used in the above covariance analysis equations. The results of the analysis will therefore be

highly dependent on the assumption of linearity, and in order for these assumptions to remain valid, the interval between measurements must be made small compared to the system truth model time constants, and perturbations about the assumed nominal trajectory in the interval, must be small.

Finally, it should be noted that the trajectory linearization is carried out about  $\underline{x}_n(t)$ . In a practice, if linearization were required then  $\hat{\underline{x}}_F(t)$  would be used. However neither  $\underline{x}_n(t)$  nor  $\hat{\underline{x}}_F(t)$  will be identical to the true system state  $\underline{x}_T(t)$  which is never available and ideally linearization would always be carried out about  $\underline{x}_T(t)$ .

## V. INITIAL CHOICE OF FILTER MODEL

Objective

The development of the true system state and measurement equations in section II resulted in a 61 state truth model which used 5 measurements. The objective of this section will be to find a filter model by simplifying the truth model equations and thus reducing the model state dimension. The filter model will then be evaluated by the covariance analysis method described in section IV.

Filter Model State Equations

Examination of the truth model state equations summarized at the end of section II shows that the basic system dynamics is represented by the states 1 to 6 and 9 to 14. States 7 and 8 were introduced to model the uncertainty in drag and solar pressure perturbations respectively due to the vehicle size and shape. The remaining states 15 to 61 were introduced to model measuring device uncertainties in the measurements of angular tracking rates, tracker acceleration, range, and tracker angular deviations.

Simplification of Equations 1 to 6

Truth model state equations 1 to 6 describing the propagation in of the vehicle orbit are:

$$\dot{X}_1 = X_4 \quad (5-1)$$

$$\dot{X}_2 = X_5 \quad (5-2)$$

$$\dot{X}_3 = X_6 \quad (5-3)$$

$$\dot{X}_4 = Ag_1 + Ad_1 + As_1 + Am_1 + Ap_1 + W_1 \quad (5-4)$$

$$\dot{X}_5 = Ag_2 + Ad_2 + As_2 + Am_2 + Ap_2 + W_2 \quad (5-5)$$

$$\dot{X}_6 = Ag_3 + Ad_3 + As_3 + Am_3 + Ap_3 + W_3 \quad (5-6)$$

Consider the low orbit problem which is investigated in particular in this study. The basic orbital profile actually tested serves as an illustrative example. The vehicle considered is in a polar, circular orbit with an altitude above the earth's surface of approximately 200 km. For this orbit, consider a typical small vehicle with a ballistic coefficient of 0.015 m<sup>2</sup>/kg and a solar pressure coefficient equivalent to a vehicle with a projected surface towards the sun of approximately 10 m<sup>2</sup>. Under these conditions, the terms in equation (5-4) for example would have deterministic values of:

$$Ag_1 = -7.55 \text{ m/s}^2 - \text{Acceleration due to full gravity}$$

$$Ad_1 = -9.0 \times 10^{-9} \text{ m/s}^2 - \text{Drag perturbation}$$

$$As_1 = +2.0 \times 10^{-9} \text{ m/s}^2 - \text{Solar perturbation}$$

$$Am_1 = +5.0 \times 10^{-7} \text{ m/s}^2 - \text{Lunar perturbation}$$

$$Ap_1 = -2.0 \times 10^{-9} \text{ m/s}^2 - \text{Solar pressure perturbation}$$

where the sun and moon are positioned for worst case effects, and the vehicle is lying in the Greenwich meridian at a latitude of approximately 30°N. The white noise driving term  $W_1$  accounts for unmodeled effects such as deviations in atmospheric density from the model and unmodeled gravitational terms.  $W_1$  would typically be zero mean white

noise with a distribution standard deviation of approximately  $10^{-9} \text{ m/s}^2$ . The two-body point mass acceleration accounts for approximately  $-7.548 \text{ m/s}^2$  in  $A_{g_1}$ . The appropriate terms driving equations (5-5) and (5-6) have similar relative magnitudes.

The model proposed for the filter therefore assumes a two-body orbit and neglects drag, luni-solar perturbations and the polar pressure perturbation. For long orbital times, this would of course be a poor approximation, but a typical tracking pass with the assumed profile lasts for only 1/20th of the orbital period. The errors introduced by these approximations are accounted for by increasing the strength of  $W_1$  to give a distribution standard deviation of approximately  $2 \times 10^{-3} \text{ m/s}^2$ . The resulting state equations are:

$$\dot{X}_1 = X_4 \quad (5-7)$$

$$\dot{X}_2 = X_5 \quad (5-8)$$

$$\dot{X}_3 = X_6 \quad (5-9)$$

$$\dot{X}_4 = \frac{-\mu_{\oplus} X_1}{r_v^3} + W_1 \quad (5-10)$$

$$\dot{X}_5 = \frac{-\mu_{\oplus} X_2}{r_v^3} + W_2 \quad (5-11)$$

$$\dot{X}_6 = \frac{-\mu_{\oplus} X_3}{r_v^3} + W_3 \quad (5-12)$$

where  $\mu_{\oplus}$  is the earth gravitational constant and  $r_v$  is the distance from earth center to vehicle;

$$r_v = \sqrt{X_1^2 + X_2^2 + X_3^2}$$

Simplification of State Equations 9 and 10

The truth model state equations 9 and 10 are:

$$\begin{aligned} \dot{\omega}_{LSY} = & -\frac{1}{R} A_{rZ} - \frac{2 V_r}{R} \omega_{LSY} + \omega_{LSZ} \omega_{TX} \\ & + \left\{ -\frac{\delta\epsilon}{R} A_{rX} + \omega_{LSZ} \left[ \delta\eta \omega_{TY} - \delta\epsilon\omega_{TZ} \right] \right\} \end{aligned} \quad (5-13)$$

$$\begin{aligned} \dot{\omega}_{LSZ} = & \frac{1}{R} A_{rY} - \frac{2 V_r}{R} \omega_{LSZ} - \omega_{LSY} \omega_{TX} \\ & + \left\{ -\frac{\delta\eta}{R} A_{rX} - \omega_{LSY} \left[ \delta\eta \omega_{TY} - \delta\epsilon\omega_{TZ} \right] \right\} \end{aligned} \quad (5-14)$$

where the bracketed terms { · } result from using tracker accelerations  $A_{rX}$ ,  $A_{rY}$ ,  $A_{rZ}$  and angular velocity  $\omega_{TX}$  rather than true line of sight parameters  $A_{relX}$ ,  $A_{relY}$ ,  $A_{relZ}$ , and  $\omega_{LSX}$ . For high accuracy tracking, the angular deviations  $\delta\epsilon$  and  $\delta\eta$  will have magnitudes on the order of  $10^{-5}$  rad or smaller. For the profile under test therefore the bracketed terms have magnitudes near  $10^{-11}$  which are approximately 5 orders smaller than the magnitudes of  $\dot{\omega}_{LSY}$  and  $\dot{\omega}_{LSZ}$ . Thus for the filter, the bracketed terms are replaced by zero mean white Gaussian driving noises each having a 1 - sigma value of approximately  $10^{-11}$ . The resulting filter model equations are:

$$\dot{\omega}_{LSY} = -\frac{1}{R} A_{rZ} - \frac{2 V_r}{R} \omega_{LSY} + \omega_{LSZ} \omega_{TX} + W_4 \quad (5-15)$$

$$\dot{\omega}_{LSZ} = \frac{1}{R} A_{rY} - \frac{2 V_r}{R} \omega_{LSZ} - \omega_{LSY} \omega_{TX} + W_5 \quad (5-16)$$

The remaining state equations are:

$$\dot{\delta\eta} = \omega_{LSZ} - \omega_{TZ} - \delta\epsilon \omega_{TX} \quad (5-17)$$

$$\dot{\delta\epsilon} = \omega_{LSY} - \omega_{TY} + \delta\eta \omega_{TX} \quad (5-18)$$

$$\dot{R} = V_R \quad (5-19)$$

$$\dot{V}_R = A_{RX} + R(\omega_{LSY}^2 + \omega_{LSZ}^2) + \delta\eta A_{RY} - \delta\epsilon A_{RZ} \quad (5-20)$$

Equation (5-20) can be simplified by removing the terms  $\delta\eta A_{RY}$  and  $\delta\epsilon A_{RZ}$ . Since  $\delta\eta$  and  $\delta\epsilon$  are small, the two terms have magnitudes 5 orders smaller than  $\dot{V}_R$ . The filter state equation for  $\dot{V}_R$  thus becomes:

$$\dot{V}_R = A_{RX} + R(\omega_{LSY}^2 + \omega_{LSZ}^2) + W_C \quad (5-21)$$

where  $W_C$  is a white Gaussian noise with a distribution standard deviation of approximately  $5 \times 10^{-5}$  m/sec.

Thus far, the orbital dynamics have been simplified, and the state equations for the true propagation of the line of sight angular velocities and  $V_R$  have been simplified. As a result, the first 14 truth model state equations are reduced to 12 filter model state equations where the two equations for the ballistic coefficient and solar pressure coefficient are no longer required.

#### Filter Model Measurement Equations

The system truth model measurement equations are summarized in section II. The 9 equations were reduced to 5 by considering the measurement of  $\omega_{TX}$ ,  $\Delta T_X$ ,  $\Delta T_Y$ , and  $\Delta T_Z$  to be parameter measurements which could be incorporated into the state equations. The measurement equations are all similar in that each equation represents a measurement of

the true quantity corrupted by other factors. For example, the measurement equation for  $\omega_{TY}$  is repeated below:

$$\omega_{MY} = \omega_{TY} + B_{gsfY} \omega_{TY} + \sum_{i=1}^3 B_{gmYi} A_i + C_{gY} + \left[ \Delta C_{gm_a} \frac{W_T}{Y} \right] + V_2 \quad (5-22)$$

In this equation,  $\omega_{TY}$  is the unknown quantity to be measured. The remaining terms are non-deterministic. The term  $B_{gsfY} \omega_{TY}$  is the product of a random bias and the deterministic but unknown quantity  $\omega_{TY}$ . Thus the product is also non-deterministic.  $C_{gY}$  is modeled as a first order exponentially time correlated random variable. In fact, there are four types of quantity, deterministic, random bias, first order exponentially correlated random variable and pure white noise.

For the truth model, in the absence of better information, the random bias terms are chosen to have zero mean, i.e.  $\hat{x} = 0$ , with variance derived from experimental data. The gyro drift parameters would also be derived using experimental data. The white noise term  $V_2$  accounts for unmodeled effects such as higher order non-linearities. For the filter model, it is assumed that in all the measurement equations the total effect of the non-deterministic terms can be accounted for by a simple white noise added to the deterministic term in each equation. The white noise is Gaussian, with zero mean and variance chosen to be approximately equal to the variance of the sum of all the non-deterministic terms.

In practice, the additive white noise term increases the uncertainty in the measurement. If the above filter measurement model gives

poor performance in the covariance analysis, it may be possible to increase the variance of the white noise further, thus indicating additional uncertainty in the measurement model. Alternatively, the model could be changed to include just the gyro drift terms for example. As a first attempt at modeling however, the additive white noise model has the simplest form.

#### Summary of State and Measurement Equations

Using the simple measurement models described above, the filter state equations and measurement equations are:

#### State Equations

$$(1) \quad \dot{X}_1 = X_4$$

$$(2) \quad \dot{X}_2 = X_5$$

$$(3) \quad \dot{X}_3 = X_6$$

$$(4) \quad \dot{X}_4 = \frac{-\mu \Theta X_1}{r_V^3} + W_1$$

$$(5) \quad \dot{X}_5 = \frac{-\mu \Theta X_2}{r_V^3} + W_2$$

$$(6) \quad \dot{X}_6 = \frac{-\mu \Theta X_3}{r_V^3} + W_3$$

$$(7) \quad \dot{\omega}_{LSY} = -\frac{1}{R} A_{rZ} - \frac{2 V_r}{R} \omega_{LSY} + \omega_{LSZ} \omega_{TX} + W_4$$

$$(8) \quad \dot{\omega}_{LSZ} = \frac{1}{R} A_{rY} - \frac{2 V_r}{R} \omega_{LSZ} - \omega_{LSZ} \omega_{TX} + W_5$$

$$(9) \quad \dot{\delta\eta} = \omega_{LSZ} - \omega_{TZ} - \delta\epsilon \omega_{TX}$$

$$(10) \quad \dot{\delta\epsilon} = \omega_{LSY} - \omega_{TY} + \delta\eta \omega_{TX}$$

$$(11) \quad \dot{R} = V_R$$

$$(12) \quad \dot{V}_R = A_{RX} + R(\omega_{LSY}^2 + \omega_{LSZ}^2) + W_6$$

#### Measurement Equations

$$(1) \quad \omega_{MX} = \omega_{TX} + V_1$$

$$(2) \quad \omega_{MY} = \omega_{TY} + V_2$$

$$(3) \quad \omega_{MZ} = \omega_{TZ} + V_3$$

$$(4) \quad A_{TXM} = A_{TX} + V_4$$

$$(5) \quad A_{TYM} = A_{TY} + V_5$$

$$(6) \quad A_{TZM} = A_{TZ} + V_6$$

$$(7) \quad \delta\epsilon_M = K_1 \delta\epsilon + V_7$$

$$(8) \quad \delta\eta_M = K_2 \delta\eta + V_8$$

$$(9) \quad R_M = K_R R + V_9$$

The measurements of  $A_{TX}$ ,  $A_{TY}$ ,  $A_{TZ}$  and  $\omega_{TX}$  as in the truth model, constitute measurements of system parameters. The measured parameters can thus be substituted into the state equations so that the actual

measurement equation will not be used as part of the filter measurement model. Now, if this is so, there is no real need for the simplified measurement models described by equations (1), (4), (5), and (6) except for the purpose of linearization. In linearizing the state equations, account must be taken of the fact that a measurement is in fact a linear or non-linear combination of system states. Thus in order to use the 12 state model, the simple measurement model must be assumed.

The remaining measurements are direct measurements of states of the system, or in the case of  $\omega_{TY}$  and  $\omega_{TZ}$ , pseudo-measurements of states of the system. Equations (2), (3), (7), (8), and (9) constitute the filter model measurement vector.

Appendix C shows how the state and measurement equations of the filter model are linearized for application to a covariance analysis of the Extended Kalman Filter.

## VI. RESULTS

Test Simulation Data

Appendix D lists the truth model simulation parameters used for the initial evaluation of the filter model. The data corresponds to a typical set of measuring instruments. Some simulation parameters were changed to improve the measuring instruments to 'state of the art' quality, and the filter model reevaluated. The actual changes will be discussed later.

Test Objective

The primary test objective was to demonstrate that good performance can be obtained using the filter model described in section V under varying conditions. These conditions were representative of differing qualities of measuring instruments. In order to achieve this objective, the filter model was first 'tuned' against the set of simulation instrument specifications described in Appendix D. The process of tuning involves adjustment of the Q and R covariance matrices in the filter model, often by trial and error, until satisfactory performance is obtained. Conceptually, the tuned filter is the best representation of the truth model, by the simplified filter model. Once the filter model had been tuned, and evaluated, some of the measuring parameters were then changed in the truth model and the filter model retuned to account for the changes.

Tuning the Filter Model

The covariance analysis method described in section IV compares the true estimation error variances resulting from the use of a particular filter, with the error variances predicted by the filter itself. Thus,

given a state vector estimate  $\hat{\underline{x}}(t)$  where the true state is  $\underline{x}_t(t)$ , the error is normally expressed by the covariance matrix:

$$P(t) = E \left\{ \left[ \hat{\underline{x}}(t) - \underline{x}_t(t) \right] \left[ \hat{\underline{x}}(t) - \underline{x}_t(t) \right]^T \right\}$$

Since this matrix may be of large dimension, it is usually more convenient to examine the square root of each diagonal element of the matrix.

Thus the error in  $x_1(t)$  is given by:

$$\sqrt{P_{11}(t)} = \sqrt{E \left\{ \left[ \hat{x}_1(t) - x_{1t}(t) \right]^2 \right\}}$$

which is the 1 - sigma value (standard deviation) for the error in  $\hat{x}_1(t)$ .

Denoting the true error in the estimate of a state as the system error, and the error predicted by the filter as the filter error, then the objective of tuning the filter model is to ensure that the system error and filter error have very nearly the same magnitude. It is quite possible for the system and filter errors to simultaneously diverge, indicating an unstable error. Even in this circumstance the filter is still tuned, provided the two magnitudes are equal. In practice it is usual to tune the filter so that the filter error standard deviations never underestimate the system error standard deviations. In this way, the filter model accurately represents or slightly overestimates the real error and therefore allows some margin of uncertainty. Fig. 6 and 7 show a typical situation where the filter error for  $X(14)$ , which is the range rate  $V_r$ , converges after 100 seconds to approximately 1.5 m/sec, whereas the system error is in fact 2 m/sec after 100 seconds. In this case, the filter is underestimating the real error and although its performance appears good, in reality it may not be acceptable. The process of tuning the filter is somewhat arbitrary in that several variables can be ad-

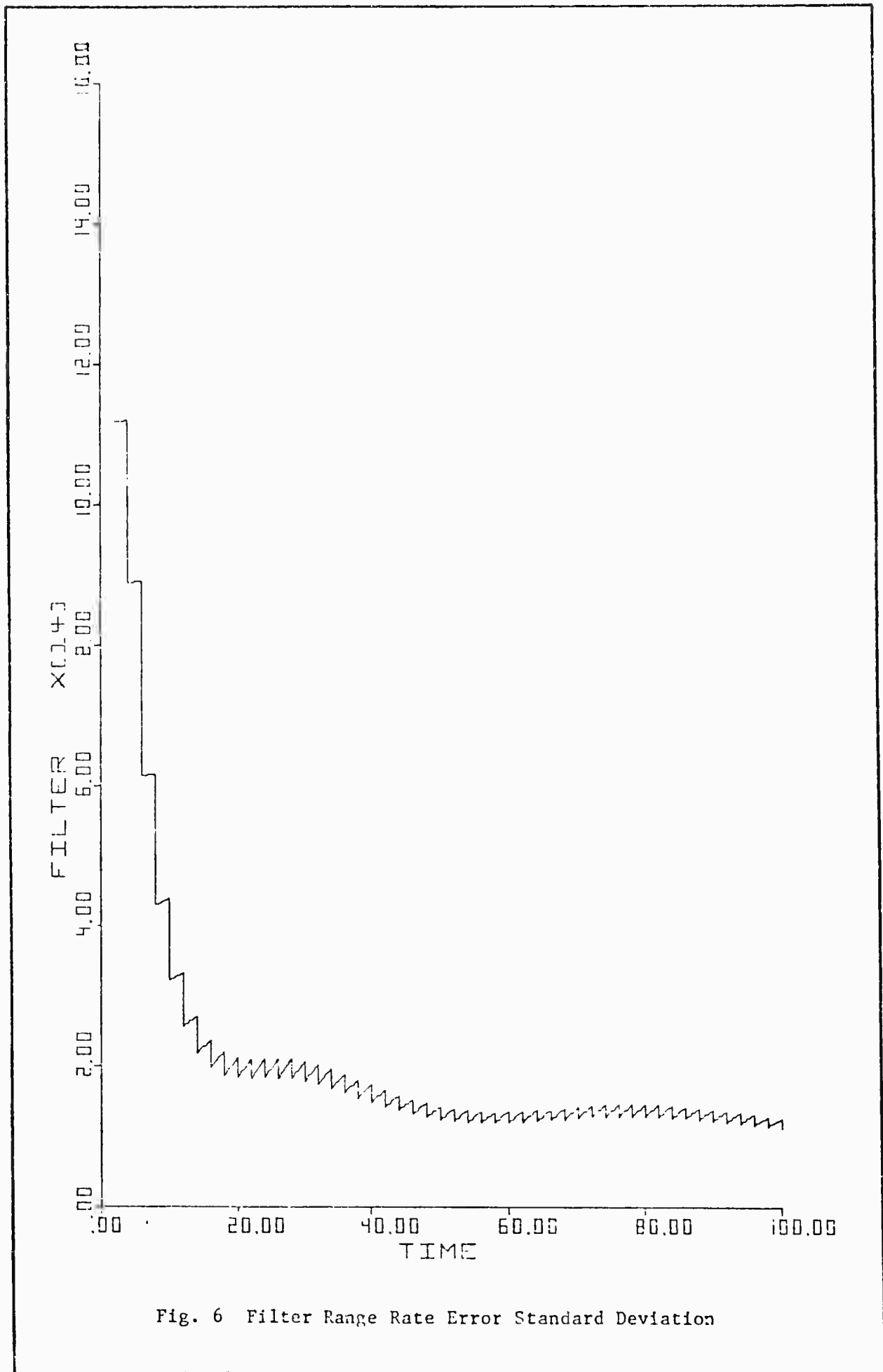


Fig. 6 Filter Range Rate Error Standard Deviation

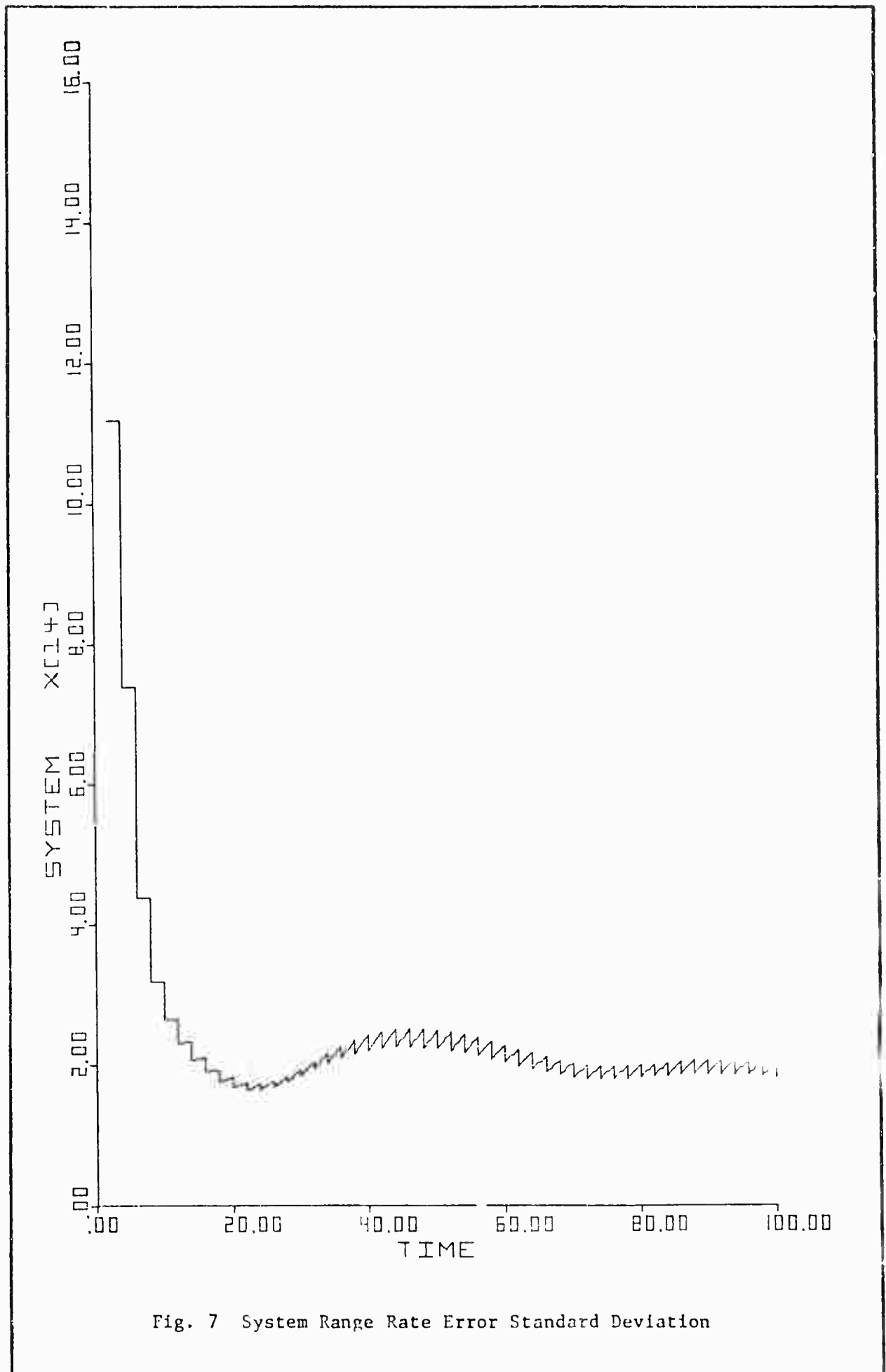


Fig. 7 System Range Rate Error Standard Deviation

justed. For example, the initial condition on the variance of a state will affect its transient behaviour, the measurement and state driving noise covariances will affect both the transient and steady state behaviour and in general there will be one set of conditions which produces the best performance. This set of conditions can be highly interdependent so that the process of finding the correct values usually requires an element of trial and error

### Transient Behaviour of Filter

The transient behaviour of the filter depends on three factors, the choice of initial conditions, the measurement noises, and the state equation driving noises for the filter model.

Initial Conditions The choice of initial conditions on both filter error and system error can severely affect the transient behaviour of the filter and can in fact cause divergence. Figs. 8 and 9 show the behaviour of the filter and system errors respectively over a 200 second time interval. The state is the inertial satellite position element  $X_1$ . The filter error initial condition  $\sqrt{P_{11}(t_0)}$  was chosen as 100 km while the system error initial condition was chosen as zero. The initial transient subsides after approximately 120 seconds, and both curves begin to show a divergent characteristic. It is interesting to note that during the divergence, the filter appears to be reasonably well tuned in that both curves show similar magnitude errors, but the filter is overestimating the error by about 20%. In this case, the divergence is not caused by the poor choice of initial conditions. Figs. 10 and 11 show the same state  $X_1$  with a different set of initial conditions on the filter and system errors respectively. Again, the divergence is apparent,

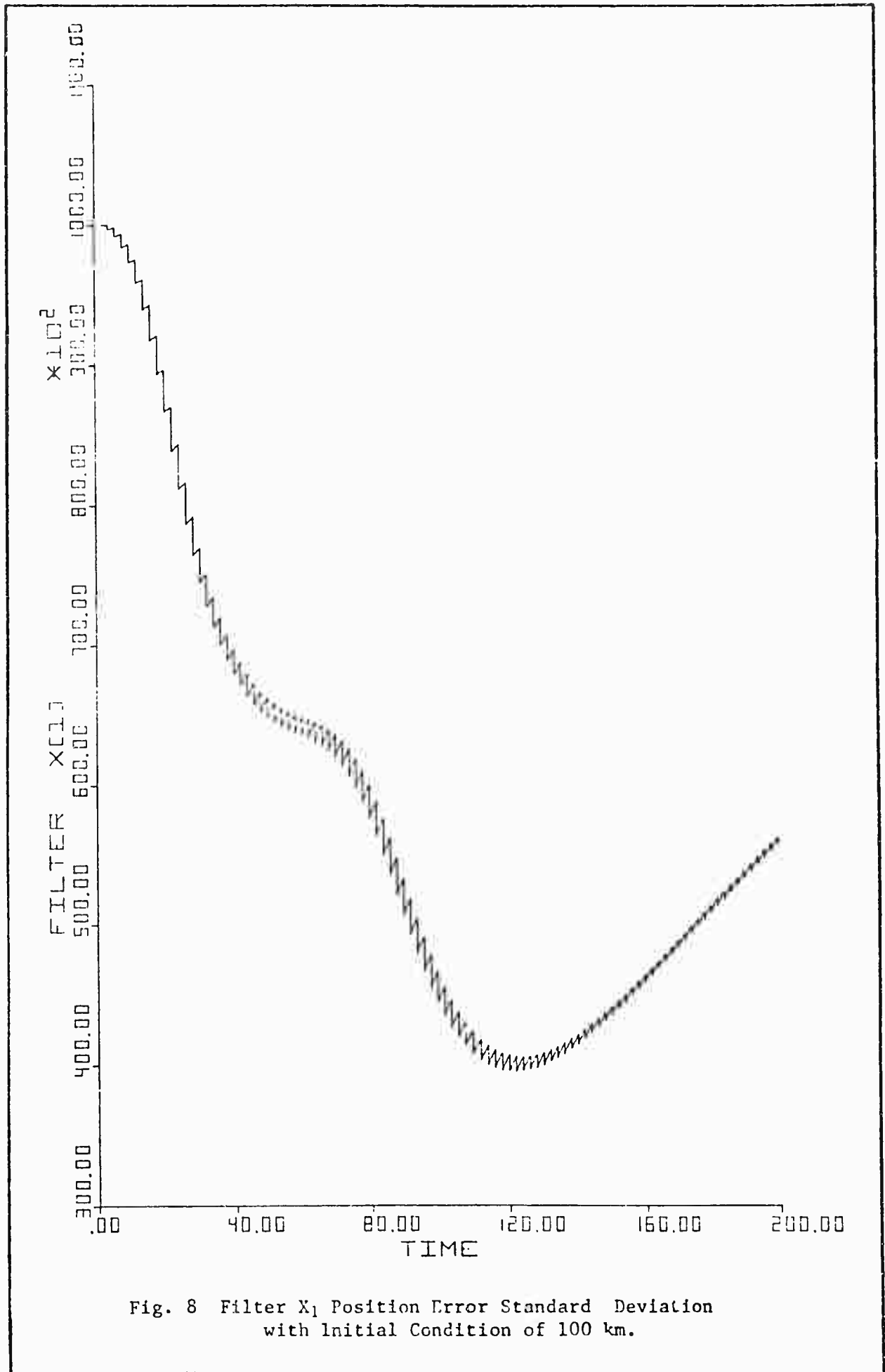


Fig. 8 Filter  $X_1$  Position Error Standard Deviation with Initial Condition of 100 km.

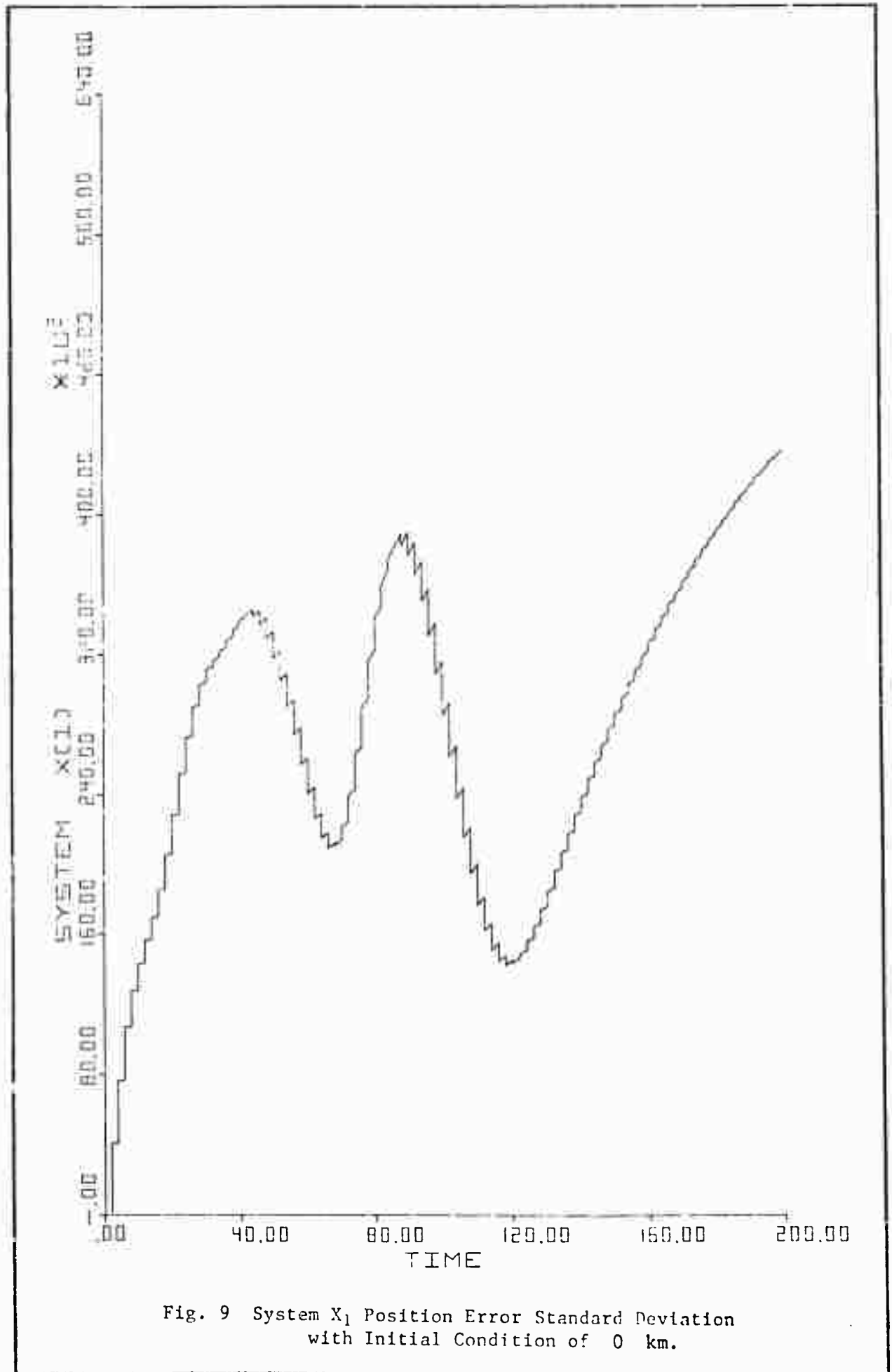


Fig. 9 System  $X_1$  Position Error Standard Deviation with Initial Condition of 0 km.

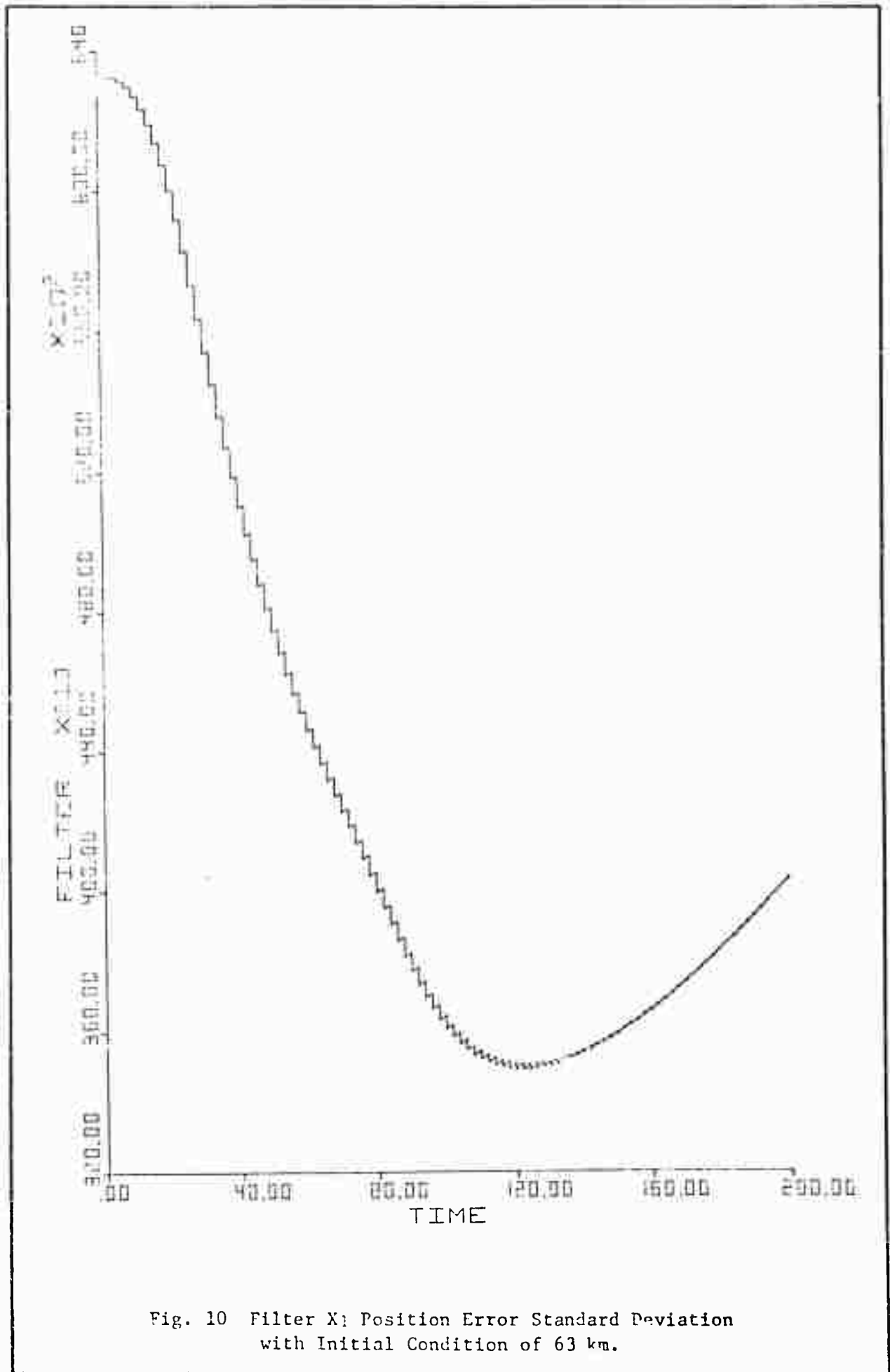


Fig. 10 Filter X1: Position Error Standard Deviation with Initial Condition of 63 km.

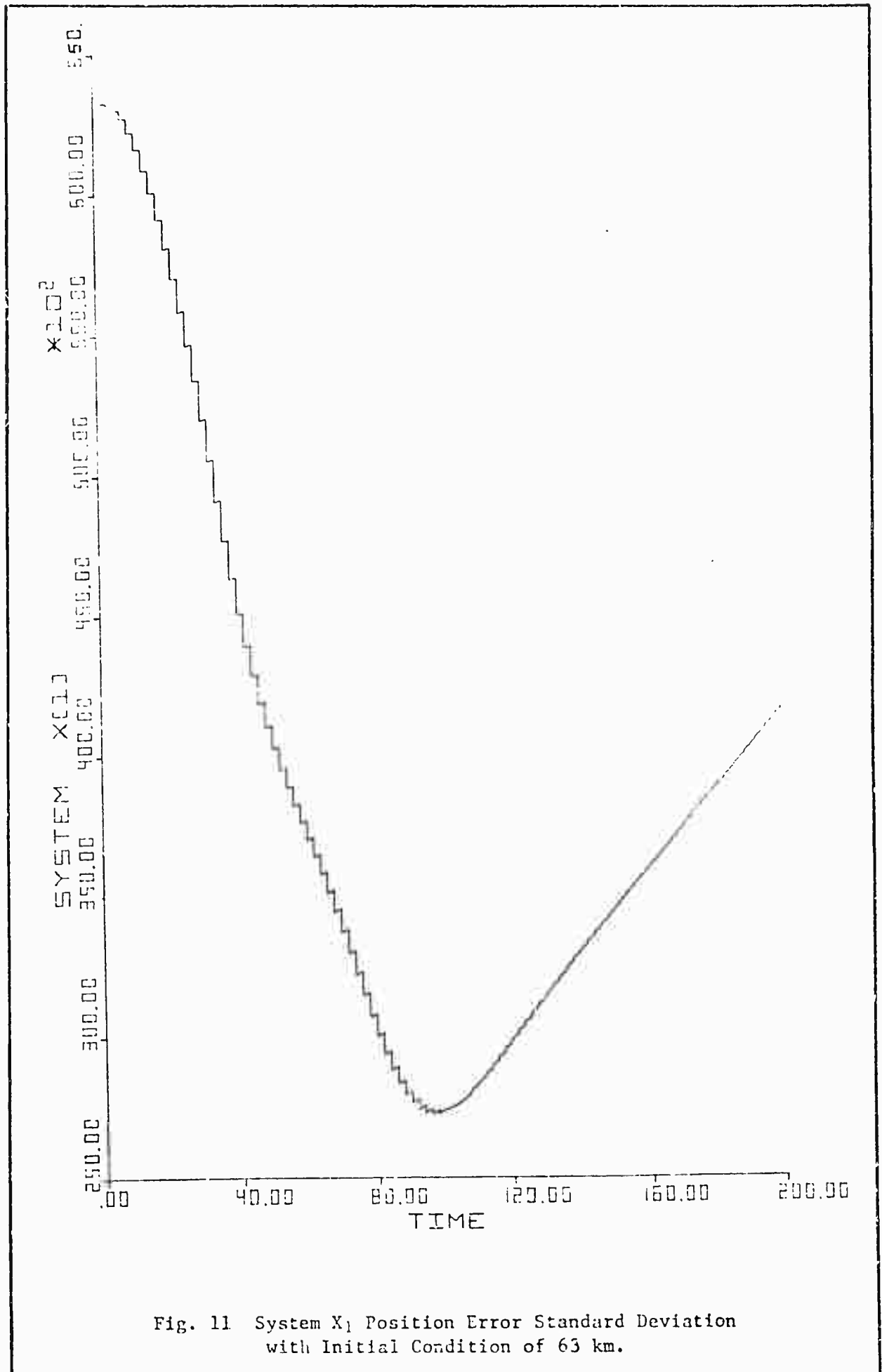


Fig. 11 System X<sub>1</sub> Position Error Standard Deviation with Initial Condition of 63 km.

and the initial transient behaviour is much improved.

Measurement and Driving Noises Consider the state  $\omega_{LSy}$  which is the line of sight angular velocity along the line of sight  $y$  - axis. Appendix C gives the state equation driving noise standard deviation as  $10^{-11}$  rad/sec<sup>2</sup> and the measurement noise standard deviation as  $1.6 \times 10^{-6}$  rad/sec. These values were derived by considering the truth model simulation data in Appendix B, and compensating for the effect of all the simplifications from truth model equations to filter model equations. Using these two values, the filter diverged rapidly. Several test runs were made in which the noise figures were adjusted to improve performance. Figs. 12 and 13 illustrated the behaviour of the filter using a driving noise standard deviation of  $2.7 \times 10^{-7}$  rad/sec and a measurement noise standard deviation of  $6.5 \times 10^{-6}$  rad/sec. In this case, an oscillatory transient occurs with a 40 second period and 100 second settling time. By further adjustments, the transient was almost removed. Figs. 14 and 15 show the final performance curves where the driving noise standard deviation was  $5 \times 10^{-7}$  rad/sec<sup>2</sup> and the measurement noise standard deviation was  $2 \times 10^{-6}$  rad/sec. The example illustrates that it is often necessary to carry out very fine adjustments to tune the filter model. Figs. 14 and 15 were obtained after 8 distinct adjustments, where each adjustment required a computer run to show the performance. Also, it is sometimes necessary to increase the strength of the state equation driving noises very considerably, in this case by a factor of  $10^4$ , to obtain good performance.

#### Determination of Vehicle Orbit

In the truth model formulation, no direct measurements of the vehicle

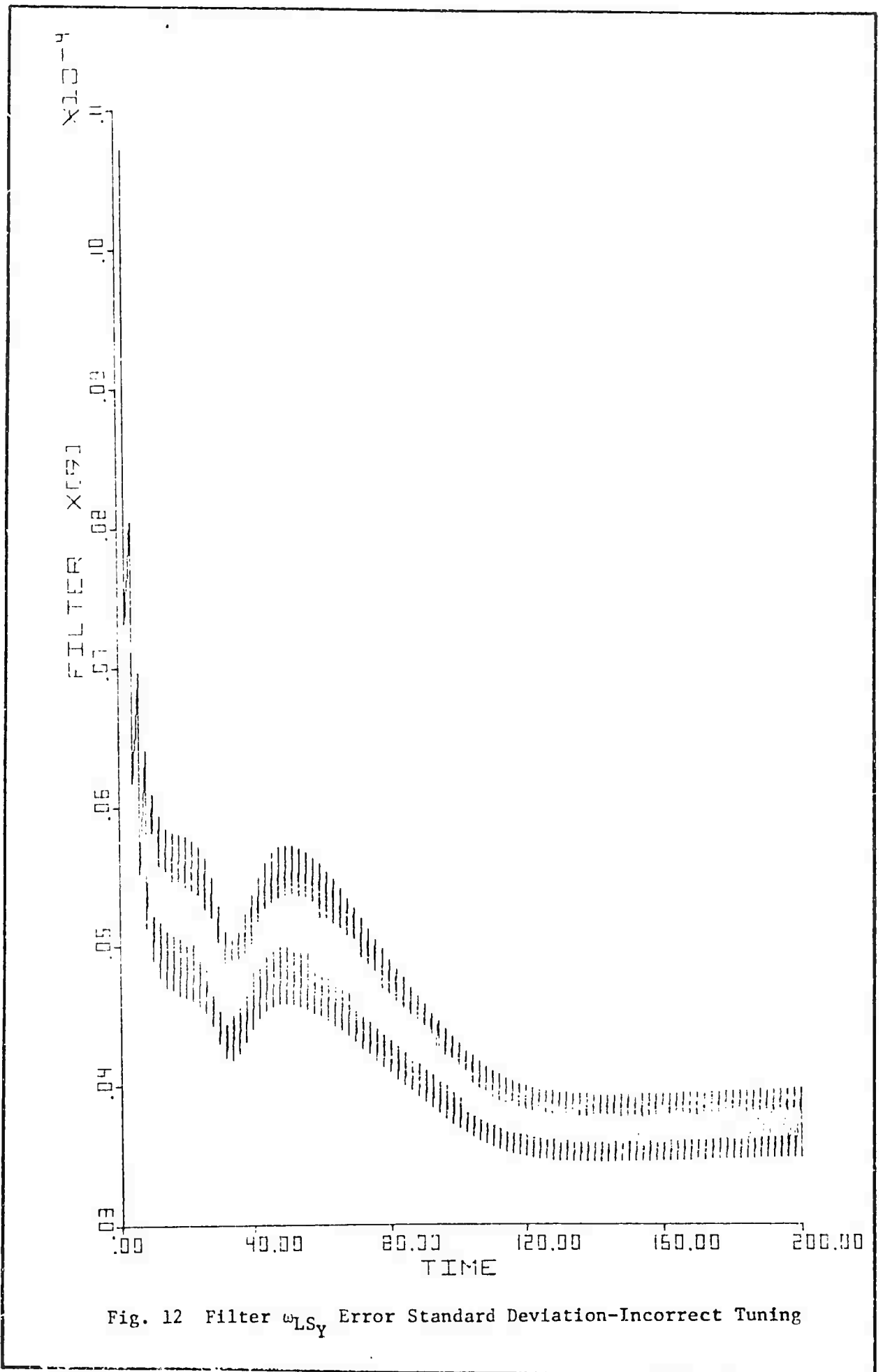


Fig. 12 Filter  $\omega_{LSy}$  Error Standard Deviation-Incorrect Tuning

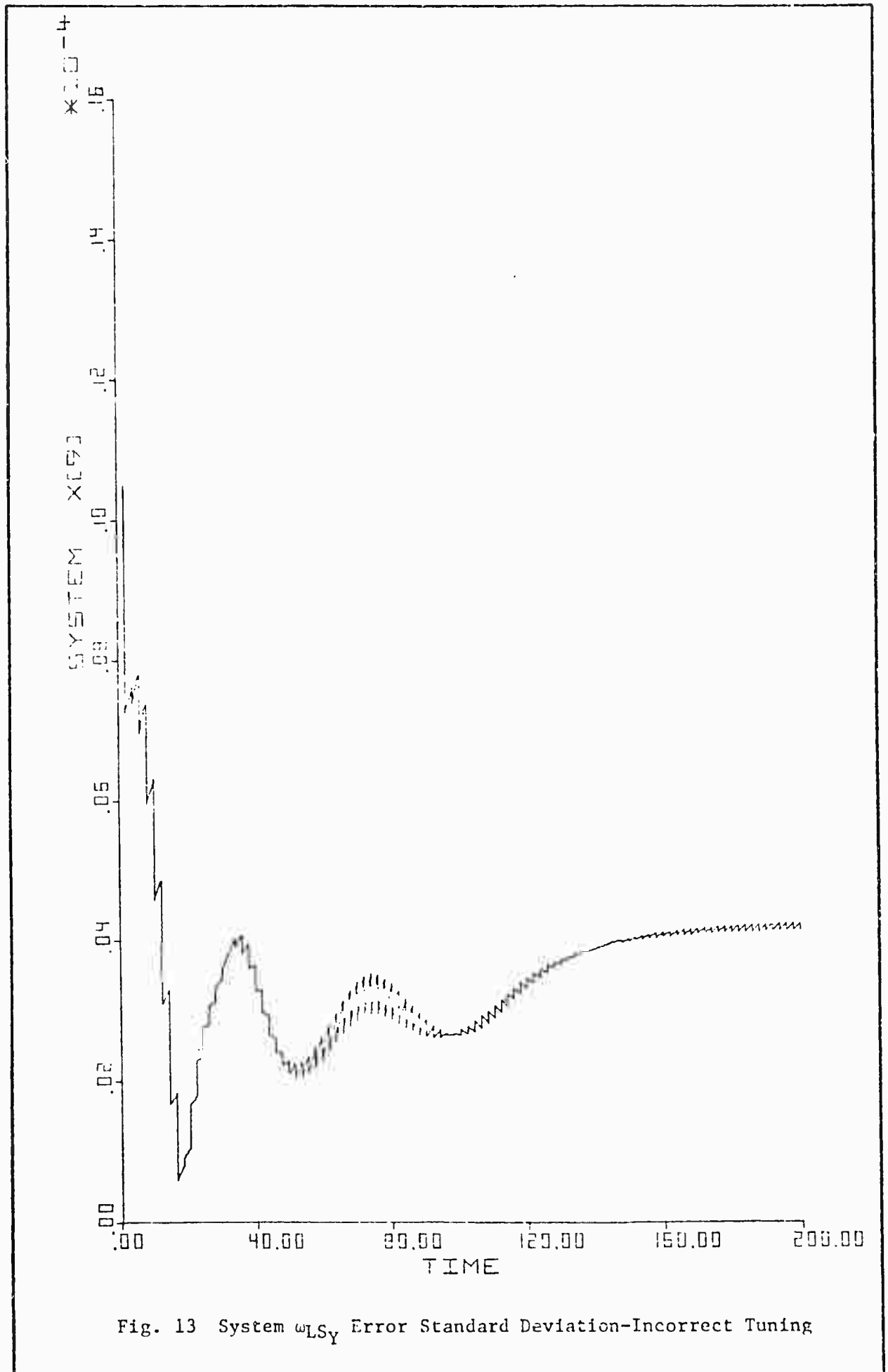
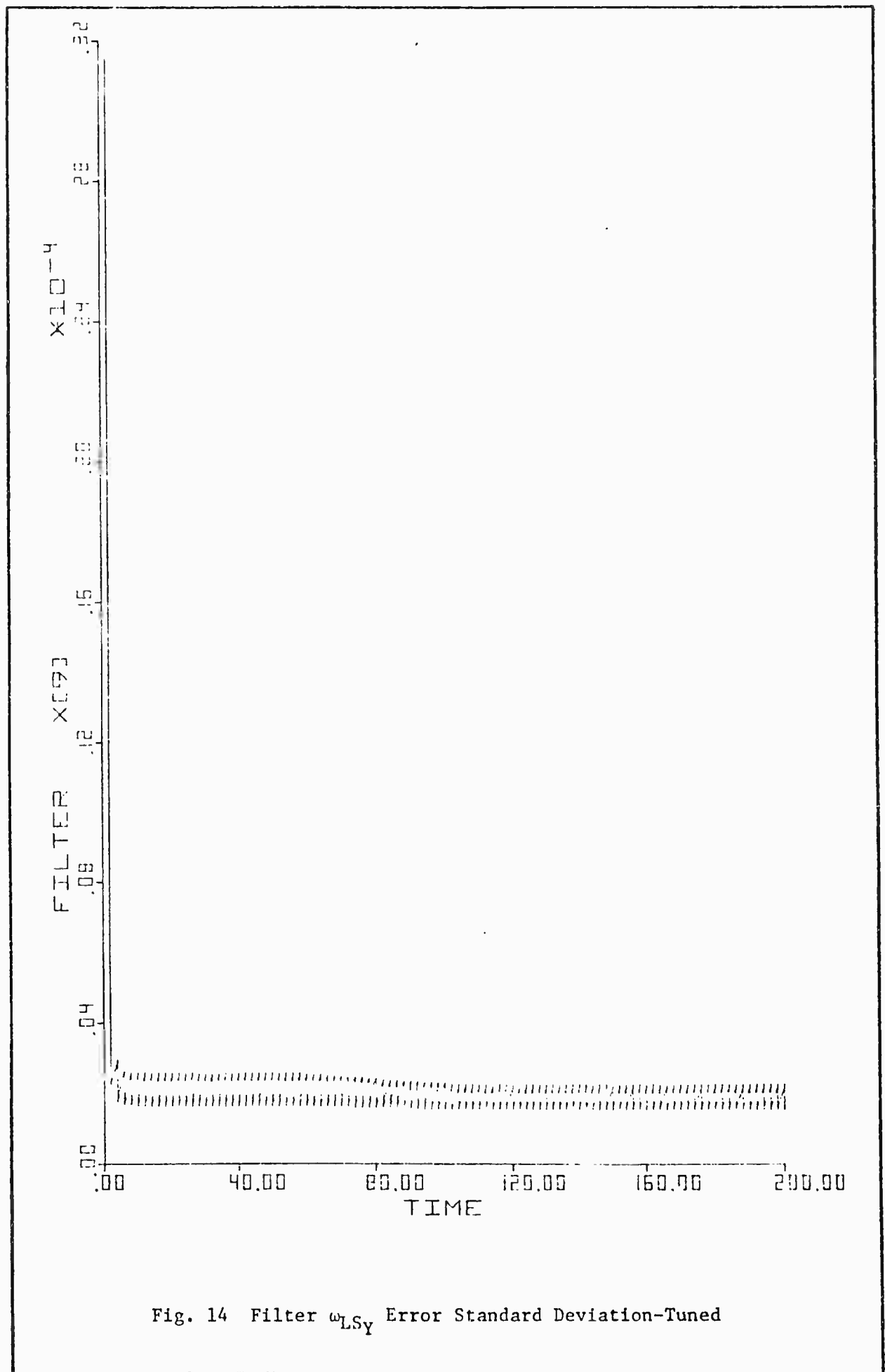


Fig. 13 System  $\omega_{LSy}$  Error Standard Deviation-Incorrect Tuning



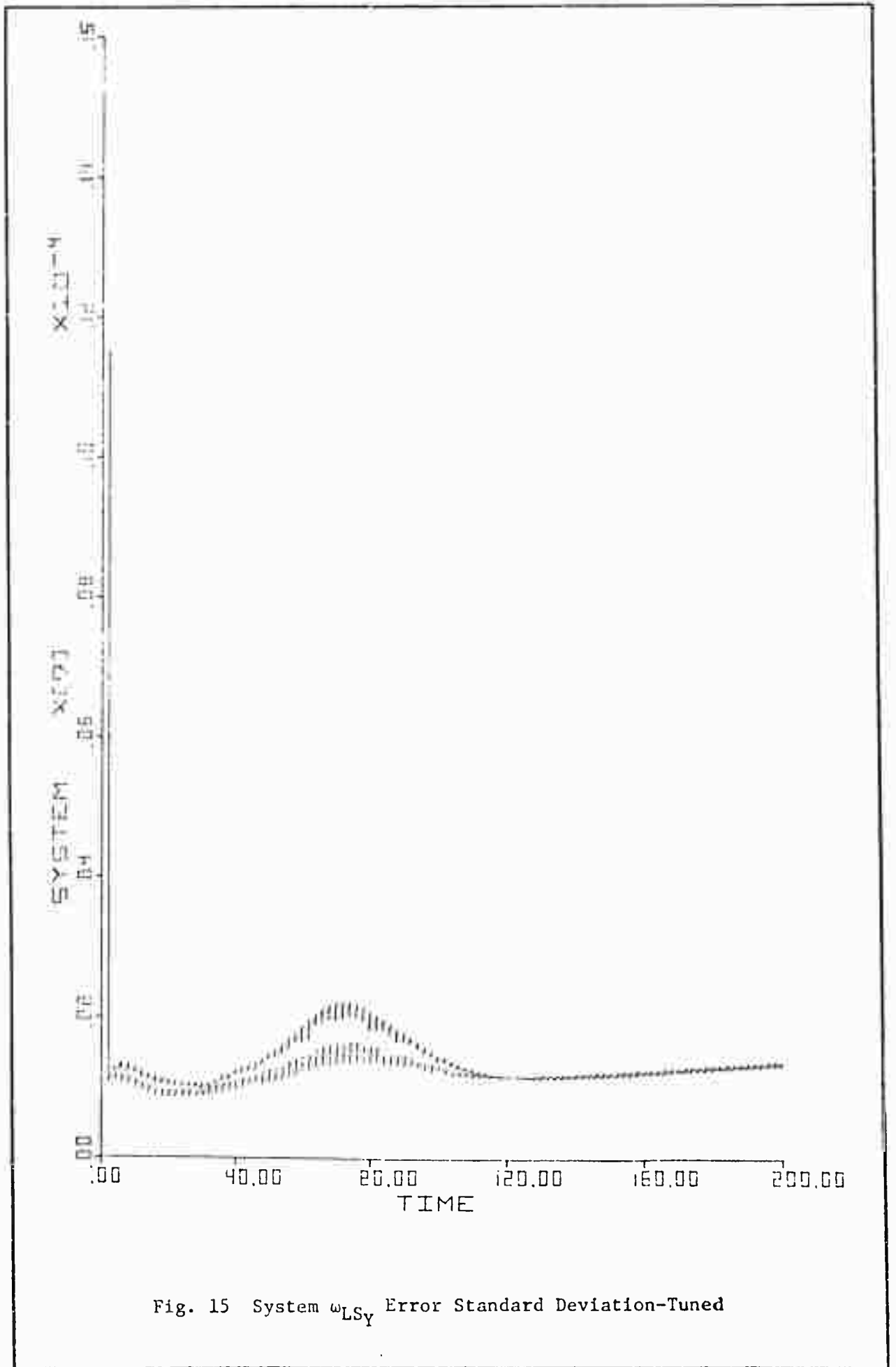


Fig. 15 System  $\omega_{LSy}$  Error Standard Deviation-Tuned

inertial position and velocity are included. In fact such measurements could not be made directly from the vehicle without using an inertial navigation system. It is feasible that measurements could be taken by a ground station and transmitted to the aircraft during the pass. However, the system was tested assuming only measurements of tracker acceleration, tracker angular velocity, misalignment angles, and range. The inclusion of further measurements might be a logical extension to this study. It is interesting to observe the behaviour of the filter with the present formulation. Figs. 10 and 11 illustrate the error standard deviation for inertial position  $X_1$ , for the filter and system respectively. Figs. 16 and 17 show a very similar trend in  $X_2$  and Figs. 18 and 19 illustrate the error in inertial velocity state  $X_4$  for filter and system respectively. The typical error standard deviation in a position component is about 40 km and that in a velocity component is about 190 m/sec. The following observations can be made:

- a. The transient performance is extremely slow.
- b. Initially (see Figs. 18 and 19) the measurements have no effect on inertial velocity errors.
- c. As the inertial position estimate improves, the measurements begin to give an improvement in the inertial velocity estimates. The time lag is approximately 40 seconds.
- d. The improvement in the inertial velocity estimate during the complete 200 second run is relatively small. With an initial condition of 200 m/sec error standard deviation, the final error standard deviation is 193 m/sec.
- e. Towards the end of the 200 second run, the position estimate errors begin to show a divergent characteristic. This could

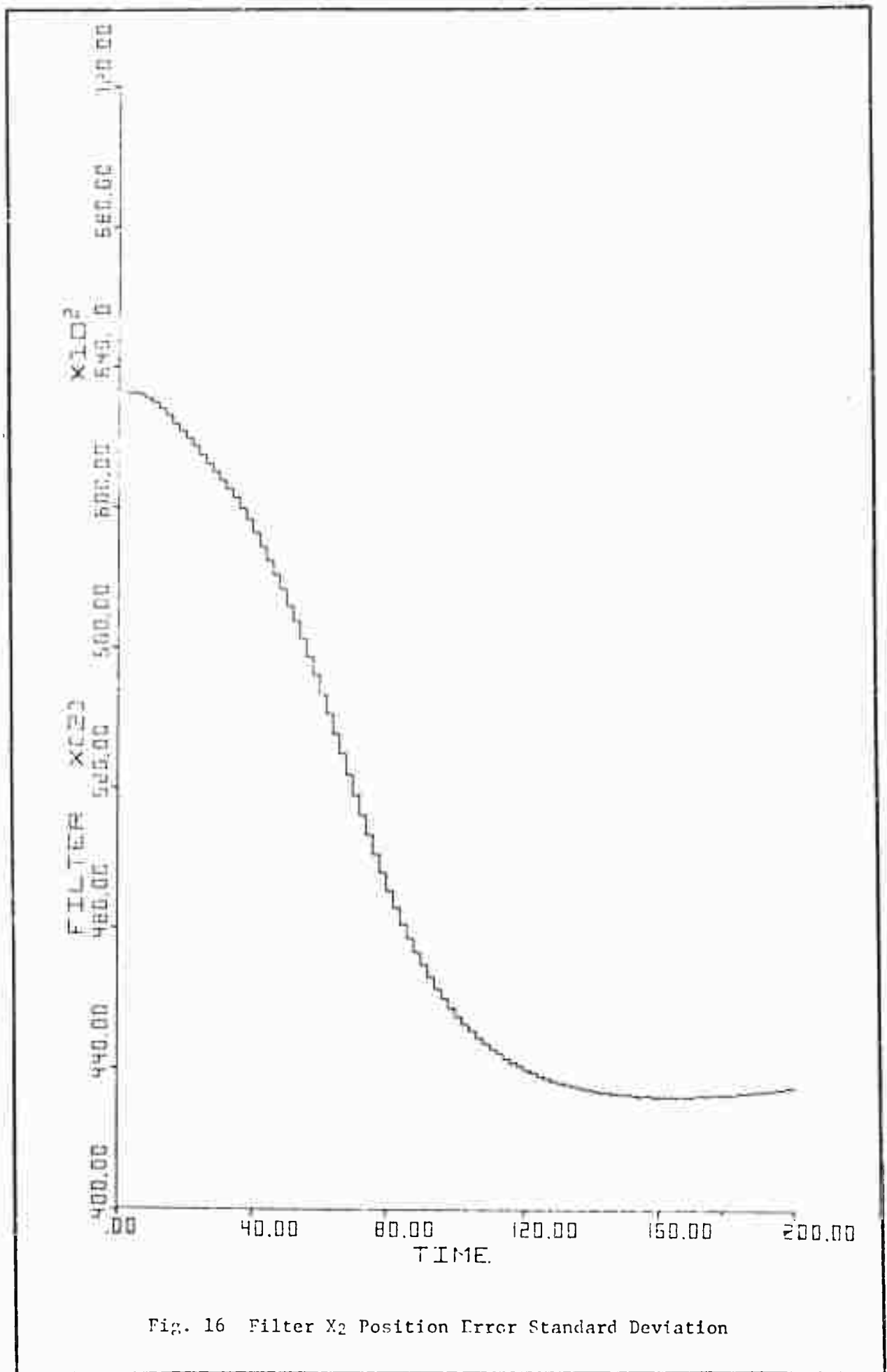


Fig. 16 Filter X2 Position Error Standard Deviation

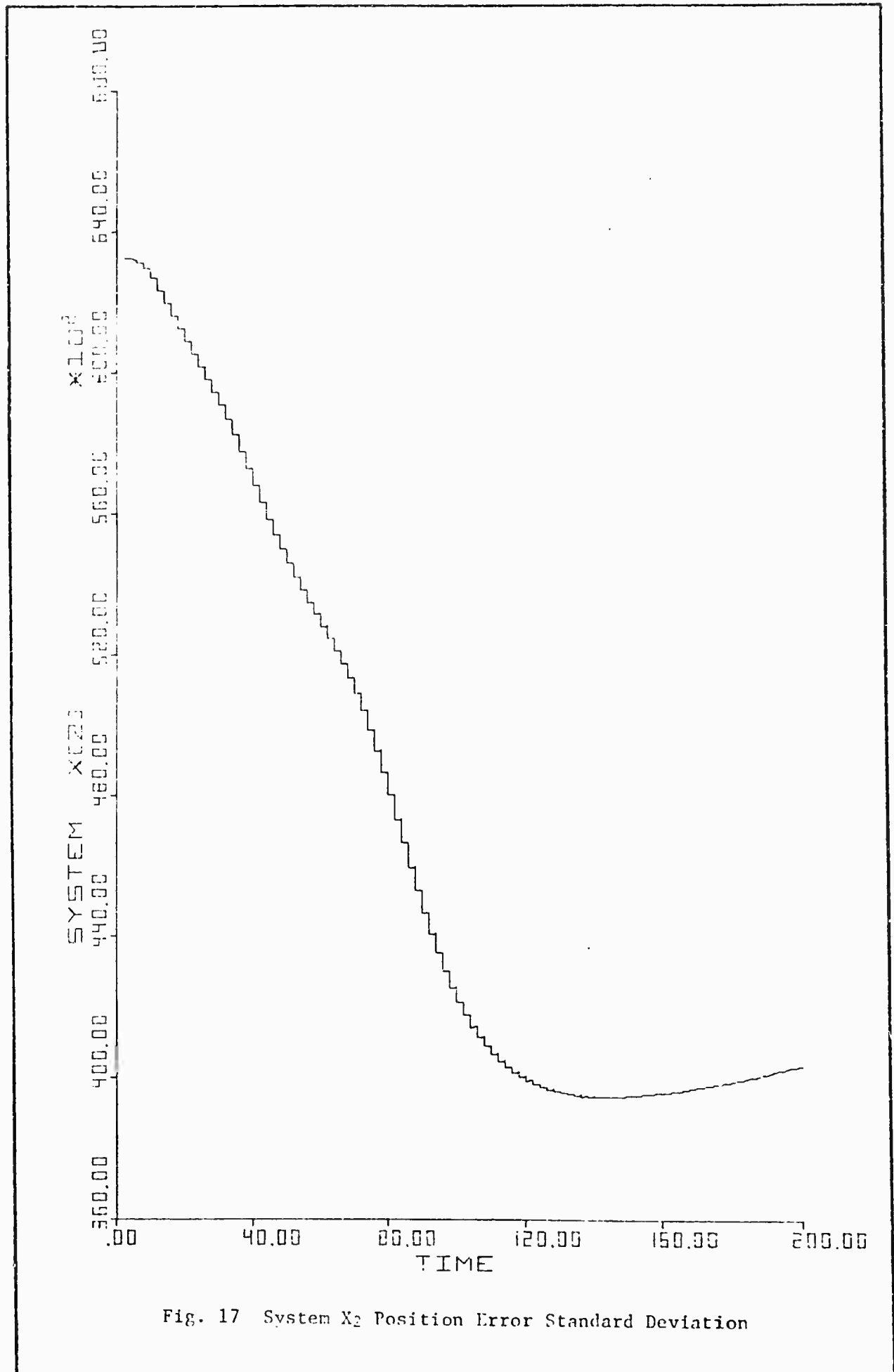


Fig. 17 System X<sub>2</sub> Position Error Standard Deviation

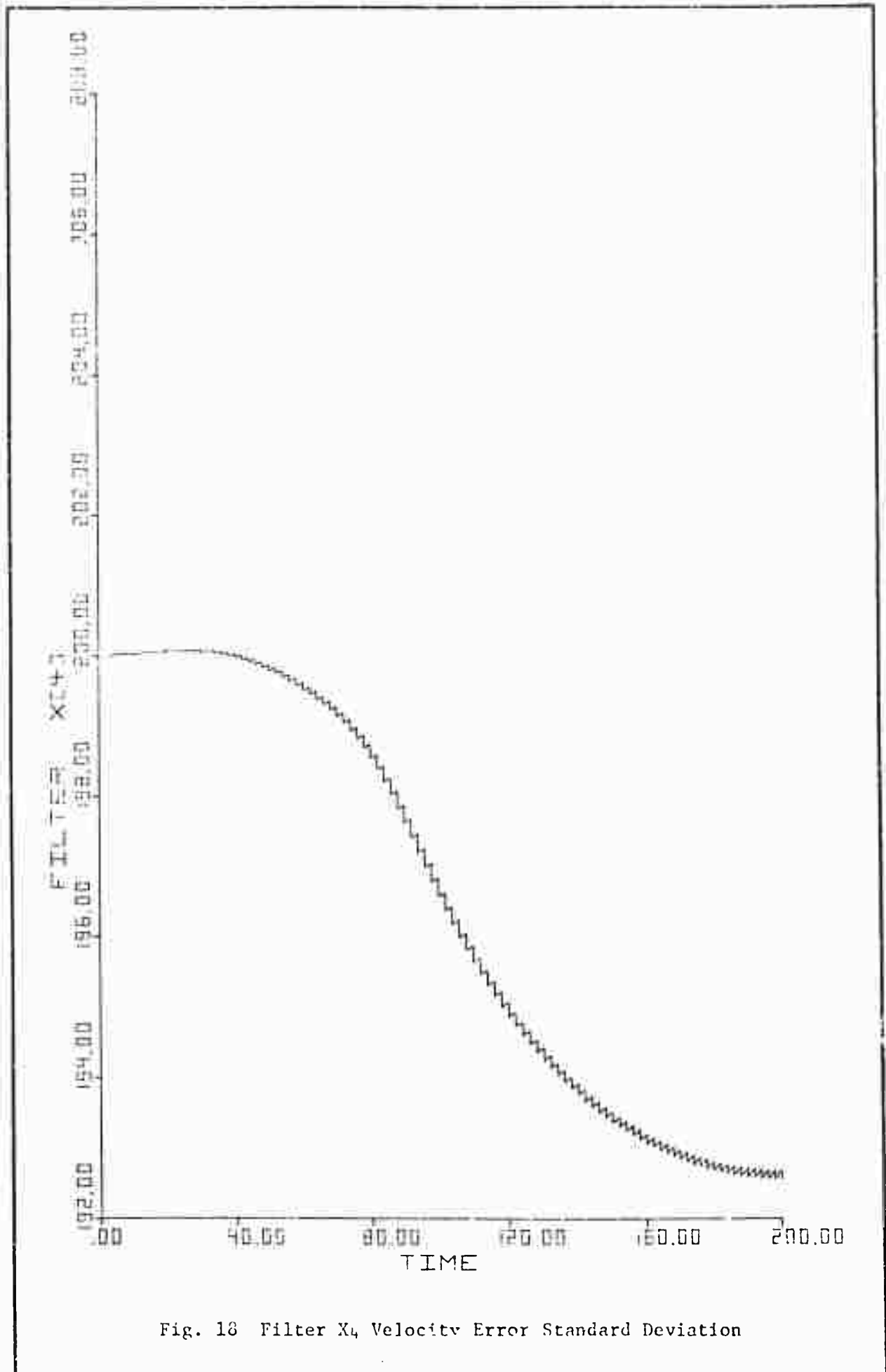


Fig. 13 Filter X4 Velocity Error Standard Deviation

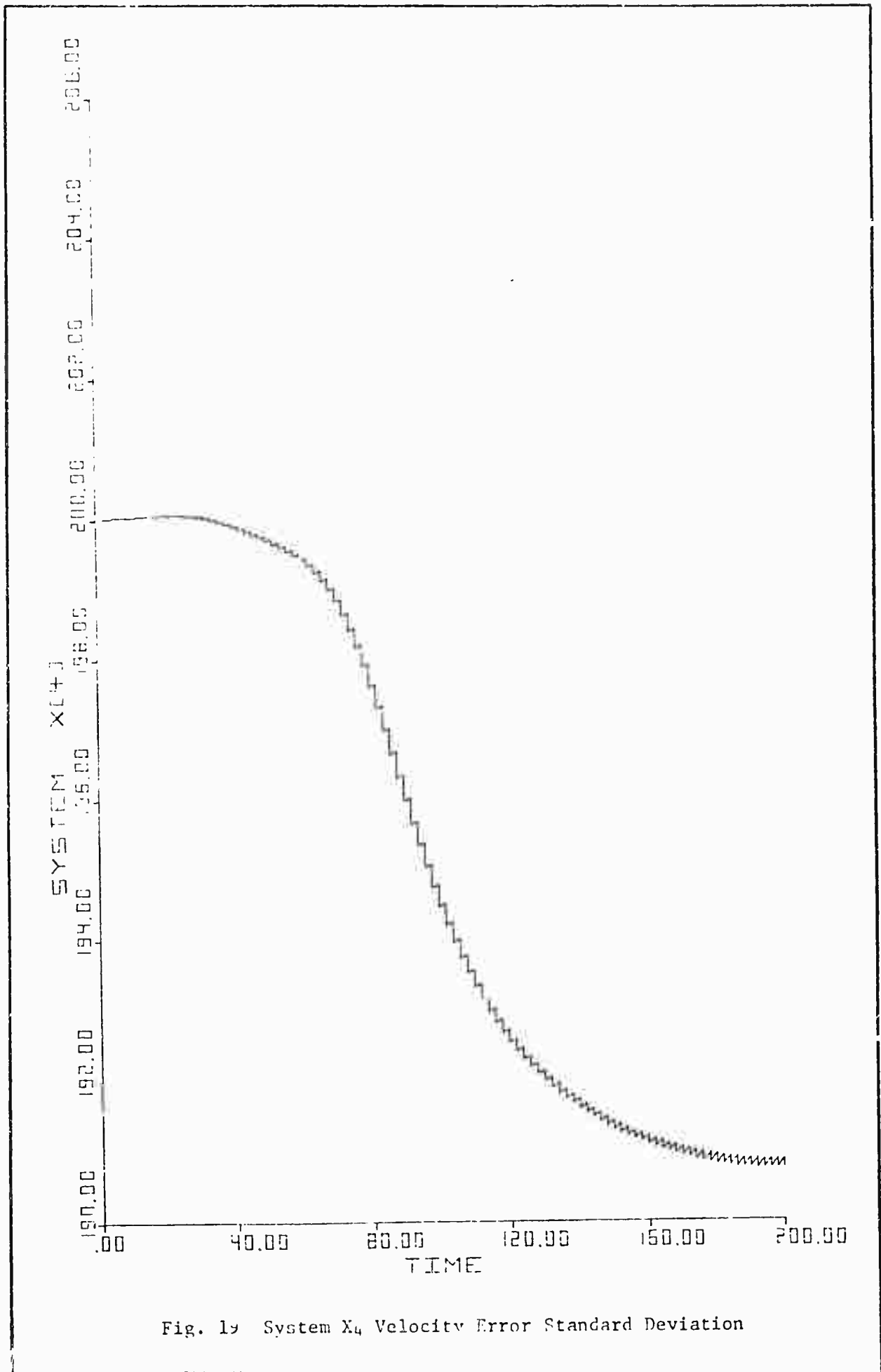


Fig. 19 System X<sub>4</sub> Velocity Error Standard Deviation

be due to the fact that as range increases and the satellite goes out of view, the measurements begin to have less effect.

The main conclusion to be drawn from these observations is that the orbital estimate is not significantly improved by the measurement information. The latter is coupled into the orbital state equations via the relative acceleration of the vehicle to the aircraft, expressed in tracker coordinates. This in turn is a function of the aircraft inertial acceleration, the vehicle inertial acceleration which is dependent on the vehicle inertial position, and the coordinate transformation matrix from tracker to inertial coordinates, which is assumed known. The coupling is complex: if a measurement of  $\omega_{LSY}$  improves the estimate of that state, then this improvement is coupled through  $A_{rZ}$  into the vehicle inertial position estimate. Recalling the filter model state equation for  $\omega_{LSY}$ :

$$\dot{\omega}_{LSY} = \frac{-A_{rZ}}{R} - \frac{2 V_r}{R} \omega_{LSY} + \omega_{LSZ} \omega_{TY} + W \quad (6-1)$$

It would seem equally important, since  $A_{rZ}$  is a function of vehicle inertial position, for the estimate of the vehicle inertial position to be good in order to maintain a good estimate of  $\omega_{LSY}$ . This loop in the coupling will be discussed later.

#### Tracking Accuracy

The accuracy in the tracking is expressed by the standard deviation of the errors in the misalignment angles  $\delta\epsilon$  and  $\delta\eta$ . These errors are in turn affected by the errors in line of sight angular velocities, range, range rate, and, as already discussed, the vehicle state. Figs. 20 and 21 show the standard deviation of the error in the misalignment angle  $\delta\eta$ . The transient is short and a mean steady state standard deviation of

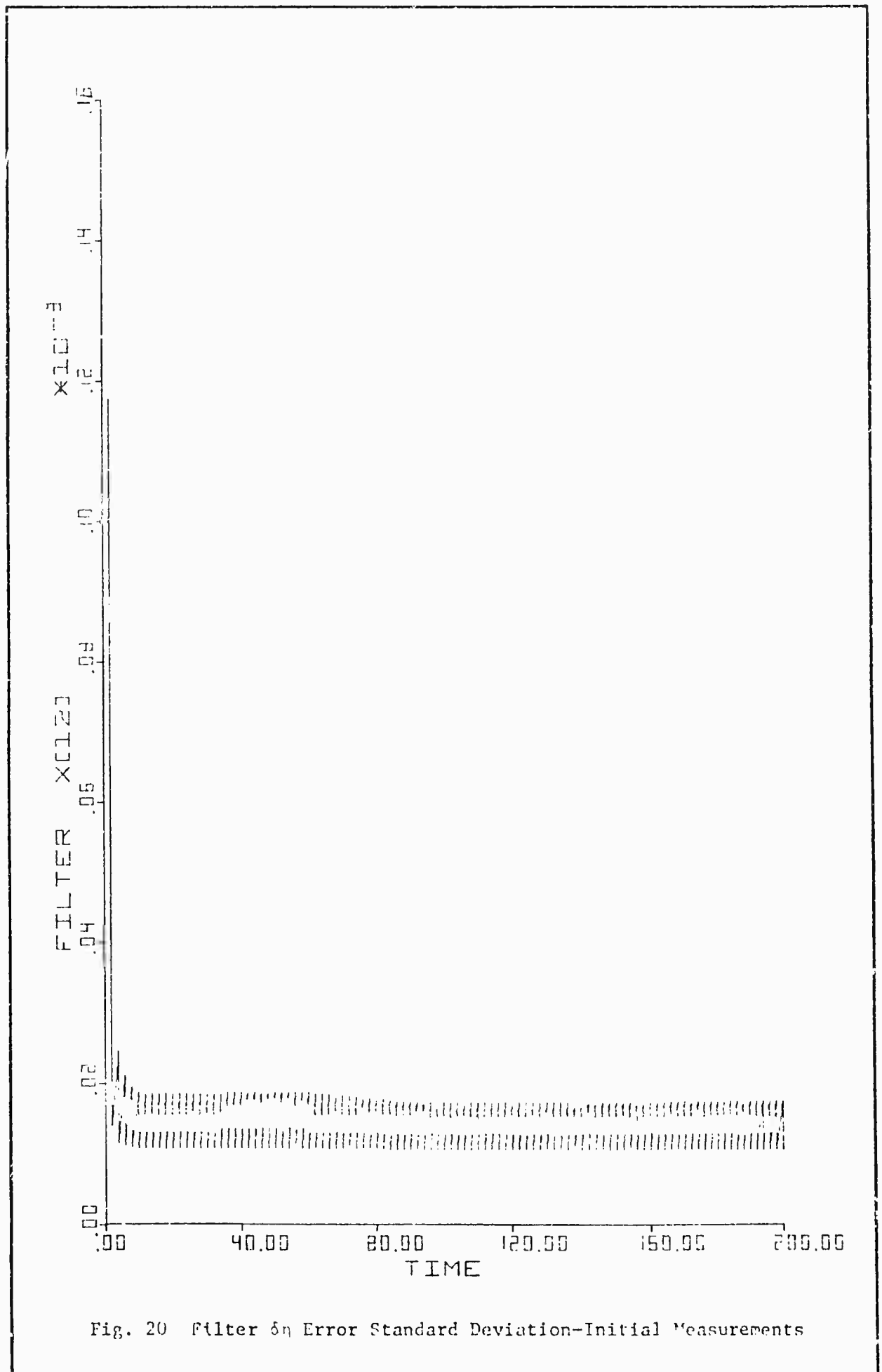


Fig. 20 Filter  $\delta\eta$  Error Standard Deviation-Initial Measurements

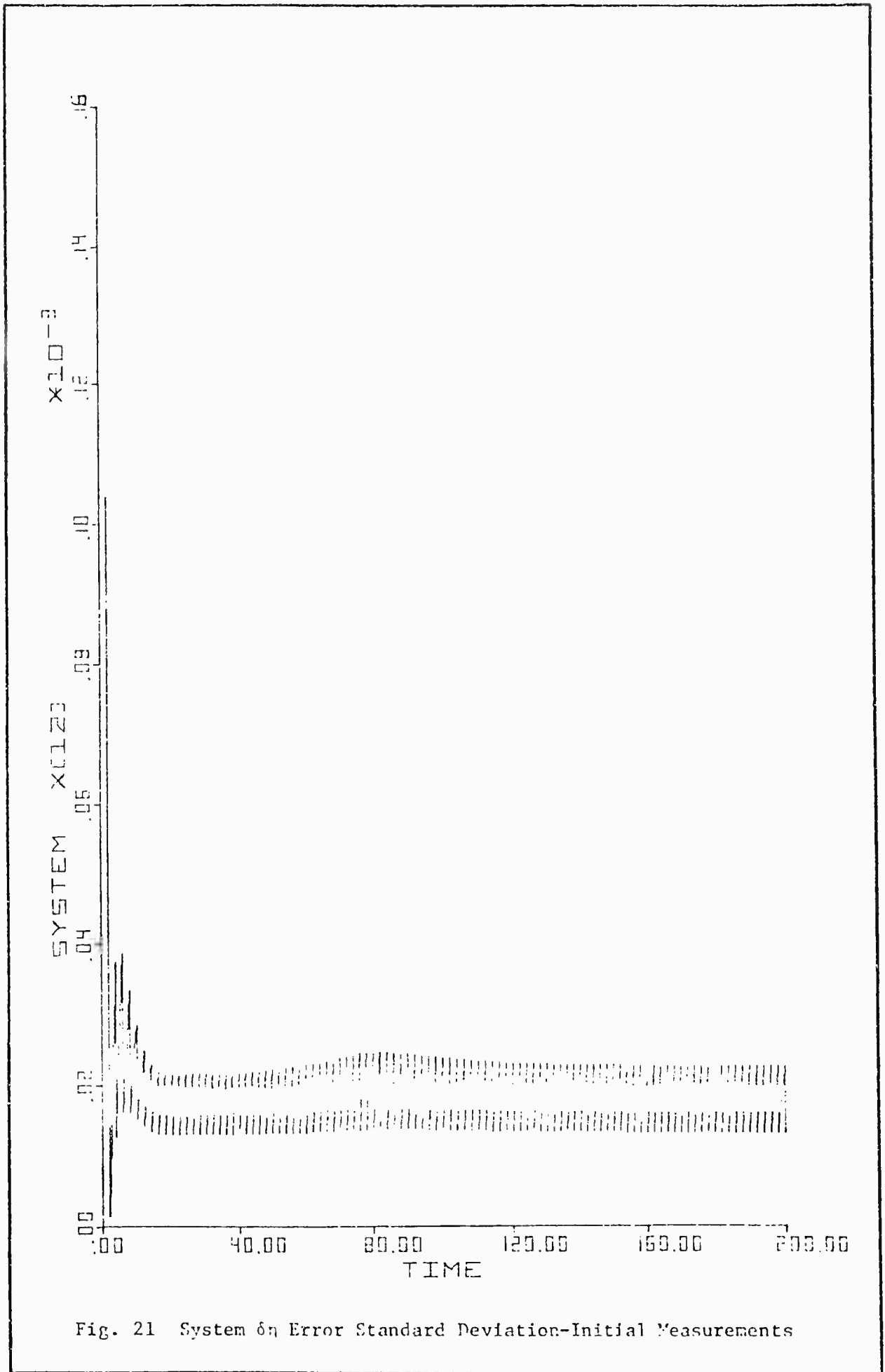


Fig. 21 System  $\delta\eta$  Error Standard Deviation-Initial Measurements

$0.15 \times 10^{-4}$  rad is achieved. This translates to about 9 m off target center for maximum range of about 600 km, and about 2 m for minimum range of about 100 km.

Effect of Orbital Estimate To determine how the orbital estimate improves or degrades the tracking, consider equation (6-1). The  $A_{rZ}$  term effectively helps to provide a prediction of the range in  $\omega_{LSy}$  between measurements. If  $A_{rZ}$  is incorrect by say 1% then the change in  $\omega_{LSy}$  between measurements will be incorrect by a similar relative magnitude. When the measurement is taken therefore, the antenna will be misaligned and some portion of this misalignment will have been caused by the original error in  $A_{rZ}$ . The measurement information in turn couples back through  $A_{rZ}$  to improve the estimate of vehicle inertial position. The loop is of course continuous and the above simplified analysis was made to illustrate the following point. Given a worst case situation, the typical error standard deviations in inertial position of 40 km as in fact produces an error in  $A_{rZ}$  of only 1%. Propagation of this error over 2 seconds results in the misalignment angle of about  $2 \times 10^{-6}$  rad. This is small compared to the error standard deviations shown by Figs. 20 and 21. In addition, it represents the worst case effect. Supposing however that a tracking accuracy equivalent to a misalignment angle error standard deviation of  $10^{-6}$  rad were required. The errors in inertial position would then be significant. There is a specific conclusion however which is quite surprising. To achieve an error standard deviation of  $10^{-5}$  rad in misalignment, an error standard deviation of 40 km in inertial position can be tolerated, provided the measurement update interval is small, i.e. of the order: 2 seconds or less.

Modifications to Truth Model

Objective. The purpose in changing the truth model was to demonstrate that the filter would perform over a reasonable range of measuring device precision. The tracking achieved with the baseline simulation parameters resulted in an error standard deviation in  $\delta\epsilon$  and  $\delta\eta$  of  $0.15 \times 10^{-4}$  rad. This is equivalent to an error standard deviation of 9 m off target at maximum range and 2 m at minimum range. Choosing arbitrarily a requirement for 1 m at maximum range implies that the  $\delta\epsilon$  and  $\delta\eta$  error standard deviations should be less than  $1.7 \times 10^{-6}$  rad at maximum range. The objective therefore was to modify the truth model to find the necessary measuring instrument quality to achieve this requirement. In so doing, the filter would be evaluated over a differing range of measurement parameters.

Approach The approach taken was to investigate the effect of improving the measurements of line of sight angular velocity, tracker misalignment, tracker acceleration, and range. The tracker acceleration and range measurements were first investigated. Adjusting the truth model measurement parameters to make these measurements perfect had no discernable effect on the tracking accuracy. In fact, the measurements could be degraded by a factor of 2 in the case of range and by a factor of approximately 5 for acceleration, before tracking accuracy became affected. The critical measurements were therefore those of line of sight angular velocity and misalignment angles.

Adjustment of Angular Velocity and Misalignment Angles The process of adjusting the truth model measurement parameters was slow and tedious since each adjustment required a retuning of the filter. The gyro drift

term in the measurements of angular velocities was found to be the largest single source of measurement error. This term was adjusted progressively from  $10^{-6}$  rad/sec to  $10^{-7}$  rad/sec. After each adjustment the filter was retuned. The resulting error standard deviation in the estimate of  $\delta\epsilon$  is shown by Figs. 22 and 23. (Note that  $\delta\epsilon$  and  $\delta\eta$  have identical error characteristics.) The mean steady state error standard deviation was  $5 \times 10^{-6}$  rad, which is equivalent to an error standard deviation of 3 m off target center at maximum range. A drift of  $10^{-7}$  rad/sec is in fact close to the region of current 'state of the art' gyros. A further improvement in gyro drift to  $0.5 \times 10^{-7}$  rad/sec did not significantly improve the estimates of  $\delta\epsilon$  and  $\delta\eta$ . It was therefore concluded at this point that a further improvement in the estimates of  $\delta\epsilon$  and  $\delta\eta$  could only be obtained by improving the measurements of those quantities.

Figs. 24 and 25 again show the error standard deviations for the misalignment angles  $\delta\epsilon$  and  $\delta\eta$ . These performance curves were obtained by improving the angle track scintillation noise from a standard deviation of  $10^{-6}$  rad to  $10^{-7}$  rad and totally removing the angle track bias. The resultant error standard deviations for  $\delta\epsilon$  is  $2 \times 10^{-6}$  rad which is equivalent to an error standard deviation of 1.2 m off target center at maximum range and 0.2 m off target center at minimum range.

Finally, Figs. 26 and 27 show the overall improvement to the error standard deviation for the estimate of vehicle inertial position  $X_1$ . The figure has been improved from about 40 km to about 20 km. Fig. 27 shows the true improvement to be nearer 10 km. This implies that the filter is overestimating the error by a factor of 2 and requires further tuning.

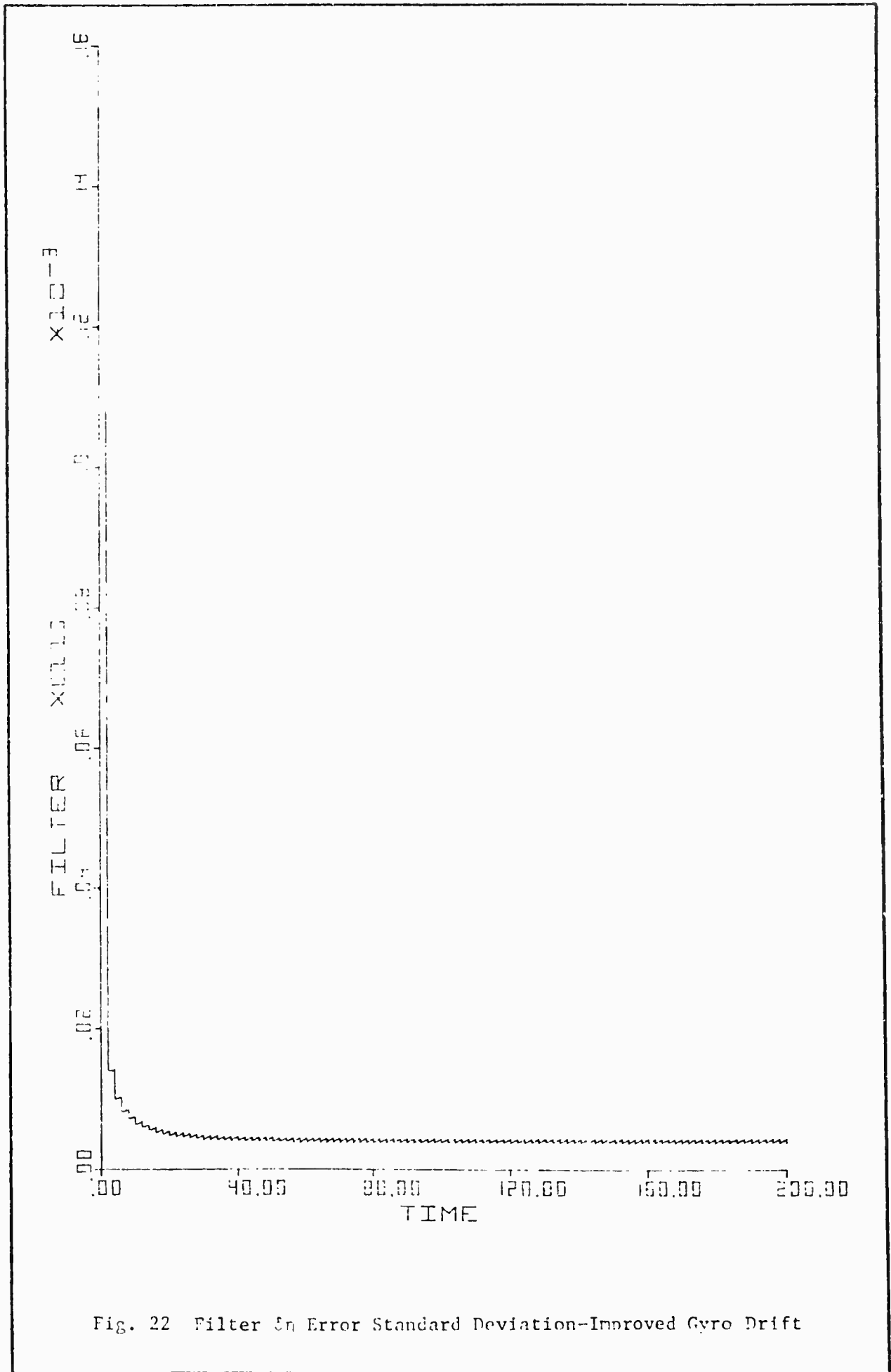


Fig. 22 Filter Error Standard Deviation-Improved Gyro Drift

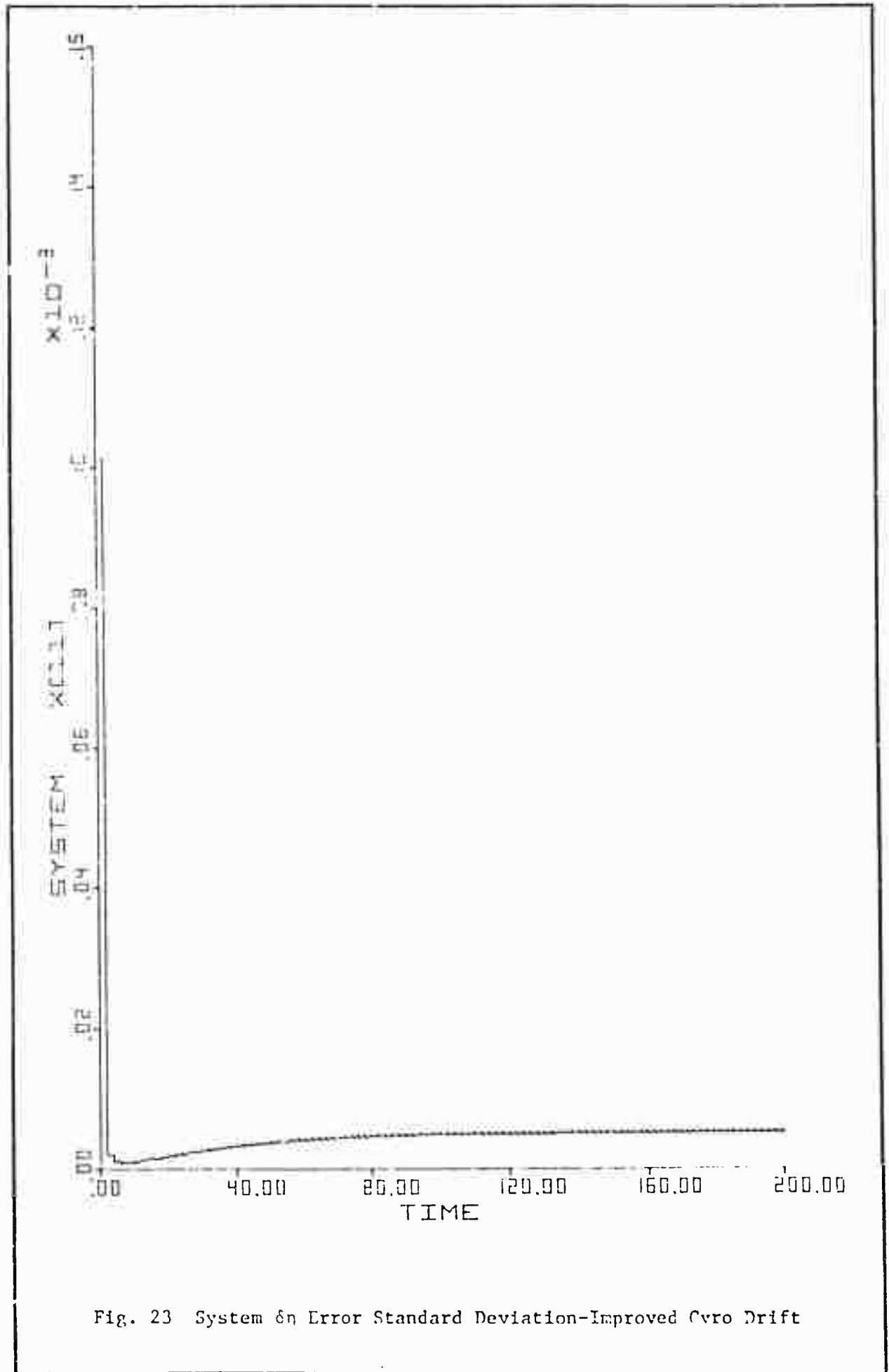


Fig. 23 System  $\delta n$  Error Standard Deviation-Improved Cyro Drift

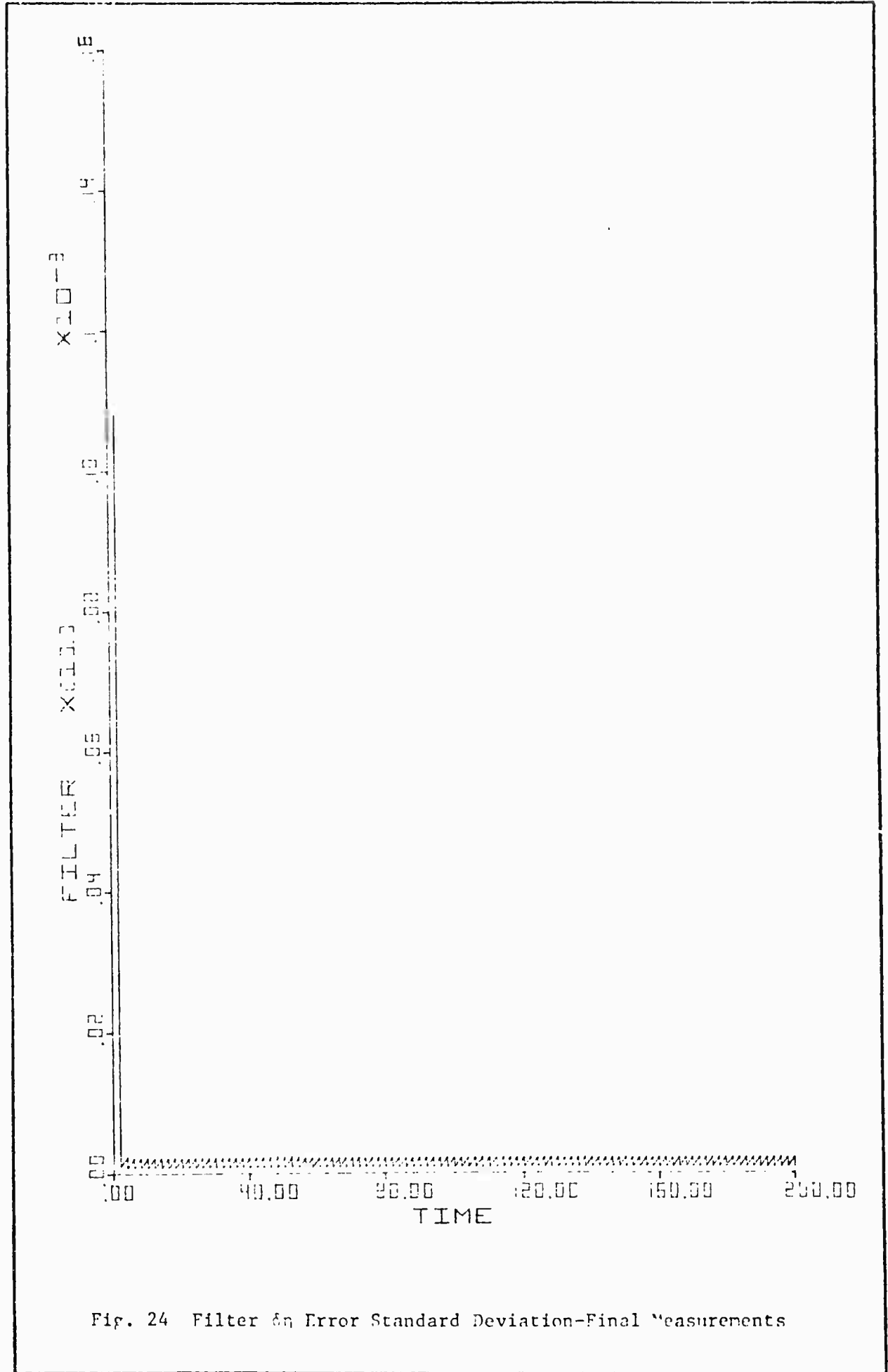


Fig. 24 Filter Error Standard Deviation-Final Measurements

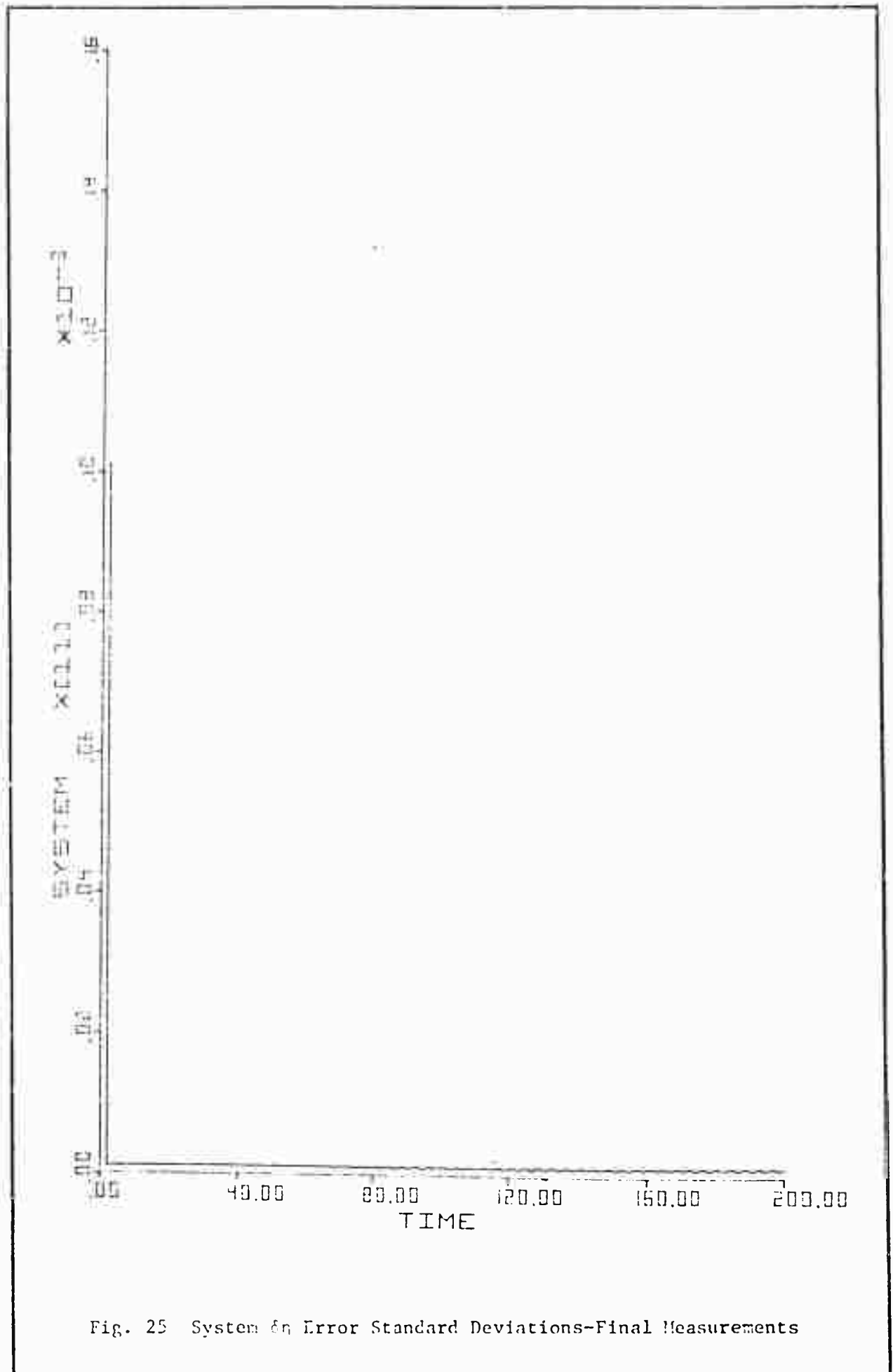


Fig. 25 System Error Standard Deviations-Final Measurements

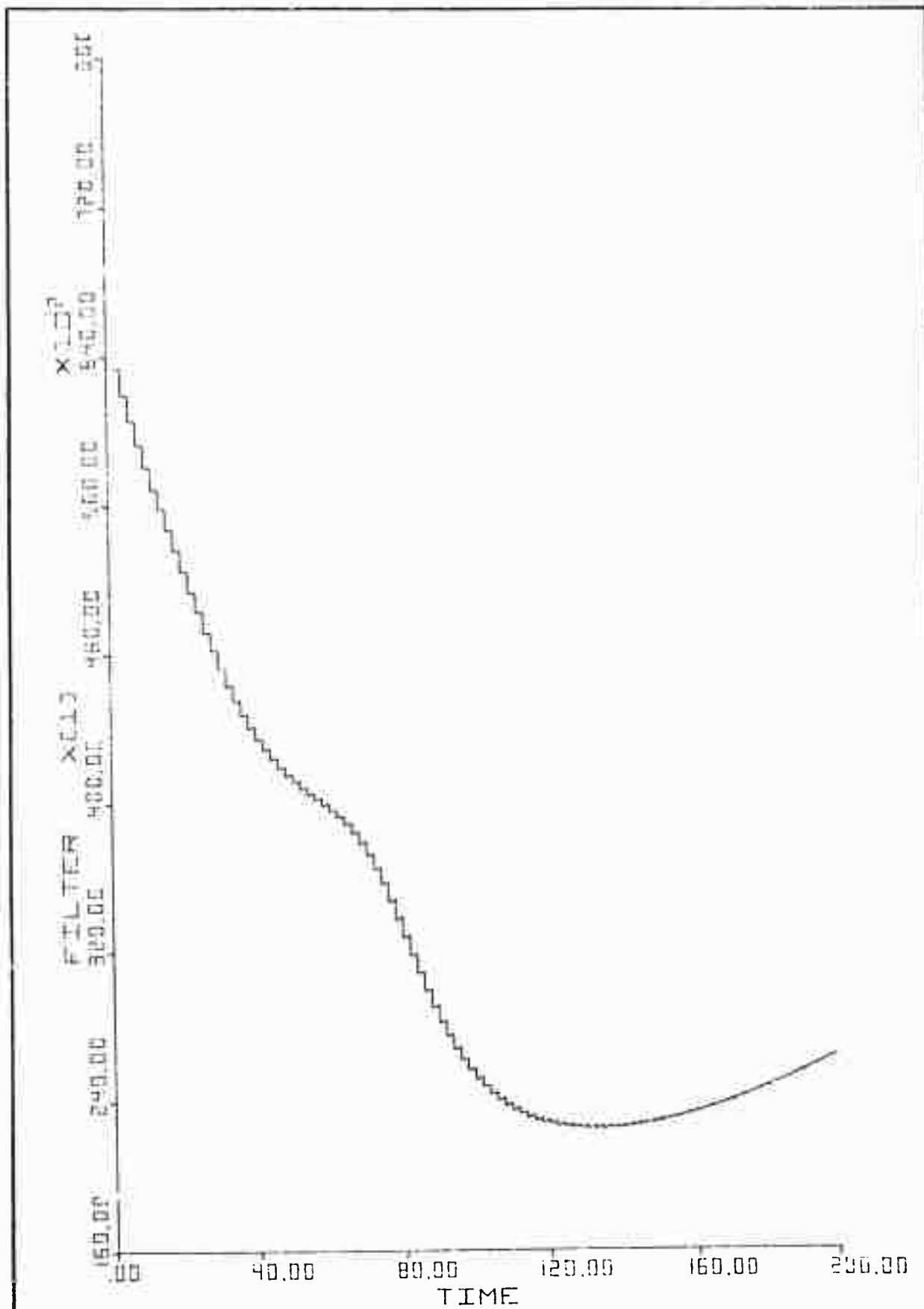


Fig. 26 Filter X1 Position Error Standard Deviation-Final Measurements

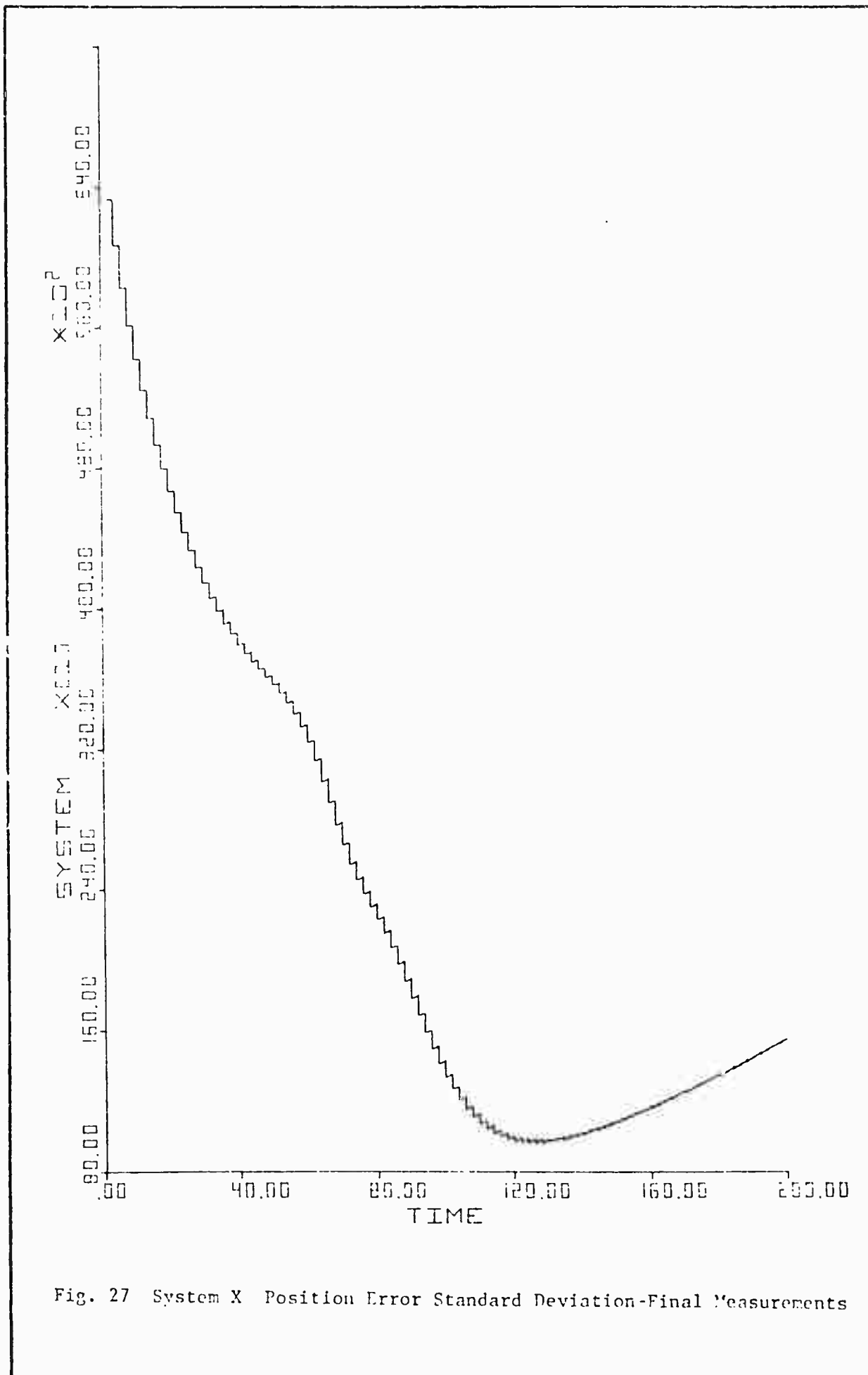


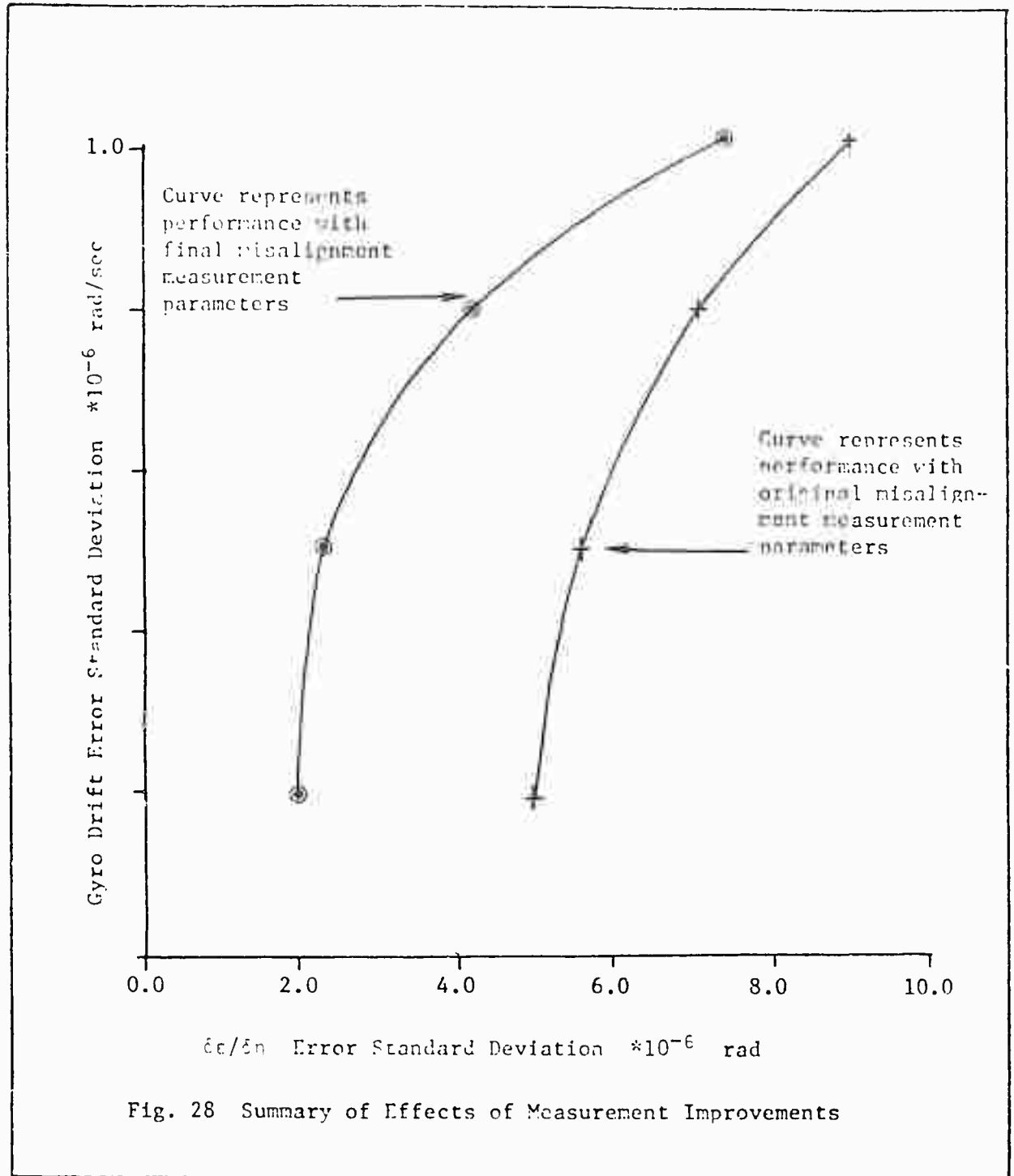
Fig. 27 System X Position Error Standard Deviation-Final Measurements

Summary of Effect of Truth Model Modifications

To achieve the requirement of approximately  $1.7 \times 10^{-6}$  rad for the error standard deviations in the estimates of  $\delta c$  and  $\delta \eta$ , it was found necessary to (1) reduce the gyro drift standard deviations from  $10^{-6}$  rad/sec to  $10^{-7}$  rad/sec, (2) remove the angle track bias errors, and (3) reduce the angle track scintillation noise standard deviation from  $10^{-6}$  rad to  $10^{-7}$  rad. Fig. 28 shows the family of error curves describing the adjustments made and the resulting performance. Each point on the curve represents some five computer runs for the system.

Clearly, these results indicate some stability in the filter formulation over a small range of measurement performance. It is emphasized however that only a small group of measurement parameters were tested and the results are by no means general.

Various recommendations for modifications to the truth model formulation will be made in the next section.



## VII. RECOMMENDATIONS AND CONCLUSIONS

Addition of Further Measurements

Coordinate Frames There are four basic coordinate frames used in the problem, the earth centered inertial and earth centered rotating coordinate frames which are related by the earth rotation rate, and the line of sight and tracker coordinate frames which are related by the misalignment angles  $\delta\epsilon$  and  $\delta\eta$ . The relationship between the tracker coordinate frame and the inertial earth centered coordinate frame was established by assuming that the tracker base could be maintained inertially stable, and that the two angles  $\theta$  and  $\phi$  (see Fig. 1, section II) were available (i.e. through perfect measurements).

It is somewhat unrealistic to assume that perfect measurements of  $\theta$  and  $\phi$  are available. In practice some type of resolver or integrating device would be used and stochastic modeling techniques might be necessary to model the device outputs accurately. Thus the inclusion of a realistic measurement model for  $\theta$  and for  $\phi$  would be desirable.

Orbit Determination The typical aircraft engaged in the long range satellite tracking role would probably be equipped with an inertial navigation system (INS) to provide aircraft inertial position information.

Now let  $\underline{R}^I$  be the range vector from aircraft to satellite expressed in inertial earth centered coordinates. Then if the aircraft inertial position vector is  $\underline{R}_A^I$  and the satellite inertial position vector is  $\underline{R}_S^I = \begin{bmatrix} X_1 \\ X_2 \\ X_3 \end{bmatrix}$

$$\begin{aligned} \underline{R}_S^I &= \underline{R}_A^I + \underline{R}^I \\ &= \underline{R}_A^I + C_T^I \underline{R}^T \end{aligned}$$

For perfect tracking,  $\underline{R}^T$  is the vector  $\begin{bmatrix} R \\ 0 \\ 0 \end{bmatrix}$ . Thus accurate knowledge of  $\underline{R}^T$ ,  $C_T^I$  which is a function of  $\theta$  and  $\phi$ , and  $\underline{R}_A^I$ , provides an accurate measurement of the satellite inertial position. Thus the measurements of  $\psi$  and  $\phi$  coupled with the INS measurement of  $\underline{R}_A^I$  can be used to provide a measurement of  $\underline{R}_S^I$ . Improvement of the estimate of satellite inertial position would lead to improvement in the estimate of satellite inertial velocity which in turn would lead to an improvement in the accuracy in orbit determination.

Now the sensitivity of tracking accuracy to the accuracy of the orbital estimate was not totally established. It was clear that the critical measurements were those of angular velocity and angular deviations. However, using 'state of the art' measuring devices, it may still be possible to achieve improved tracking performance with a better orbital estimate. The inclusion of INS position information is therefore considered desirable.

#### Alternate Methods of Modeling

Extending the above discussion further, if INS velocity information were also available then an alternate model formulation is possible. The state of the satellite vehicle is completely described by inertial position and velocity vectors. Similarly, the aircraft state is completely described by inertial position and velocity vectors. In fact, the relative position and velocity vectors from aircraft to satellite would also be completely described by these four vectors. The tracking problem is in essence a problem of estimating the relative position and velocity vectors, so that one method of modeling the system would be to use inertial states for the aircraft and satellite. This would result

in a 12 state model which is of the same dimension as the current filter model and additional states could be included if necessary to account for measurement parameters.

Considering the geometry of the tracking problem, the inertial formulation might be better conditioned numerically when target and tracker are widely separated in the inertial coordinate frame. If the target and tracker are in a close configuration, in which the magnitude of the range vector is small compared to the magnitudes of the two inertial position vectors, then modeling the problem in the line of sight coordinate frame would probably be better conditioned numerically. When tracking a low orbit satellite, both situations exist. Initially, as the satellite appears over the horizon, the two vehicles are widely separated inertially. As the satellite passes near to the aircraft however, the range vector can become small in magnitude. The incorporation of aircraft inertial position measurements into the present formulation is one method of meeting both situations.

#### Method of Analysis

The filter was tested using the covariance analysis method. The performance results are therefore valid only if the various approximations and assumptions described in section IV are also valid. The Monte-Carlo analysis method does not make such approximations and assumptions. The method involves making multiple runs using the non-linear state equations and artificially generated white Gaussian noises. Thus, provided a large number of runs are made, a general run performance trend can be obtained. The usual problem with the Monte-Carlo method is the practical limit on computational time. If the method is compared to

the covariance analysis method however, this is not such a severe problem. The latter generally requires a very large and complex computer program and multiple runs are often necessary in any case, to ensure satisfactory performance of the program. It should be recalled also that the covariance analysis is the first step analysis for a filtering problem. It is therefore recommended that further analysis of the problem should be carried out with the Monte Carlo method.

#### Summary of Recommendations

- a. The addition of realistic measurements for the angles  $\theta$  and  $\phi$  in the coordinate transformation matrix  $C_T^I$  should be investigated.
- b. Measurements of aircraft inertial position and velocity should be investigated and incorporated if performance benefits so dictate.
- c. The possibility of system modeling entirely using inertial coordinates should be investigated.
- d. With the present formulation, further work could now be carried out using the Monte-Carlo analysis technique. If the filter is significantly redesigned, then the covariance analysis method should again be used as the first step analysis.

#### Conclusions

The work carried out in this study falls into three categories:

- a. Development of the truth model and filter model state and measurement equations.
- b. Description of the Extended Kalman Filter and covariance analysis method equations.
- c. Testing of the filter.

Part c. represents the majority of the work. Where possible, existing computer programs were used. This was done to save program development time which essentially detracts from the real thrust of the study. However, in retrospect, it might have been better to develop new programs since the redevelopment of existing programs was a very time consuming task.

The most difficult part of the actual testing was the filter tuning. This basically involved changing various parameters in the filter model to maximize filter performance. The task is similar to an optimization problem where several parameters are simultaneously adjusted for optimum filter performance. Since each computer run required considerable computational time and storage, the optimization process was slow and time consuming.

As a whole, however, the study was an informative experience. There is much work still to be done in the area of aircraft to satellite tracking, but this study has certainly indicated some of the areas where problems can be expected, and some of the methods through which they can be solved.

Bibliography

1. Bate, R. et al, Fundamentals of Astrodynamics, New York: Dover Publications, Inc.
2. Asher, Robert B. and Watjen, David P., Kalman Filtering for Precision Pointing and Tracking Applications, AF Avionics Laboratory, Wright-Patterson AFB, AFAL Technical Report to be published.
3. Pearson, John B. and Stear, Edwin B., Kalman Filter Applications in Airborne Radar Tracking, IEEE Transactions, Vol. AES-10, No. 3, May 1974.
4. Fitts, John M., Aided Tracking as Applied to High Accuracy Pointing Systems, IEEE Transactions, Vol. AES-9, No. 3, May 1973.
5. Pearson, John B., Basic Studies in Airborne Radar Tracking Systems, PhD Dissertation, University of California at Los Angeles, September 1970.
6. Wrigley, Walter, et al, Gyroscope Theory, Design and Instrumentation, Cambridge Massachusetts and London England, MIT Press, 1969.
7. Broxneyer, Charles, Inertial Navigation Systems, New York, McGraw-Hill, 1964.
8. Baker, Robert M. L., Jr., and Makemson, Maud W., An Introduction to Astrodynamics, 2nd Ed., New York, London, Academic Press, 1967.
9. Baker, Robert M. L., Jr., Astrodynamics Applications and Advanced Topics, New York, London, Academic Press, 1967.
10. Escobol, Pedro R., Methods of Astrodynamics, New York, London, John Wiley & Sons, Inc., 1968.
11. Herrick, Samuel, Astrodynamics, Vol. II, New York, Van Nostrand Reinhold Company, London, 1972.
12. Meditch, J. S., Stochastic Optimal Linear Estimation and Control, New York, McGraw-Hill, 1969.
13. Maybeck, Peter S., Notes for a Course in Nonlinear Filtering Theory, Given at the Air Force Institute of Technology, WPAFB, Course Title EE7.66, 1974.
14. D, Appolito, Joseph A., The Evaluation of Kalman Filter Designs for Multisensor Integrated Navigation Systems, Report prepared by The Analytic Sciences Corporation for the Avionics Laboratory at WPAFB, Technical Report AFAL-TR-70-271, January 1971.

15. Kavton, Myron and Fried, Walter R., Avionics Navigation Systems, New York, John Wiley & Sons, 1969.
16. Pollard, Joseph, J., Orbital Parameter Determination by Weighted Least Square Error and Kalman Filtering Methods, Thesis submitted for the degree of Master of Science, Air Force Institute of Technology, WPAFB, 1973.

## Appendix A

Derivation of Gravitational Forces Due to Earth (Refs. 8, 9, 10, 11)

Fig. 29 below shows the inertial earth centered coordinate frame (I - frame) and the rotating earth centered coordinate frame (r - frame). The two frames align when  $\theta = 0$ .

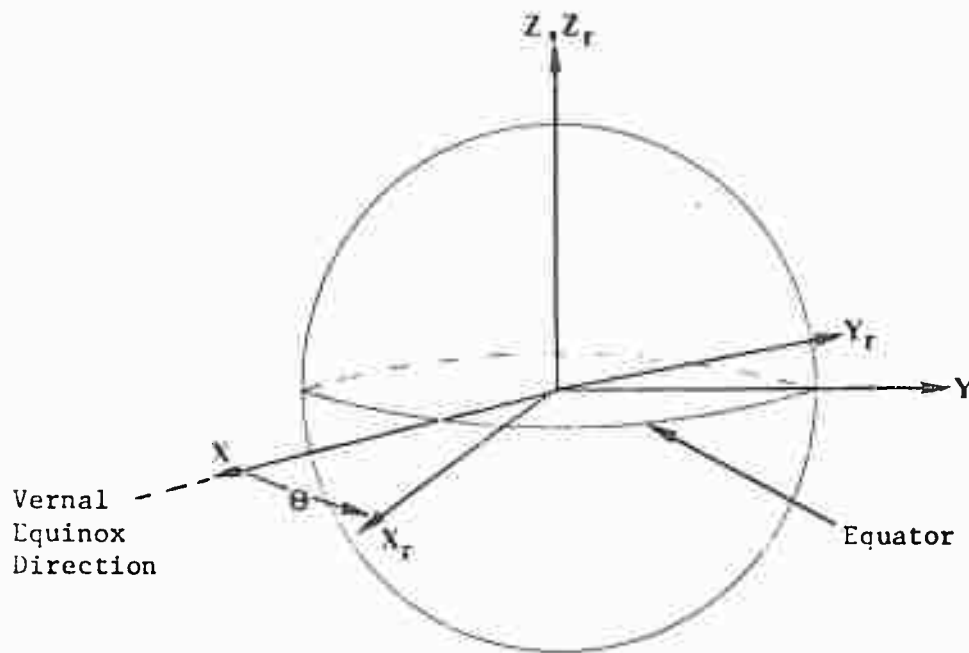


Fig. 29 Inertial and Rotating Coordinate Frames

Defining the Earth's gravitational potential as  $U$  which is a function of position  $X_r, Y_r, Z_r$  in the rotating frame i.e.  $U = U(X_r, Y_r, Z_r)$ , then at any point in space, the three components of gravitational force expressed in the rotating coordinate frame can be defined as  $A_{P_{X_r}}, A_{g_{Y_r}}$ , and  $A_{g_{Z_r}}$  such that:

$$A_{gX_r} = \frac{\partial U}{\partial X_r}$$

$$A_{gY_r} = \frac{\partial U}{\partial Y_r}$$

$$A_{gZ_r} = \frac{\partial U}{\partial Z_r}$$

If  $U$  is defined therefore, the gravitational forces in the rotating frame can be calculated. The forces are required however in the inertial coordinate frame so a coordinate transformation from rotating to inertial coordinates must be defined. Let  $C_r^I$  be the coordinate transformation matrix from rotating to non-rotating (inertial) coordinates, then:

$$C_r^I = \begin{bmatrix} \cos(\theta) & -\sin(\theta) & 0 \\ \sin(\theta) & \cos(\theta) & 0 \\ 0 & 0 & 1 \end{bmatrix}$$

where:

$$\theta = \theta_{go} + WE t$$

$$\theta_{go} = \text{Local Greenwich hour angle at } t = 0$$

$$WE = \text{Earth rotation rate}$$

$$t = \text{time}$$

and if the force due to gravity in the inertial coordinate system is the vector:

$$\underline{A_g} = \begin{bmatrix} A_{g_1} \\ A_{g_2} \\ A_{g_3} \end{bmatrix}$$

then:

$$\begin{bmatrix} A_{g_1} \\ A_{g_2} \\ A_{g_3} \end{bmatrix} = C_R^I \begin{bmatrix} A_{g_{X_r}} \\ A_{g_{Y_r}} \\ A_{g_{Z_r}} \end{bmatrix}$$

#### Gravitational Potential Model $U(X_r, Y_r, Z_r)$

The problem under consideration examines the tracking problem for a near earth satellite. In order to express the gravitational forces due to the earth for a low orbit satellite accurately, the following gravitational potential model was chosen:

$$U = \frac{k_e^2 m}{r} \left[ 1 + \sum_{k=2}^6 \left( \sum_{m=0}^k \frac{P_k^{(m)}(\sin \phi)}{r^k} \left\{ C_{k,m} \cos(m\lambda_E) + S_{k,m} \sin(m\lambda_E) \right\} \right) \right] \quad (a-1)$$

where the terms in equation (a-1) are defined as follows:

$k_e$  is the gravitational constant for the earth

$m$  is the mass of the earth

$r$  is the radial distance of the body from the earth center

$P_k^{(m)}$  are Legendre functions, that is the functions;

$$P_k^{(m)}(x) = (1-x^2)^{m/2} \frac{d^m}{dx^m} \left\{ P_k(x) \right\}$$

and  $P_k(x)$  is the Legendre polynomial with argument  $x$ .

Note that in equation (3), the argument of the Legendre polynomials is  $\sin \theta$ .

$\lambda_E$  is the longitude of the satellite with respect to the Greenwich meridian

$\theta$  is the geocentric declination angle for the satellite

The  $C_{k,m}$  and  $S_{k,m}$  are harmonic coefficients for the gravitational potential such that:

$$C_{k,0} = -J_k^{(0)} \quad \text{and} \quad S_{k,0} = 0$$

and the  $J_k^{(0)}$  coefficients are termed 'zonal harmonic'

$C_{k,m}$  and  $S_{k,m}$  are termed 'tesseral harmonic' if  $m \neq k$ ,  $m > 0$

and 'sectorial harmonic' if  $m = k$

The significance of the terms zonal, tesseral, and sectorial is illustrated by Fig. 30(Ref. 9)

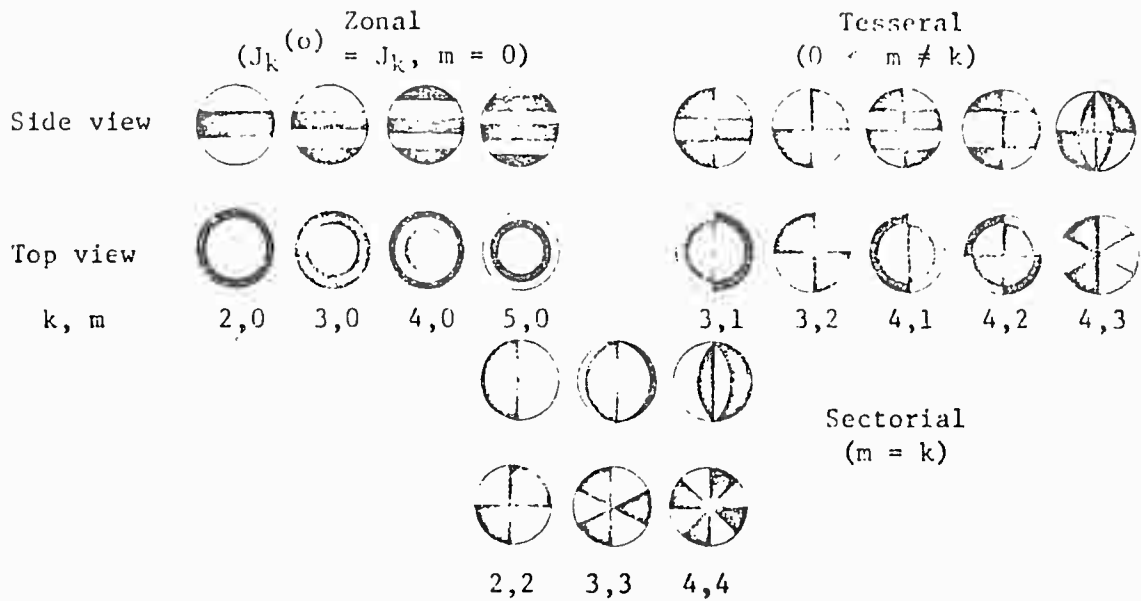


Fig. 30 Gravity Harmonics

Equation (3) could be extended to include higher harmonics than 6,6. This would largely depend on the type of orbit and the accuracy required. For the purposes of this study, the harmonics up to and including 6,6 are defined to represent the true gravitational field. Thus any filter model which might use a lower order model will be compared against this particular truth model, and the inclusion of higher terms in the truth model would not significantly improve this comparison.

#### Calculation of the Second Partial Derivatives of U (Ref. 16)

In order to linearize the state equations for use with the Extended Kalman Filter, it will be necessary to find the second partial derivatives of the gravitational potential  $U$  with respect to the satellite inertial position  $(X_1, X_2, X_3)$  measured along the  $X, Y$  and  $Z$  axes respectively of the inertial frame (see Fig. 1). The analytic calculations of the first partials only are long and complex and result in several hundred terms. An analytic calculation of the second partials would be complex,

prone to error and too time consuming computationally. In Ref. 16, it was shown that for this type of orbit, a one sided differencing method provided an accurate value for the second partials providing the differencing step size is kept small. A step size of 1 meter was chosen since any further reduction did not change the numerical result while at the same time, a calculation using 1 meter did not introduce round-off errors. Calculation of these second partials is carried out in the rotating coordinate frame to give the matrix of second partial derivatives:

$$U_{2r} = \begin{bmatrix} \frac{\partial^2 U}{\partial X_r^2} & \frac{\partial^2 U}{\partial X_r \partial Y_r} & \dots \\ \dots & \dots & \dots \\ \dots & \dots & \frac{\partial^2 U}{\partial Z_r^2} \end{bmatrix} \quad (a-2)$$

where the notation indicates the matrix is with respect to the rotating frame. Defining  $U_{2I}$  as the matrix of second partial derivatives taken with respect to the inertial non-rotating earth centered coordinate frame (I - frame) then:

$$U_{2I} = C_r^I T U_{2r} C_r^I$$

$$= \begin{bmatrix} \frac{\partial^2 U}{\partial X_1^2} & \frac{\partial^2 U}{\partial X_1 X_2} & \dots \\ \dots & \dots & \dots \\ \dots & \dots & \frac{\partial^2 U}{\partial X_3^2} \end{bmatrix} \quad (a-3)$$

## Appendix B

Linearization of Truth Model State and Measurement Equations

## Definitions:

$X_1, X_2, X_3$	Inertial satellite position vector
$X_4, X_5, X_6$	Inertial satellite velocity vector
$x_s, y_s, z_s$	Position vector of sun in earth centered inertial coordinates
$x_m, y_m, z_m$	Position vector of moon in earth centered inertial coordinates
$r_v$	Distance from earth center to satellite
$r_s$	Distance from earth center to sun
$r_m$	Distance from earth center to moon
$\rho$	Atmospheric density at altitude h
$\rho_0$	Sea level atmospheric density
$\beta$	Altitude atmospheric density decay rate
$V_a$	Magnitude of satellite velocity relative to rotating atmosphere
$r_{vs}$	Distance from satellite to sun
$r_{vm}$	Distance from satellite to moon

- WE Earth rotation rate
- $U_{2I}$  Matrix of second partials of gravity gradient with respect to satellite position in earth centered inertial coordinates
- $u(i, j)$  Element in  $i^{\text{th}}$  row and  $j^{\text{th}}$  column of  $U_{2I}$
- $U_{2T}$  Matrix of second partials of gravity gradient with respect to satellite position in tracker coordinates
- $$(U_{2T} = (C_I^T)^T U_{2I} C_I^T)$$
- $\bar{u}(i, j)$  Element in  $i^{\text{th}}$  row and  $j^{\text{th}}$  column of  $U_{2T}$
- $\mu_{\odot}$  Sun's gravitational constant
- $\mu_{\text{D}}$  Moon's gravitational constant

#### System F - Matrix

Given the non-linear state equation:

$$\dot{\underline{x}}(t) = \underline{f}_s(\underline{x}(t), t) + G_s(t) \underline{w}_s(t)$$

$$F_s(t) = \left. \frac{\partial \underline{f}_s}{\partial \underline{x}} \right|_{\underline{x}_n(t)}$$

where  $\underline{x}_n(t)$  is the nominal reference state trajectory.

Using the non-linear state equation defined in the summary to section II, the matrix  $F_s(t)$  is:

$$F_S \Delta = \begin{bmatrix} F_1(8 \times 8) & & & & 0(8 \times 53) \\ \dots & & & & \dots \\ F_2(6 \times 8) & F_3(6 \times 6) & F_4(6 \times 11) & F_5(6 \times 36) \\ \dots & & & & \dots \\ 0(47 \times 14) & & F_6(11 \times 11) & & 0(47 \times 36) \\ \dots & & & & \dots \\ & & & & 0(36 \times 11) \end{bmatrix}$$

which is evaluated along  $x_n(t)$ . The figures in brackets indicate the dimensions of the various sub-matrices.

$$F_1 = \begin{bmatrix} 0(3 \times 3) & & & I(3 \times 3) & & & 0(3 \times 2) \\ \dots & & & \dots & & & \dots \\ f_1 & f_2 & f_3 & f_4 & f_5 & 0 & f_6 & f_7 \\ f_8 & f_9 & f_{10} & f_{11} & f_{12} & 0 & f_{13} & f_{14} \\ f_{15} & f_{16} & f_{17} & f_{18} & f_{19} & 0 & f_{20} & f_{21} \\ \dots & & & & & & \dots \\ & & & & & & & 0(2 \times 8) \end{bmatrix}$$

where:

$$f_1 = u(1, 1) + \left\{ \frac{0.5 X_7 V_a \beta \rho X_1 (X_4 + WE X_2)}{r_v} \right\} \\ + \left\{ \frac{0.5 X_7 WE \rho (X_5 - WE X_1)(X_4 + WE X_2)}{V_a} \right\} \\ - \frac{\mu_0}{r_{vs}^3} + \frac{3\mu_0 (x_s - X_1)^2}{r_{vs}^5} - \frac{\mu_D}{r_{vm}^3} + \frac{3\mu_D (x_m - X_1)^2}{r_{vm}^5}$$

$$\begin{aligned}
 f_2 = & u(1, 2) + \left\{ \frac{0.5 X_7 V_a \beta \rho X_2 (X_4 + WE X_2)}{r_v} \right\} \\
 & - \left\{ \frac{0.5 X_7 WE \rho (X_4 + WE X_2)^2}{V_a} \right\} - \left\{ 0.5 X_7 \rho WE V_a \right\} \\
 & + \left\{ \frac{3\mu_{\odot} (x_s - X_1) (y_s - X_2)}{r_{vs}^5} \right\} + \left\{ \frac{3\mu_{\oplus} (x_m - X_1) (y_m - X_2)}{r_{vm}^5} \right\}
 \end{aligned}$$

$$\begin{aligned}
 f_3 = & u(1, 3) + \left\{ \frac{0.5 X_7 V_a \beta \rho X_3 (X_4 + WE X_2)}{r_v} \right\} \\
 & - \left\{ \frac{0.5 X_7 \rho X_3 (X_4 + WE X_2)}{V_a} \right\} \\
 & + \left\{ \frac{3\mu_{\odot} (x_s - X_1) (z_s - X_3)}{r_{vs}^5} \right\} + \left\{ \frac{3\mu_{\oplus} (x_m - X_1) (z_m - X_3)}{r_{vm}^5} \right\}
 \end{aligned}$$

$$f_4 = -0.5 X_7 \rho \left\{ \frac{(X_4 + WE X_2)^2}{V_a} + V_a \right\}$$

$$f_5 = \frac{-0.5 X_7 \rho (X_4 + WE X_2) (X_5 - WE X_1)}{V_a}$$

$$f_6 = -0.5 \rho V_a (X_4 + WE X_2)$$

$$f_7 = -4.5 \times 10^{-7} \frac{x_s}{r_s}$$

$$\begin{aligned}
 f_8 = u(2, 1) &+ \left\{ \frac{0.5 X_7 Va \beta \rho X_1 (X_5 - WE X_1)}{r_v} \right\} \\
 &+ \left\{ \frac{0.5 X_7 WE \rho (X_5 - WE X_1)^2}{Va} \right\} \\
 &+ \left\{ 0.5 X_7 Va \rho WE \right\} + \left\{ \frac{3\mu_{\odot} (y_s - x_2)(x_s - X_1)}{r_{vs}^5} \right\} \\
 &+ \left\{ \frac{3\mu_{\mathcal{D}} (y_m - X_2)(x_m - X_1)}{r_{vm}^5} \right\}
 \end{aligned}$$

$$\begin{aligned}
 f_9 = u(2, 2) &+ \left\{ \frac{0.5 X_7 Va \beta \rho X_2 (X_5 - WE X_1)}{r_v} \right\} \\
 &- \left\{ \frac{0.5 X_7 WE \rho (X_5 - WE X_1)(X_4 + WE X_2)}{Va} \right\} \\
 &- \frac{\mu_{\odot}}{r_{vs}^3} + \frac{3\mu_{\odot} (y_s - X_2)^2}{r_{vs}^5} - \frac{\mu_{\mathcal{D}}}{r_{vm}^3} \\
 &+ \frac{3\mu_{\mathcal{D}} (y_m - X_2)^2}{r_{vm}^5}
 \end{aligned}$$

$$\begin{aligned}
 f_{10} = & u(2, 3) + \left\{ \frac{0.5 X_7 Va \beta \rho X_3 (X_5 - WE X_1)}{r_v} \right\} \\
 & - \left\{ \frac{0.5 X_7 \rho WE X_3 (X_5 - WE X_1)}{Va} \right\} \\
 & + \left\{ \frac{3\mu_{\odot} (y_s - X_2)(z_s - X_3)}{r_{vs}^5} \right\} \\
 & + \left\{ \frac{3\mu_{\oplus} (y_m - X_2)(z_m - X_3)}{r_{vm}^5} \right\}
 \end{aligned}$$

$$f_{11} = \frac{-(X_4 + WE X_2)(X_5 - WE X_1) 0.5 X_7 \rho}{Va}$$

$$f_{12} = -0.5 X_7 \rho \left\{ \frac{(X_5 - WE X_1)^2}{Va} + Va \right\}$$

$$f_{13} = -0.5 \rho Va (X_5 - WE X_1)$$

$$f_{14} = -4.5 \times 10^{-7} \frac{y_s}{r_s}$$

$$\begin{aligned}
 f_{15} = & u(3, 1) + \left\{ \frac{0.5 X_7 \beta \rho X_1 Va X_3}{r_v} \right\} \\
 & + \left\{ \frac{0.5 X_7 \rho WE X_3 (X_5 - WE X_1)}{Va} \right\} \\
 & + \left\{ \frac{3\mu_{\odot} (z_s - X_3)(x_s - X_1)}{r_{vs}^5} \right\} + \left\{ \frac{3\mu_{\oplus} (z_m - X_3)(x_m - X_1)}{r_{vm}^5} \right\}
 \end{aligned}$$

$$\begin{aligned}
 f_{16} = & u(3, 2) + \left\{ \frac{0.5 X_7 \beta \rho X_2 Va X_3}{r_v} \right\} \\
 & - \left\{ \frac{0.5 X_7 \rho WE X_3 (X_4 + WE X_2)}{Va} \right\} \\
 & + \left\{ \frac{3\mu_{\odot} (z_s - X_3) (y_s - X_2)}{r_{vs}^5} \right\} \\
 & + \left\{ \frac{3\mu_{\mathcal{D}} (z_m - X_3) (y_m - X_2)}{r_{vm}^5} \right\}
 \end{aligned}$$

$$\begin{aligned}
 f_{17} = & u(3, 3) + \left\{ \frac{0.5 X_7 \beta \rho Va X_3^2}{r_v} \right\} - \frac{0.5 X_7 \rho X_3^2}{Va} \\
 & - 0.5 X_7 \rho Va - \frac{\mu_{\odot}}{r_{vs}^3} + \frac{3\mu_{\odot} (z_s - X_3)^2}{r_{vs}^5} \\
 & - \frac{\mu_{\mathcal{D}}}{r_{vm}^3} + \frac{3\mu_{\mathcal{D}} (z_m - X_3)^2}{r_{vm}^5}
 \end{aligned}$$

$$f_{18} = \frac{-0.5 X_7 \rho (X_4 + WE X_2) X_3}{Va}$$

$$f_{19} = \frac{-0.5 X_7 \rho (X_5 - WE X_1) X_3}{Va}$$

$$f_{20} = -0.5 \rho Va X_3$$

$$f_{21} = -4.5 \times 10^{-7} \frac{z_s}{r_s}$$

$$F_2 = \begin{bmatrix} g_1 & g_2 & g_3 & | & \\ g_4 & g_5 & g_6 & | & \\ \hline & & & & 0(6 \times 5) \\ & 0(3 \times 3) & & & \\ \hline g_7 & g_8 & g_9 & | & \end{bmatrix}$$

where:

$$g_1 = \frac{-\bar{u}(3, 1)}{R} - \frac{\delta \epsilon \bar{u}(1, 1)}{R}$$

$$g_2 = \frac{-\bar{u}(3, 2)}{R} - \frac{\delta \epsilon \bar{u}(1, 2)}{R}$$

$$g_3 = \frac{-\bar{u}(3, 3)}{R} - \frac{\delta \epsilon \bar{u}(1, 3)}{R}$$

$$g_4 = \frac{-\bar{u}(2, 1)}{R} - \frac{\delta \eta \bar{u}(1, 1)}{R}$$

$$g_5 = \frac{-\bar{u}(2, 2)}{R} - \frac{\delta \eta \bar{u}(1, 2)}{R}$$

$$g_6 = \frac{-\bar{u}(2, 3)}{R} - \frac{\delta \eta \bar{u}(1, 3)}{R}$$

$$g_7 = \bar{u}(1, 1) + \delta\eta \bar{u}(2, 1) - \delta\varepsilon \bar{u}(3, 1)$$

$$g_8 = \bar{u}(1, 2) + \delta\eta \bar{u}(2, 2) - \delta\varepsilon \bar{u}(3, 2)$$

$$g_9 = \bar{u}(1, 3) + \delta\eta \bar{u}(2, 3) - \delta\varepsilon \bar{u}(3, 3)$$

$$\begin{bmatrix}
 -\frac{2 V_I}{R} & \omega_{TX} + \delta \eta \omega_{TY} & \omega_{LSZ} \omega_{TY} & -\frac{A_{TX}}{R} & \frac{2 V_I \omega_{LSY}}{R^2} + \frac{A_{TY}}{R^2} & -\frac{2 \omega_{LSY}}{R} \\
 -\omega_{TX} + \delta \epsilon \omega_{TZ} & -2 \omega_{LSZ} \omega_{TZ} & -\frac{A_{TX}}{R} - \omega_{LSY} \omega_{TZ} & \omega_{LSY} \omega_{TZ} & \frac{2 V_I \omega_{LSZ}}{R^2} - \frac{A_{TY}}{R^2} & -\frac{2 \omega_{LSZ}}{R} \\
 0 & 1 & 0 & -\omega_{TX} & 0 & 0 \\
 1 & 0 & \omega_{TX} & 0 & 0 & 0 \\
 0 & 0 & 0 & 0 & 0 & 1 \\
 2 \omega_{LSY} R & 2 \omega_{LSZ} R & A_{TY} & -A_{TZ} & (\omega_{LSY}^2 + \omega_{LSZ}^2) & 0
 \end{bmatrix}$$

$$\begin{bmatrix}
 0 & 0 & 0 & \omega_{LSZ} & \delta\eta & \omega_{LSZ} & -(\omega_{LSZ})^2 & \frac{\delta\epsilon}{R} & 0 & \frac{1}{R} & 0 & 0 \\
 0 & 0 & 0 & -\omega_{LSY} & -\delta\eta & \omega_{LSY} & \delta\epsilon & \omega_{LSY} & \frac{1}{R} & 0 & 0 & 0 \\
 0 & 0 & 0 & -\delta\epsilon & 0 & 0 & -1 & 0 & 0 & 0 & 0 & 0 \\
 0 & 0 & 0 & \delta\eta & -1 & 0 & 0 & 0 & 0 & 0 & 0 & 0 \\
 0 & 0 & 0 & 0 & 0 & 0 & 0 & 0 & 0 & 0 & 0 & 0 \\
 0 & 0 & 0 & 0 & 0 & 0 & 0 & -1 & -\delta\eta & \delta\epsilon & 0 & 0
 \end{bmatrix}$$

$$F_4 =$$

$$F_5 = \begin{bmatrix} F_{5_1} & F_{5_2} & F_{5_3} & F_{5_4} & F_{5_5} & F_{5_6} \\ (6 \times 6) & (6 \times 6) & (6 \times 6) & (6 \times 7) & (6 \times 7) & (6 \times 4) \end{bmatrix}$$

$\omega_{LSZ}$	$A_{TX}$	$\omega_{LSZ}$	$A_{TY}$	$\omega_{LSZ}$	$A_{TZ}$	$\delta n$	$\omega_{LSZ}$	$A_{TY}$	$\delta n$	$\omega_{LSZ}$	$A_{TZ}$
$- \omega_{LSY}$	$A_{TX}$	$- \omega_{LSY}$	$A_{TY}$	$- \omega_{LSY}$	$A_{TZ}$	$- \delta n$	$\omega_{LSY}$	$A_{TY}$	$- \delta n$	$\omega_{LSY}$	$A_{TZ}$
$- \delta \epsilon$	$A_{TX}$	$- \delta \epsilon$	$A_{TY}$	$- \delta \epsilon$	$A_{TZ}$	$0$	$0$	$0$	$0$	$0$	$0$
$\delta n$	$A_{TX}$	$\delta n$	$A_{TY}$	$\delta n$	$A_{TZ}$	$- A_{TX}$	$- A_{TY}$	$- A_{TZ}$	$0$	$0$	$0$
$0$	$0$	$0$	$0$	$0$	$0$	$0$	$0$	$0$	$0$	$0$	$0$
$0$	$0$	$0$	$0$	$0$	$0$	$0$	$0$	$0$	$0$	$0$	$0$

F 51

$$\begin{bmatrix}
 -\omega_{LSZ}^2 A_{TX} & -\omega_{LSZ}^2 A_{TY} & -\omega_{LSZ}^2 A_{TZ} & \frac{\delta \epsilon A_{TX}}{R} & 0 & \frac{A_{TZ}}{R} \\
 \delta \epsilon \omega_{LSY} A_{TX} & \delta \epsilon \omega_{LSY} A_{TY} & \delta \epsilon \omega_{LSY} A_{TZ} & \frac{\delta \eta A_{TX}}{R} & -\frac{A_{TY}}{R} & 0 \\
 -A_{TX} & -A_{TY} & -A_{TZ} & 0 & 0 & 0 \\
 0 & 0 & 0 & 0 & 0 & 0 \\
 0 & 0 & 0 & 0 & 0 & 0 \\
 0 & 0 & 0 & -A_{TX} & -\delta \eta A_{TY} & \delta \epsilon A_{TZ}
 \end{bmatrix}$$

F5<sub>2</sub> =

$$\begin{bmatrix}
 -\omega_{LSZ} & \omega_{TY} & \omega_{LSZ} & \omega_{TZ} & \delta\eta & \omega_{LSZ} & \omega_{TX} & -\omega_{LSZ}^2 & \omega_{TY} \\
 \omega_{LSY} & \omega_{TY} & -\omega_{LSY} & \omega_{TZ} & -\delta\eta & \omega_{LSY} & \omega_{TX} & \delta\epsilon & \omega_{LSY} \omega_{TY} \\
 \delta\epsilon & \omega_{TY} & -\delta\epsilon & \omega_{TZ} & 0 & \omega_{TX} & -\omega_{TY} & & \\
 -\delta\eta & \omega_{TY} & \delta\eta & \omega_{TZ} & -\omega_{TX} & \omega_{TZ} & 0 & 0 & 0 \\
 0 & 0 & 0 & 0 & 0 & 0 & 0 & 0 & 0 \\
 0 & 0 & 0 & 0 & 0 & 0 & 0 & 0 & 0
 \end{bmatrix}$$

F53

$\frac{-\delta\epsilon \Delta_{TY}}{R}$	$\frac{\delta\epsilon \Delta_{TZ}}{R}$	0	$\frac{-\Delta_{TX}}{R}$	0	$\frac{\delta\epsilon \Delta_{TX}^2}{R}$
$\frac{-\delta\eta \Delta_{TY}}{R}$	$\frac{\delta\eta \Delta_{TZ}}{R}$	$\frac{-\Delta_{TX}}{R}$	0	$\frac{\Delta_{TZ}}{R}$	$\frac{\delta\epsilon \Delta_{TX}}{R}$
0	0	0	0	0	0
0	0	0	0	0	0
0	0	0	0	0	0
$\Delta_{TY}$	$-\Delta_{TZ}$	$-\delta\eta \Delta_{TX}$	$-\delta\epsilon \Delta_{TX}$	$\delta\eta \Delta_{TZ}$	$-\Delta_{TX}^2$

F<sub>54</sub> =

$\frac{\delta \epsilon A_{TX}^3}{R}$	0	0	$\frac{A_{TZ}^3}{R}$	0	0
$\frac{\delta \eta A_{TX}^3}{R}$	$-\frac{A_{TY}^2}{R}$	$-\frac{A_{TY}^3}{R}$	0	0	0
0	0	0	0	0	0
0	0	0	0	0	0
0	0	0	0	0	0
$-A_{TX}^3$	$-\delta \eta A_{TY}^2$	$-\delta \eta A_{TY}^3$	$\delta \epsilon A_{TZ}^2$	$\delta \epsilon A_{TZ}^3$	0

F<sub>55</sub> =



System  $Q_S$  - matrix and  $G_S$  - matrix

If  $Q_1$  is the variance of the white noise  $W_1$  driving the state equation for  $X_4$ ,  $Q_2$  is the variance for  $W_2$  and  $Q_3$  is the variance for  $W_3$ , then:

$$Q_S = \left[ \begin{array}{ccc|c} Q_1 & 0 & 0 & | \\ 0 & Q_2 & 0 & | \quad 0(3 \times 11) \\ 0 & 0 & Q_3 & | \\ \hline & & & | \\ 0(11 \times 3) & & & | \quad I(11 \times 11) \\ & & & | \end{array} \right]$$

and  $G_S$  is given by:

$$G_S = \left[ \begin{array}{ccc|c} 0(3 \times 3) & & & | \\ \hline & & & | \quad 0(14 \times 11) \\ I(3 \times 3) & & & | \\ \hline & & & | \\ 0(55 \times 3) & & & | \\ \hline & \sqrt{2\beta_1} \sigma_1 & & | \\ & & \sqrt{2\beta_2} \sigma_2 & | \\ & & & \sqrt{2\beta_3} \sigma_3 \\ & & & \vdots \\ & & & \sqrt{2\beta_{11}} \sigma_{11} \\ \hline & & & | \\ & & & | \quad 0(36 \times 11) \\ & & & | \end{array} \right]$$

System  $H_S$  - matrix and  $R_S$  - matrix

---

Given the non-linear measurement equation:

$$\underline{z}_S(t_i) = \underline{h}_S(\underline{x}(t_i), t_i) + \underline{v}_S(t_i)$$

$$H_S = \left. \frac{\partial \underline{h}_S}{\partial \underline{x}} \right|_{\underline{x}_n(t)}$$

where  $\underline{x}_n(t)$  is the nominal reference state trajectory.

Using the non-linear measurement equations defined in the summary to section II, and defining the components of  $\underline{z}_S(t_i)$  as:

$$\underline{z}_S(t_i) = \begin{bmatrix} \omega_{MY} \\ \omega_{MZ} \\ \delta_{nM} \\ \delta_{\epsilon M} \\ R_M \end{bmatrix}$$

and assuming the constants  $K_1$ ,  $K_2$ , and  $K_R$  are all unity, then  $H_S(t)$  is given by:

$$H_S(t) = \begin{bmatrix} H_{S1} & & \\ (5 \times 16) & H_{S2} & \\ & (5 \times 10) & H_{S3} \\ & & (5 \times 11) \end{bmatrix}$$









## Appendix C

Linearization of Filter Model State and Measurement Equations

## Definitions:

$X_1, X_2, X_3$  Inertial satellite position vector

$X_4, X_5, X_6$  Inertial satellite velocity vector

$r_v$  Distance from earth center to satellite

$U_{2_I}$  Matrix of 2nd partials of gravity gradient with respect to satellite position in earth centered inertial coordinates

$u(i, j)$  Element in  $i^{\text{th}}$  row and  $j^{\text{th}}$  column of  $U_{2_I}$

$U_{2_T}$  Matrix of 2nd partials of gravity gradient with respect to satellite position in tracker coordinates

$\bar{u}(i, j)$  Element in  $i^{\text{th}}$  row and  $j^{\text{th}}$  column of  $U_{2_T}$

$\mu_{\oplus}$  Earth's gravitational constant

Filter Model F - matrix

Using the non-linear state equations defined in the summary to section V, the filter model F - matrix denoted  $F_F$  is given by:

$$F_F = \begin{bmatrix} F_1 & 0 \\ (6 \times 6) & (6 \times 6) \\ F_2 & F_3 \\ (6 \times 6) & (6 \times 6) \end{bmatrix}$$



$$\begin{bmatrix}
 \frac{-2 V_I}{R} & \omega_{TX} & 0 & 0 & 0 & \frac{2 V_I \omega_{LSY} + A_{TZ}}{R^2} & \frac{-2 \omega_{LSY}}{R} \\
 -\omega_{TX} & \frac{-2 V_I}{R} & 0 & 0 & 0 & \frac{2 V_I \omega_{LSZ} - A_{TY}}{R^2} & \frac{-2 \omega_{LSZ}}{R} \\
 0 & 1 & 0 & 0 & -\omega_{TX} & 0 & 0 \\
 1 & 0 & \omega_{TX} & 0 & 0 & 0 & 0 \\
 0 & 0 & 0 & 0 & 0 & 0 & 1 \\
 2 \omega_{LSY} R & 2 \omega_{LSZ} R & 0 & 0 & 0 & (\omega_{LSY}^2 + \omega_{LSZ}^2) & 0
 \end{bmatrix}$$

F<sub>3</sub> =

Filter Model  $Q_F$  and  $G_F$  Matrices

Let  $Q_F$  be defined as the covariance matrix  $E \{ \underline{\omega}(t) \underline{\omega}^T(t) \}$

where:

$$\underline{\omega}(t) = \begin{bmatrix} W_1 \\ W_2 \\ W_3 \\ W_4 \\ W_5 \\ W_6 \end{bmatrix}$$

$W_1$  to  $W_6$  are independent Gaussian white noise processes so that  $Q_F$  is a diagonal 6 x 6 matrix and:

$$Q_F = \begin{bmatrix} 4 \times 10^{-6} & & & & & \\ & 4 \times 10^{-6} & & & & \\ & & 4 \times 10^{-6} & & & \\ & & & 1 \times 10^{-22} & & \\ & & & & 1 \times 10^{-22} & \\ & & & & & 2.5 \times 10^{-9} \end{bmatrix}$$

$$G_F = \begin{bmatrix} 0 & & & & & \\ (3 \times 3) & & & & & \\ \hline & I & & & & \\ (3 \times 3) & & & & & \\ \hline & & & & I & \\ & & & & (2 \times 2) & \\ \hline & 0 & & & & \\ (6 \times 3) & & & & & \\ & & & & & 0 \\ & & & & & (4 \times 2) \end{bmatrix}$$

Filter Model  $M_F$  and  $R_F$  Matrices

Let  $R_F$  be the covariance matrix  $E \left\{ \underline{v}(t) \underline{v}^T(t) \right\}$  where:

$$\underline{v}(t) \triangleq \begin{bmatrix} v_2 \\ v_3 \\ v_7 \\ v_8 \\ v_9 \end{bmatrix}$$

The elements of the vector are independent Gaussian white noise processes so that  $R_F$  is a diagonal 5 x 5 matrix and:

$$R_F = \begin{bmatrix} 2.5 \times 10^{-12} & & & & \\ & 2.5 \times 10^{-12} & & & \\ & & 6 \times 10^{-12} & & \\ & & & 6 \times 10^{-12} & \\ & & & & 450 \end{bmatrix}$$

where the figures are derived using the truth model data set in Appendix D.  $H_F$  is the 5 x 5 identity matrix.

## Appendix D

Initial Truth Model Simulation Parameters

The following simulation parameters are used initially in the truth model measurement equations.

Rate Gyro Measurements

The figures are based on Ref. 15, page 302 representing a typical aircraft gyro.

<u>Quantity</u>	<u>Steady State Standard Deviation</u>	<u>Process Correlation Time</u>
Gyro drift	$1 \times 10^{-6}$ rad/sec	1 hr
Gyro scale factors	$5 \times 10^{-4}$	$\infty$
Gyro mass unbalance coefficients	$3 \times 10^{-6}$ rad-sec/m	$\infty$
Gyro misalignment coefficients	$1 \times 10^{-4}$	$\infty$
Additive white noise	$1 \times 10^{-9}$ rad/sec	0

The gyro drift correlation time is typically much larger than 1 hour. The time was reduced to 1 hour to model a worst case drift. The misalignment coefficients have been approximately estimated and the white noise is based on uncertainty in the gyro drift.

Accelerometer Measurements

The figures are based on Ref. 15, page 291, representing a typical accelerometer.

<u>Quantity</u>	<u>Steady State Standard Deviation</u>	<u>Process Correlation Time</u>
Accelerometer drift	0.05 m/sec <sup>2</sup>	1 hr
Accelerometer scale factors	1 x 10 <sup>-3</sup>	∞
Accelerometer g <sup>2</sup> non-linear coefficients	1 x 10 <sup>-3</sup> sec <sup>2</sup> /m	∞
Accelerometer g <sup>3</sup> non-linear coefficients	2 x 10 <sup>-4</sup> sec <sup>4</sup> /m <sup>2</sup>	∞
Accelerometer misalignment coefficients	5 x 10 <sup>-4</sup>	∞
Additive white noise	1 x 10 <sup>-7</sup> m/sec <sup>2</sup>	0

where the accelerometer drift process correlation time has been reduced to 1 hour to represent worst case drift and the white noise results from the additive effects of dead zone, hysteresis and temperature effects.

#### Angular Deviations

The exact means of measuring angular deviations will vary depending on the type of tracking device employed. The following figures are therefore approximately estimated as representative of a typical device.

<u>Quantity</u>	<u>Steady State Standard Deviation</u>	<u>Process Correlation Time</u>
Angle track scintillations	1 x 10 <sup>-6</sup> rad	10 sec
Angle measurement scale factors	10 <sup>-4</sup>	300 sec
Angle track bias	2 x 10 <sup>-6</sup> rad	∞
Additive white noise	1 x 10 <sup>-6</sup> rad	0

Range Measurement

Again, the range measurement parameters will vary depending on the device used. The following figures are therefore approximately estimated as representative of a typical device.

<u>Quantity</u>	<u>Steady State Standard Deviation</u>	<u>Process Correlation Time</u>
Range scintillation	20 m	10 sec
Range bias	5 m	$\infty$
Additive white noise	5 m	0

Vita

Robert Arthur Kirk Mitchell was [REDACTED]

[REDACTED] In [REDACTED]

[REDACTED] and subsequently was awarded a

cadetship at the Royal Air Force Technical College Henlow, Bedfordshire and the Royal Air Force College Cranwell, Lincolnshire.

He graduated from Cranwell in 1969 with a Bachelor of Science degree in Aeronautical Engineering with an Electrical specialisation. As an Engineer, he served as Maintenance Officer for Radar and Communications systems at RAF Patrington, Yorkshire during the period 1969 to 1971. Until May 1973 he served at RAF Coldhanger, Hampshire as the Skyjet Spacecraft Operations Officer where he was responsible for on-orbit satellite control functions and project work for new satellite systems. In May 1973 he entered the Graduate Aeronautical Engineering program at the Air Force Institute of Technology, Wright-Patterson Air Force Base, Ohio, USA.